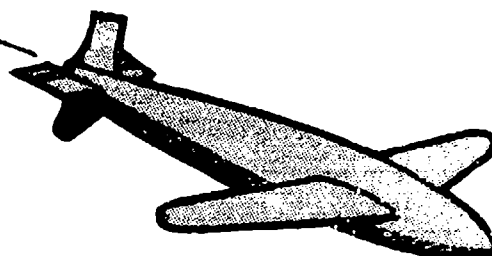


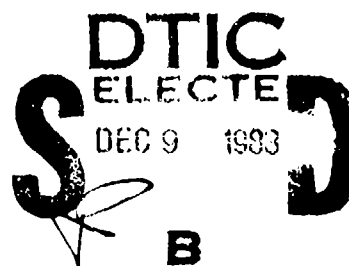
Defence Fellowship Paper 1980

AD-A135605

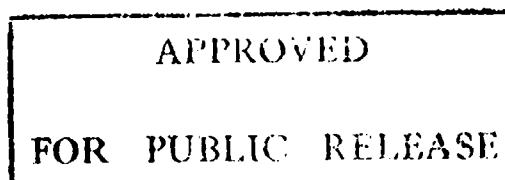
Linearised Optimal Control and Application
to a Gliding Projectile

by

G. Jepps

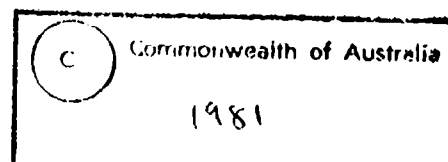


DTIC FILE COPY



Department of Defence

83 12 09 059



THE UNITED STATES NATIONAL
TECHNICAL INFORMATION SERVICE
IS AUTHORIZED TO
REPRODUCE AND SELL THIS REPORT

- - -
Department of Defence

Defence Fellowship Paper

LINEARISED OPTIMAL CONTROL AND APPLICATION TO A GLIDING PROJECTILE

G. Jepps

DRCS

Salisbury, South Australia

This paper represents the views of the author and not necessarily those of either the Department of Defence or the Minister for Defence.

Preface

The studies which led to this paper were carried out under the Defence Fellowship Scheme during the year 1980 in the Electrical Engineering Department of the University of Adelaide. The objects of these studies were to pursue the latest developments in modern control system theory, to examine applications to the design of flight control systems in particular, and to apply the theory to some problem of interest to the Department of Defence. The problem selected was the mid-course control of a gliding projectile and this has a direct application to glide bomb design.

Studies also included short courses on the use of microprocessors and experience was gained in using computer-aided design packages under the guidance of Dr. M.J. Gibbard of the Electrical Engineering Department.

This paper has been submitted to the University of Adelaide as a Master of Engineering Science thesis.

G. Jepps, Aeroballistics Division, Weapons Systems Research Laboratory


Copyright assigned to the Commonwealth, 1981.

Accession For	
NTIS GRA&I	<input checked="checked" type="checkbox"/>
DTIC TAB	<input type="checkbox"/>
Unannounced	<input type="checkbox"/>
Justification	<input type="checkbox"/>
By	
Distribution/	
Availability Codes	
Dist	Avail. and/or Special
A-1	



- 2 -

SUMMARY



The standard results of linearized² optimal control theory are explored and examined to see how they can be applied to flight control systems. A feedback control system operating on the elevators of an aircraft-like gliding projectile is investigated. The projectile is required to closely follow a predetermined maximum range trajectory in the face of initial disturbances.

Equations of motion are set up and linearized¹. Approximate solutions for the maximum range trajectory are given and approximate analytical expressions for the eigenvalues of the plant matrix are derived. After assigning weighting values to the state and control variables in the integral quadratic performance index, solutions to the Riccati matrix equation are computed and used to evaluate optimal state feedback gain vectors. The effect of this optimal feedback on glider performance is observed from computed trajectory simulations. An optimal feedback gain vector is selected subject to limitations on angle of attack, elevator deflection angle, and attitude.

The question of incomplete state variable feedback is considered in the interest of simpler engineering design. Using a reduced order system representation, relationships between performance index weights and closed loop poles are established and a sub-optimal system based on feedback of only one state variable is investigated.




TABLE OF CONTENTS

	Page
1. INTRODUCTION	1
2. EQUATIONS OF MOTION	6
3. OPTIMAL GLIDE PATH	12
4. PERTURBED EQUATIONS OF MOTION	16
5. LINEAR OPTIMAL CONTROL THEORY	19
5.1 Properties of Riccati Matrix R	23
5.1.1 Relationship between R and Integral Performance Index	24
5.1.2 Link between R and Liapunov Stability	25
5.1.3 Asymptotic behaviour of R	25
5.1.4 Time invariant, infinite upper limit performance integral	26
5.1.5 Alternative to Riccati Matrix Solution	27
5.1.6 Selection of Weighting Matrices	28
6. CONTROL SYSTEM DESIGN	30
6.1 Choice of Performance Index Weights and Determination of Feedback	31
6.2 Integrity	39
6.3 Implementation	41

	Page
7. SUB OPTIMAL CONTROL	42
7.1 Reduced Order Approximation	43
7.2 Single State Feedback	53
8. DISCUSSION AND RESULTS	57
REFERENCES	66

LIST OF APPENDICES

I PROJECTILE MASS AND AERODYNAMIC PROPERTIES	68
II CHARACTERISTIC EQUATION AND SOLUTION	74

LIST OF TABLES

1. SYSTEM 11 POLES FOR EACH FEEDBACK FAILURE	40
2. COMPARATIVE FEATURES OF 3 FEEDBACK CONTROL SYSTEMS	60
3. COMPARATIVE PERFORMANCE OF 3 FEEDBACK CONTROL SYSTEMS	61

LIST OF FIGURES

1. Aircraft-like projectile with elevator controls
2. Total projectile trajectory
3. Phugoid oscillation
4. Force, moment and axes systems for projectile

5. Velocity response to initial velocity perturbation 20 m s^{-1} for
projectile with no control and control system I
6. Attitude response to initial velocity perturbation 20 m s^{-1} for
projectile with no control and control system I
7. Altitude response to initial velocity perturbation 20 m s^{-1} for
projectile with no control and control system I
8. Positional response to initial velocity perturbation 20 m s^{-1}
for projectile with no control and control system I
9. State variable feedback scheme
10. Optimal state feedback gains for control system II
11. Velocity response to initial velocity perturbation 20 m s^{-1}
for projectile with no control and control system II
12. Attitude response to initial velocity perturbation 20 m s^{-1}
for projectile with no control and control system II
13. Altitude response to initial velocity perturbation 20 m s^{-1}
for projectile with no control and control system II
14. Positional response to initial velocity perturbation 20 m s^{-1}
for projectile with no control and control system II

15. Angle of attack response to initial velocity perturbation 20 m s^{-1}
for projectile with control system 11
16. Elevator angle response to initial velocity perturbation 20 m s^{-1}
for projectile with control system 11
17. Random vertical wind gust sequence
18. Random horizontal wind gust sequence
19. Velocity response to initial velocity perturbation 20 m s^{-1}
and random gusts for projectile with control system 11
20. Attitude response to initial velocity perturbation 20 m s^{-1}
and random gusts for projectile with control system 11
21. Altitude response to initial velocity perturbation 20 m s^{-1}
and random gusts for projectile with control system 11
22. Positional response to initial velocity perturbation 20 m s^{-1}
and random gusts for projectile with control system 11
23. Angle of attack response to initial velocity perturbation 20 m s^{-1}
and random gusts for projectile with control system 11
24. Elevator angle response to initial velocity perturbation 20 m s^{-1}
and random gusts for projectile with control system 11
25. Scheme for estimation of feedback states from incomplete measurements
26. Optimal feedback gains and relative weights for complex poles of
reduced order system

27. Optimal velocity feedback gain and relative weights for largest
real poles of reduced order system
28. Optimal flight path angle feedback gain and relative weights
for largest real poles of reduced order system
29. Velocity response to initial velocity perturbation 20 m s^{-1}
for projectile with reduced order system control
30. Attitude response to initial velocity perturbation 20 m s^{-1}
for projectile with reduced order system control
31. Positional response to initial velocity perturbation 20 m s^{-1}
for projectile with reduced order system control
32. Initial angle of attack response to initial velocity perturbation
 20 m s^{-1} for projectile with reduced order system control
33. Initial velocity response to initial velocity perturbation
 20 m s^{-1} for projectile with reduced order system control
34. Initial attitude response to initial velocity perturbation
 20 m s^{-1} for projectile with reduced order system control
35. Velocity response to initial velocity perturbation 20 m s^{-1}
and random gusts for projectile with reduced order control system
36. Angle of attack response to initial velocity perturbation 20 m s^{-1}
and random gusts for projectile with reduced order control system

37. Attitude response to initial velocity perturbation 20 m s^{-1}

and random gusts for projectile with reduced order control system

38. Positional response to initial velocity perturbation 20 m s^{-1}

and random gusts for projectile with reduced order control system

39. Performance index for feedback of velocity only

40. Velocity response to initial velocity perturbation 20 m s^{-1}

for projectile with velocity feedback control only

41. Attitude response to initial velocity perturbation 20 m s^{-1}

for projectile with velocity feedback control only

42. Altitude response to initial velocity perturbation 20 m s^{-1}

for projectile with velocity feedback control only

43. Angle of attack response to initial velocity perturbation 20 m s^{-1}

for projectile with velocity feedback control only

1. INTRODUCTION

In recent years, technological advances have opened up new concepts in the design of flight control systems for aircraft, guided missiles, and military projectiles. The products of these advances, which are now manifest in sensors, microprocessors, and computing techniques, are already being exploited in modern advanced aircraft and guided missile design. Now, with the development of smaller robust sensors together with small and even cheaper microprocessor chips, the possibility of monitoring and controlling the flight of such military projectiles as bombs, shells, and artillery rockets, is emerging.

These new developments have brought with them new approaches to control system design which are particularly relevant to flight systems. In flight, when speed and altitude vary, system parameters are often time-dependent and often performance over only a limited time of flight is of interest. Modern control system theory can take account of such time variations and limited times of flight. Traditional classical control system design theory is, in the main, applicable to linear systems with time-invariant parameters and these systems are required to be asymptotically stable as time becomes large. The basic mathematical tool used in the traditional methods is the Laplace transform whereas matrices are basic to modern control theory. The handling of matrices has been facilitated by the interactive computer aided design packages which are now becoming available and which really have turned the use of modern control theory by engineers into a practical proposition.^{1,2,3} Such matrix methods can readily cope with the multi-input-output control systems frequently needed in flight, as for instance on an aircraft with rudder, elevator, and aileron controls. For systems which are sensibly time-invariant, matrix methods can be readily reduced to the well known classical representation thus rendering such systems amenable to treatment by the well-developed classical design techniques.

Another attraction of the modern theory in applications to flight control system design is that it has a natural connection with optimisation theory, and this in turn enables characteristics of the desired flight path to be used directly as criteria while developing a feedback control design. For example, in the case of a feedback control system for a projectile which is required to follow a desired trajectory, the modern method could be used to find a set of optimal feedback gains which would serve to minimise the time integral of weighted squares of deviations from the required trajectory values. Another use would be to determine optimal feedback gains for a terminal guidance system to minimise miss distance subject to limitations on the amount of available control. A virtue of the linear control system, which results from this method of minimising the integral of weighted squares of errors of deviations in system variables, is that by following simple rules governing selection of weights the system is inherently stable and also, the effects of random variations or noise are suppressed. In fact, the art of linear system design by this method often lies in the choice of suitable weights. In general, the optimal feedback gains will be time-varying and an on-board microprocessor will be needed to generate the gain values together with desired values of system variables to be compared with actual values measured by sensors.

This thesis aims at exploiting modern control theory, to investigate how it can be applied to the mid-course flight of a gliding projectile and to see how it reveals the physical flight behaviour. The sort of projectile considered is a standard bomb configuration to which an aircraft-like wing has been added together with a pair of elevator controls at the rear tail fins as shown in figure 1. The wing provides the bomb with a gliding capability, significantly increasing its range so that the position of launch may remain at a safe stand-off distance from a heavily defended target. A complete trajectory from launch to target would consist of three phases, as shown in figure 2, launch, mid-course, and terminal. Launch may occur by release from an aircraft or by



Figure 1. Aircraft-like Projectile with Elevator Controls.

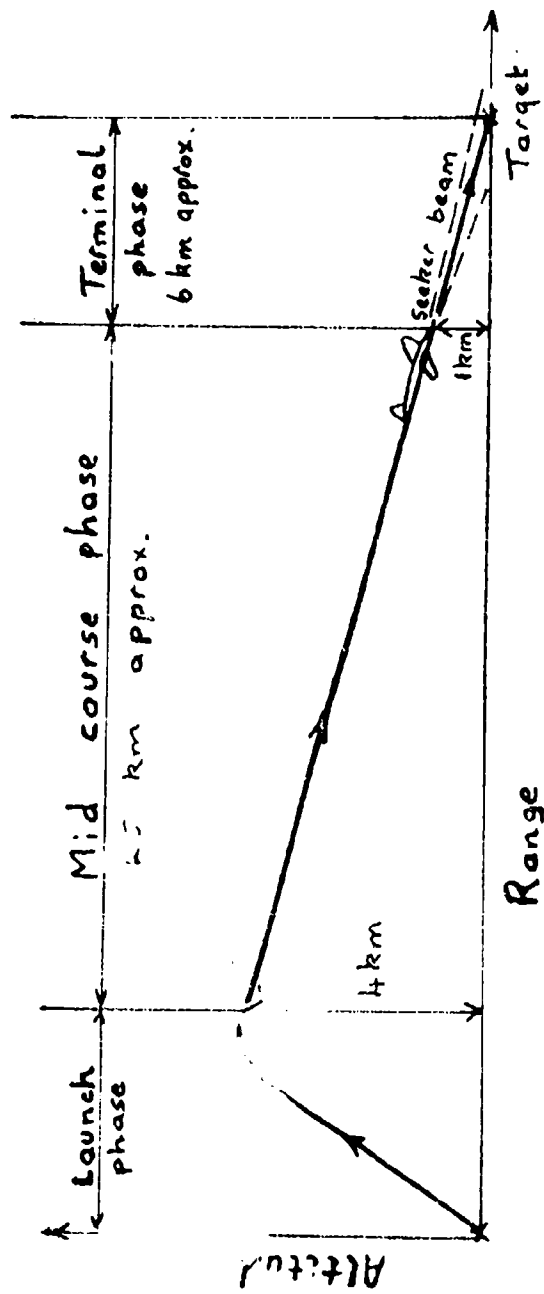


Figure 2. Total Projectile Trajectory

rocket boost from a ground launcher and the launch phase of the trajectory must terminate in favourable starting conditions for the mid-course gliding flight. Mid-course flight must take the projectile to within acquisition range of the target, such that the terminal phase seeker can see the target. However, the greater the mid-course range the greater the terminal errors due to initial disturbances will be, and hence the need for some corrective control, and for some assessment of allowable tolerance in mid-course initial conditions.

The main influence of elevator controls is on pitching motion which, for an aircraft at zero bank or roll angle, means that the main influence is on those system variables which affect motion in a vertical plane. Such motion is termed longitudinal motion as distinct from the lateral motion which governs rolling and yawing behaviour. For conventional aircraft it is well-established that the longitudinal and lateral motions can be decoupled as long as roll angle variations do not exceed first order magnitudes.^{4,5} On the ideal mid-course trajectory where there is no call for side manoeuvre there is no demand for large roll angles and hence for the purpose of preliminary control system design, the lateral and longitudinal motions can be treated separately. For aircraft, the longitudinal motion typically possesses two characteristic modes, a well-damped short period mode and a lightly damped long period mode. Oscillatory motion of the short period mode is prominent in the angle of attack and angular pitching velocity behaviour whilst the long period oscillations dominate the velocity and attitude behaviour. The damping agency for the long period mode, or phugoid as it is called, is the aerodynamic drag. In order to maximise range it is necessary to minimise drag and hence, damping is of necessity, small. This means that initial errors in velocity and attitude would tend to persist throughout mid-course flight without some form of control. Using figure 3, a simple physical explanation of the phugoid oscillation can be given. For the undisturbed or equilibrium flight path, the vertical component of aerodynamic lift is a little less than

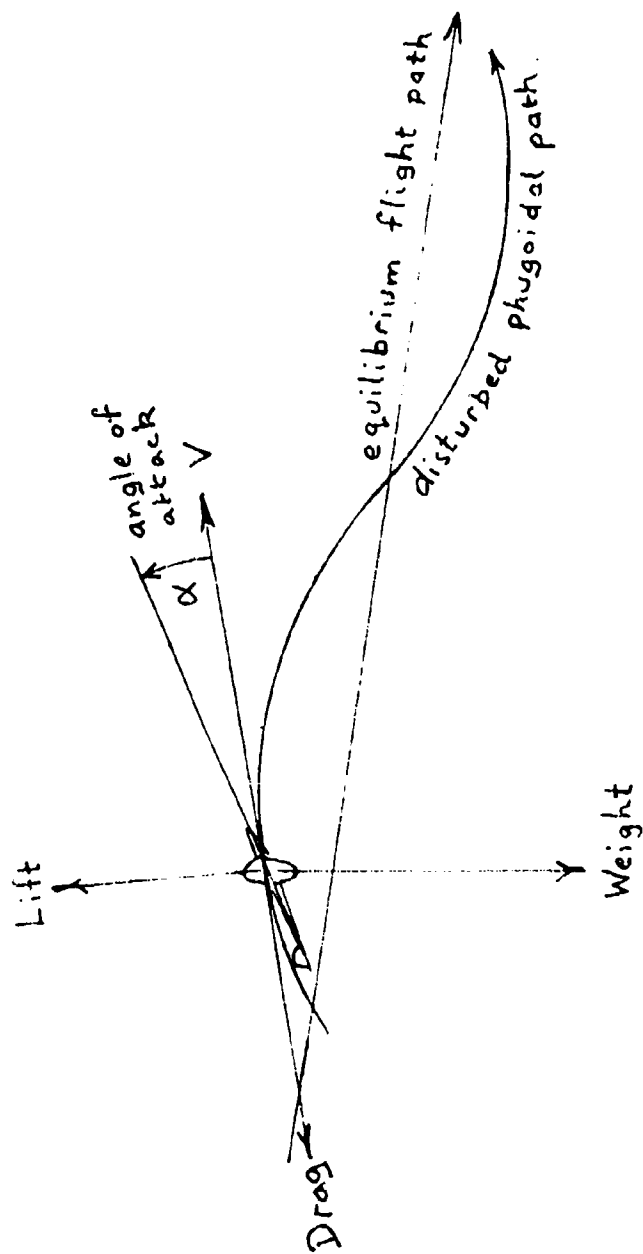


Figure 3. Phugoid Oscillation

the weight, allowing the glider to sink at a rate at which the potential energy loss just balances the energy dissipated by drag. Suppose that the glider flies at a constant angle of attack, then a disturbance which causes the velocity to increase will cause the lift to increase and the glider will rise, increasing its potential energy at the expense of its kinetic energy. Velocity then decreases, causing lift to decrease until the glider eventually sinks and the process is repeated in reverse setting up a phugoid oscillation about the equilibrium flight path. Aerodynamic drag dampens this oscillation. To counter this oscillation, the angle of attack would need to be continuously controlled so that the equilibrium balance between lift and weight of the undisturbed flight path is maintained. This is what the elevator controls seek to do by their pitching effect on angle of attack.

In a powered aircraft the phugoid would be controlled by regulating velocity through engine throttle control, relying on elevators for attitude control. In a piloted glider the pilot is usually able to counter phugoid motion because of its relatively long period. The unpiloted glider relying on automatic control of phugoid motion through elevators has not attracted much attention in the literature although it is interesting to note that automatic control systems which fed back attitude and velocity to elevator controls were devised for both British and German bomber aircraft early in the second world war.⁶ When a gliding projectile is to be released from an aircraft it is likely that the error in initial attitude reference will exceed the magnitude of attitude measurements needed for feedback during gliding flight, so it is worthwhile briefly considering the consequences of sensing velocity alone. One way of counteracting the phugoid is for the elevators to cause the glider to climb for velocities in excess of equilibrium and attempt to maintain the increased altitude, when velocity falls to the equilibrium value. Although this diminishes the phugoid it results in a displaced equilibrium flight path and loses positional accuracy. To maintain positional accuracy it is necessary to try to maintain oscillations about the equilibrium flight path.

This could be achieved by allowing angle of attack to decrease for velocities in excess of equilibrium values, thus diminishing the excess of lift over weight and hence phugoid amplitude, but also diminishing drag and hence damping. This tends to maintain equilibrium flight path position, but unless the control system is carefully designed, too large a decrease in angle of attack in response to increased velocity could lead to an unrecoverable downward plunge. In this respect, phugoid motion is not unlike that of a simple pendulum which executes small oscillations about its equilibrium position for small disturbances, but for large disturbances a projectile can loop the loop whereas the pendulum encircles the pivot.

If, on the other hand, the angle of attack is caused to increase for velocities greater than the equilibrium value then the opposite effects occur and phugoid oscillations are enhanced. The amplitude of oscillations is initially increased but the increased angle of attack increases the drag and hence the damping has a more marked effect in reducing excess velocity.

The consequences of the foregoing discussion are that we can expect to regulate velocity and attitude at the expense of position, velocity and position at the expense of attitude, or attitude and position at the expense of velocity. These observations will be useful later on when weights are selected for constructing the performance indexes used in optimal feedback design. For the projectile considered in this thesis, the objects of the mid-course control then are to maximise range by preserving gliding flight and, to within constraints on control deflection and angle of attack, to reduce terminal effects arising from initial errors and flight disturbances.

Elements of linearised optimal control theory are introduced in section 5 and application of this theory to the design of a feedback control system for the glider is carried out in section 6. A consequence of linearised optimal control theory is that all state variables should be fed back to the controller thus it is of interest to investigate the performance of simpler

sub optimal systems with partial feedback. A sub optimal feedback control system based on a reduced order mathematical model which considers only phugoid motion in isolation is studied in detail in section 7. Also considered in section 7 is a sub optimal system in which only velocity is fed back to the controller.

In the next section the equations of motion for a gliding projectile are derived and include the effects of wind disturbances. In section 3, the equations of motion are used to extract conditions for optimal flight paths and in section 4 the equations for first order perturbations about optimal conditions are derived and form the basic equations for applying the linear optimal control theory in the section following on.

2. EQUATIONS OF MOTION

The full equations of motion for an aircraft can be obtained from such texts as references 4 or 5. It is found that when large sideways manoeuvres are not needed then roll angles can remain small, and horizontal and vertical components of the motion become uncoupled. Thus for the purpose of preliminary design of a feedback control system operating on the projectile's elevators, only motion in a vertical plane will be considered. Equations of motion for flight in a vertical plane, subject to wind disturbances, will now be derived in a form convenient for treating gliding flight and for subsequent linearisation for the purpose of control system design. Nomenclature together with force, moment, and axes systems for flight in a vertical plane are shown in figure 4. In the figure

\bar{V} is the velocity vector of the projectile's centre of gravity,

\bar{V}_w is the velocity vector of the atmospheric wind,

and $\bar{V}_R = -\bar{V} + \bar{V}_w$, the velocity vector of the air relative to the projectile and thus the velocity on which the magnitude and direction of the aerodynamic forces depend.

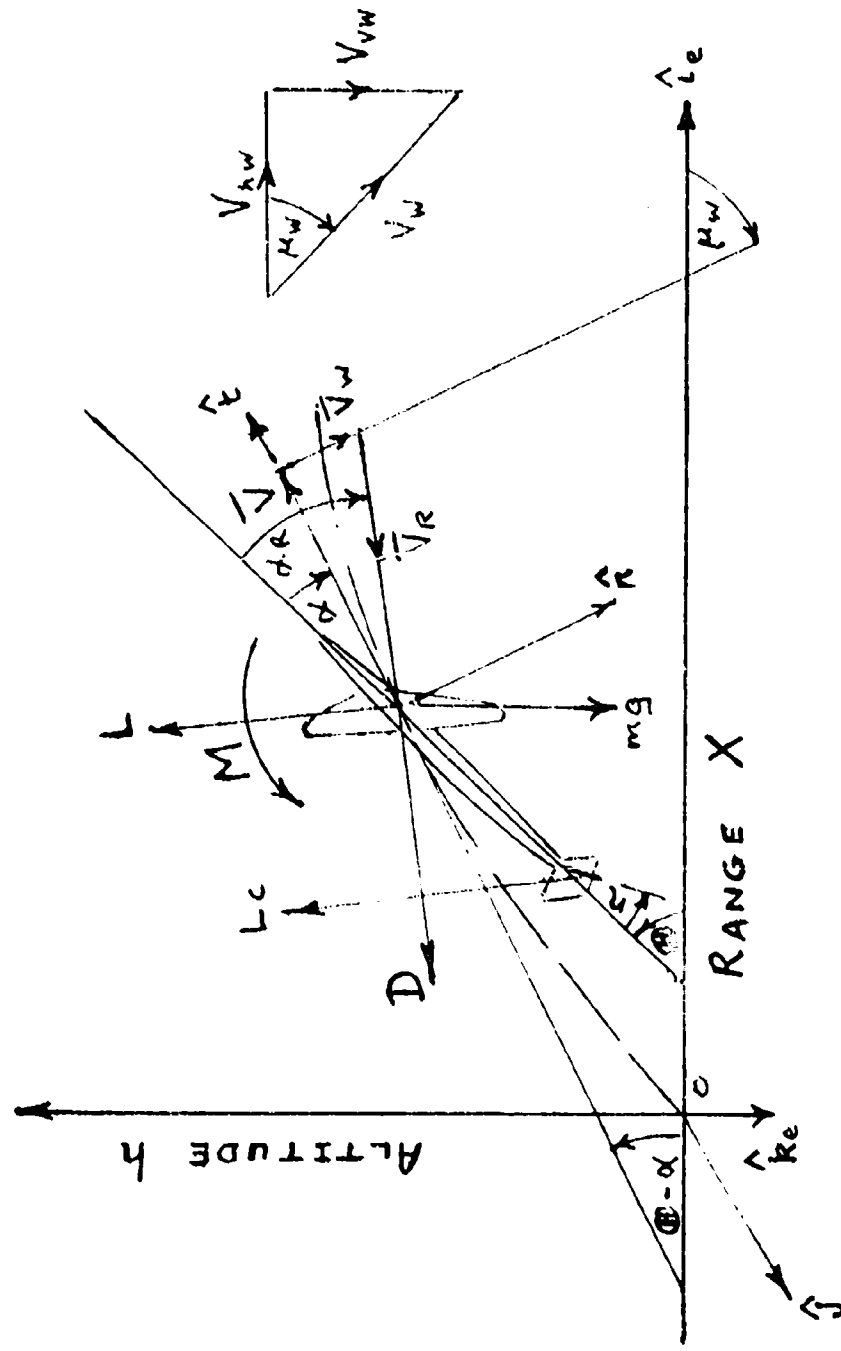


Figure 4. Force, Moment and Axes Systems for Projectile

The aerodynamic forces are:-

- L the lift force acting normal to \bar{V}_R not including the elevators component,
- L_C the lift force component of the elevators,
- and D the drag force acting in the direction of \bar{V}_R .
- M is the pitching moment about the centre of gravity,
- and m is the mass of the projectile.

The angles in figure 4 are:-

- α the angle of attack, which is the angle between \bar{V} and the projectile's longitudinal axis, positive for nose up,
- α_R the relative angle of attack, which is the angle between \bar{V}_R and the projectile's longitudinal axis,
- η the elevator control deflection angle, positive downwards as shown
- and θ the angle between the projectile's longitudinal axis and the horizontal lying in the same vertical plane.

There are two sets of three dimensional axes systems shown in figure 4 and these are defined by the mutually perpendicular unit vector triads $\hat{i}_e, \hat{j}, \hat{k}_e$ and $\hat{i}, \hat{j}, \hat{n}$.

The $\hat{i}_e, \hat{j}, \hat{k}_e$ system is fixed relative to earth with \hat{i}_e and \hat{j} contained in a horizontal plane such that \hat{i}_e is directed along the range X and \hat{k}_e is vertically downwards. The $\hat{i}, \hat{j}, \hat{n}$ system with origin at the centre of gravity, rotates with angular velocity $\hat{j}(\dot{\theta}-\dot{\alpha})$ and \hat{i} is along the tangent to the flight path and \hat{n} is along the inward drawn normal.

The linear acceleration of the centre of gravity is found by differentiating the velocity vector $\bar{V} = V\hat{i}$.

Thus
$$\dot{\bar{V}} = \dot{V}\hat{i} + V\dot{\hat{i}}.$$

where
$$\dot{\hat{i}} = \hat{j}(\dot{\theta}-\dot{\alpha}) \wedge \hat{i} = -\hat{n}(\dot{\theta}-\dot{\alpha}),$$

giving the result $\dot{\vec{V}} = \dot{V}\hat{t} - V(\dot{\theta}-\dot{\alpha})\hat{n}$.

From figure 4, the force acting on the projectile is

$$\begin{aligned} &= \{D \cos(\alpha_R - \alpha) - (L + L_C) \sin(\alpha_R - \alpha) + mg \sin(\theta - \alpha)\}\hat{t} \\ &= \{(L + L_C) \cos(\alpha_R - \alpha) + D \sin(\alpha_R - \alpha) - mg \cos(\theta - \alpha)\}\hat{n} \end{aligned}$$

Equating this force to $m\dot{\vec{V}}$ gives the two scalar equations

$$m\dot{V} = -D \cos(\alpha_R - \alpha) + (L + L_C) \sin(\alpha_R - \alpha) - mg \sin(\theta - \alpha) \quad (1)$$

$$\text{and } mV(\dot{\theta} - \dot{\alpha}) = (L + L_C) \cos(\alpha_R - \alpha) + D \sin(\alpha_R - \alpha) - mg \cos(\theta - \alpha) \quad (2)$$

In addition there is the moment equation

$$B\ddot{\theta} = M \quad (3)$$

where B is the pitching moment of inertia of the projectile about a transverse axis through its centre of gravity.

Additionally, the range X and altitude h satisfy

$$\dot{X} = V \cos(\theta - \alpha) \quad (4)$$

$$\dot{h} = V \sin(\theta - \alpha) \quad (5)$$

It is now necessary to define the aerodynamic forces and moments appearing in equations (1), (2) and (3). The drag is expressed in the form⁽⁴⁾

$$D = (\rho V_R^2 S / 2) \times \{C_{D0} + \alpha_R^2 S (\partial C_{L'} / \partial \alpha)^2 / (\pi e A S_w)\}$$

where ρ is air density

S is the reference area on which aerodynamic coefficients are based,

C_{D0} is the drag coefficient at zero angle of attack,

$\partial C_L / \partial \alpha$ is the wing lift coefficient derivative evaluated at $\alpha=0$
and $S/(\pi e A S_w)$ is a constant.

The α_R^2 term in the expression for drag D, represents the component of drag induced by vorticity shed from a finite span wing and would disappear only for a wing of infinite span. The lift on the projectile, apart from that arising from deflected elevators, is given by

$$L = (\rho V_R^2 S / 2) C_L(\alpha_R),$$

and the lift on the deflected elevator control by

$$L_C = (\rho V_R^2 S / 2) (\partial C_L / \partial \eta) \eta,$$

where $C_L(\alpha_R)$ is the lift coefficient for the projectile

and $\partial C_L / \partial \eta$ is the lift coefficient derivative for the elevator control evaluated for $\eta=0$.

The drag coefficient C_{D0} and the lift coefficient derivatives $\partial C_L / \partial \eta$ and $\partial C_L / \partial \alpha$ are Mach number dependent, but for the Mach number range considered here, which is less than 0.5, these aerodynamic coefficients can reasonably be taken as constants. Thus the projectile lift will be expressed as

$$(\rho V_R^2 S / 2) (\partial C_L / \partial \alpha) \alpha_R$$

where $(\partial C_L / \partial \alpha)$ is evaluated at $\alpha=0$.

Similarly, the pitching moment is expressed as

$$M = (\rho V_R^2 S b / 2) \{ \alpha_R (\partial C_m / \partial \alpha) + (q b / 2 V_R) (\partial C_m / \partial q) + (\dot{\alpha}_R b / 2 V_R) (\partial C_m / \partial \dot{\alpha}) + \eta (\partial C_m / \partial \eta) \}$$

where b is a reference length

C_m is the aerodynamic pitching moment coefficient

$$\text{and } \dot{q} = \dot{\theta}$$

and the partial derivatives of C_m are evaluated for zero values of their arguments. The moment components in $\partial C_m / \partial \alpha$ and $\partial C_m / \partial \eta$ represent the static pitching moment due to angle of attack and elevator deflection respectively, while the components in $\partial C_m / \partial \dot{q}$ and $\partial C_m / \partial \dot{\alpha}$ represent damping effects.

The air density ρ appearing in the aerodynamic forces and moments is dependent upon altitude h and a frequently used analytical relationship is given by

$$\rho = \rho_{\text{ref}} e^{-h/H}, \text{ where}$$

ρ_{ref} is a constant reference density

and H is a constant scale height.

Using this relationship for ρ and expressing the relative velocity V_R and angle of attack α_R in terms of wind velocity V_w and wind direction with the horizontal μ_w , as shown in figure 4, equations (1) to (5) together with

$$\dot{\theta} = \dot{q}$$

give the following set of equations for the motion of the projectile.

$$\begin{aligned} \dot{V} = & -(D/m) \{V - V_w \cos(\mu + \theta - \alpha)\} / V_R \\ & -(L/m)(V_w/V_R) \sin(\mu_w + \theta - \alpha) - g \sin(\theta - \alpha) \\ & - (\rho_{\text{ref}} S/2m) (\partial C_L / \partial \eta) \eta V_R V \sin(\mu + \theta - \alpha) \exp(-h/H) \end{aligned} \quad (6)$$

$$\begin{aligned} \dot{\alpha} = & (D/mV)(V_w/V_R) \sin(\mu_w + \theta - \alpha) \\ & -(L/mV) \{V - V_w \cos(\mu_w + \theta - \alpha)\} / V_R \\ & + (g/V) \cos(\theta - \alpha) + \dot{q} \\ & - (\rho_{\text{ref}} S/2m) (\partial C_L / \partial \eta) \eta V_R \{V - V_w \cos(\mu + \theta - \alpha)\} \end{aligned} \quad (7)$$

$$\dot{\theta} = q \quad (8)$$

$$\begin{aligned} \dot{q} = & (\rho_{rel} S b / 2 B) V_R^2 \{ \alpha_R (\partial C_m / \partial \alpha) + (q b / 2 V_R) (\partial C_m / \partial q) \\ & + (\dot{\alpha}_R b / 2 V_R) (\partial C_m / \partial \dot{\alpha}) + \eta (\partial C_m / \partial \eta) \} e^{-h/H} \end{aligned} \quad (9)$$

$$\dot{X} = V \cos(\theta - \alpha) \quad (10)$$

$$\dot{h} = V \sin(\theta - \alpha) \quad (11)$$

Equations (6) to (11) thus represent a set of six equations for the state variables V , α , θ , q , X , h and control variable η where

$$\begin{aligned} (D/m) = & (\rho_{rel} S / 2 m) V_R^2 e^{-h/H} \\ & \times \{ C_{Do} + \alpha_R^2 S (\partial C_L / \partial \alpha)^2 / \pi c A S w \} \end{aligned} \quad (12)$$

$$(L/m) = (\rho_{rel} S / 2 m) V_R^2 (\partial C_L / \partial \alpha) \alpha_R e^{-h/H} \quad (13)$$

$$V_R^2 = V^2 + V_w^2 - 2 V V_w \cos(\mu_w + \theta - \alpha) \quad (14)$$

$$\alpha_R = \sin^{-1} \{ (V \sin \alpha - V_w \sin(\mu_w + \theta)) / V_R \} \quad (15)$$

$$\begin{aligned} \dot{\alpha}_R = & \dot{\alpha} \{ V^2 - V V_w \cos(\mu_w + \theta - \alpha) \} / V_R^2 \\ & + (\dot{\mu}_w + q) \{ V^2 - V V_w \cos(\mu_w + \theta - \alpha) \} / V_R^2 \\ & + \{ (\dot{V} V_w - \dot{V}_w V) \sin(\mu_w + \theta - \alpha) \} / V_R^2 \end{aligned} \quad (16)$$

The values of the aerodynamic coefficients appearing in equations (6) to (13) can be found from data handbooks such as references 7 and 8.

3. OPTIMAL GLIDE PATH

The desired glide path is one which maximises the range X for a given decrease in altitude for flight in still air. Descent rate is governed by the elevator control setting so that the mathematical problem is to find the time variation of control angle $\eta(t)$ which maximises

$$\int_{t_i}^{t_f} \dot{X}(t) dt$$

subject to the constraints imposed by equations (6) to (16) with $V_w=0$. When $V_w=0$, equations (6) to (16) become,

$$\dot{V} = -(\rho_{ref} S/2m) V^2 C_D(\alpha) e^{-h/H} - g \sin(\theta - \alpha) \quad (17)$$

$$\begin{aligned} \dot{\alpha} = & -(\rho_{ref} S/2m) V \{ \alpha (\partial C_L / \partial \alpha) \\ & + \eta (\partial C_L / \partial \eta) \} e^{-h/H} + \alpha + (g/V) \cos(\theta - \alpha) \end{aligned} \quad (18)$$

$$\dot{\theta} = q \quad (19)$$

$$\begin{aligned} \dot{q} = & (\rho_{ref} S b/2B) V^2 e^{-h/H} \{ \alpha (\partial C_m / \partial \alpha) + (qb/2V) (\partial C_m / \partial q) \\ & + (\dot{\alpha} b/2V) (\partial C_m / \partial \dot{\alpha}) + \eta (\partial C_m / \partial \eta) \} \end{aligned} \quad (20)$$

where

$$C_D(\alpha) = C_{D0} + \alpha^2 S (\partial C_L / \partial \alpha)^2 / \pi \epsilon A S_w \quad (21)$$

However, a good engineering approximate solution is available for this problem and is based on physical reasoning. It is argued that maximum range flight paths will be flat and hence changes in θ and α will be small. Hence, the

approximation $\dot{\theta} = \dot{q} = \dot{\alpha} = 0$ is attempted in equations (17) to (21), giving

$$\dot{V} = -(\rho_{\text{ref}} S/2m) V^2 C_D(\alpha) e^{-h/H} - g \sin(\theta - \alpha) \quad (22)$$

$$0 = -(\rho_{\text{ref}} S/2m) V \{ \alpha (\partial C_L / \partial \alpha) + \eta (\partial C_L / \partial \eta) \} e^{-h/H} + (g/V) \cos(\theta - \alpha) \quad (23)$$

$$0 = \alpha (\partial C_m / \partial \alpha) + \eta (\partial C_m / \partial \eta) \quad (24)$$

The physical interpretation of these equations is, first, from (23) that the lift is approximately equal to the weight of the projectile and that changes in velocity are due to changes in altitude. For small changes in velocity, or that is, kinetic energy, equation (22) implies that the rate of loss in potential energy is approximately balanced by the energy dissipated in drag. Equation (24) is the trim equation giving the relative values of α and η which reduce the pitching moment to zero. As shown in reference (9), equations (22) and (23) can be combined to give

$$d(V^2 + gh)/dt = -g X C_D(\alpha) / \{ \alpha (\partial C_L / \partial \alpha) + \eta (\partial C_L / \partial \eta) \} \quad (25)$$

where, from equation (24), $\eta = -\alpha (\partial C_m / \partial \alpha) / (\partial C_m / \partial \eta)$,

so that integration of equation (25) with α assumed to be sensibly constant yields

$$X - X_i = \{ (V_i^2 - V^2) / 2g + (h_i - h) \} \{ \alpha / C_D(\alpha) \} \times \{ (\partial C_L / \partial \alpha) + (\eta / \alpha) (\partial C_L / \partial \eta) \} \quad (26)$$

where subscript i denotes initial value. It is possible to obtain further close approximations for trajectory parameters when α is assumed to be invariant. For example, equations (23) and (24) give

$$V^2 = \frac{g e^{h/H} \cos(\theta-\alpha)}{(\rho_{ref} S/2m) \{ (\partial C_L / \partial \alpha) + (\eta/\alpha) (\partial C_L / \partial \eta) \} \alpha} \quad (27)$$

Differentiating equation (27) with respect to time and ignoring changes in $(\theta-\alpha)$ gives

$$\dot{V} = (V^2/2H) \sin(\theta-\alpha) \quad (28)$$

which when substituted into equation (22) gives for the glide path angle,

$$\tan(\theta-\alpha) = \frac{-g C_D(\alpha)}{(g+V^2/2H) \{ (\partial C_L / \partial \alpha) + (\eta/\alpha) (\partial C_L / \partial \eta) \}} \quad (29)$$

The time of flight can be found by putting

$$t = \int_{h_i}^h \frac{dh}{\dot{h}} = \int_{h_i}^h \frac{dh}{\{V \sin(\theta-\alpha)\}}.$$

Equations (27) and (29) enable $\{V \sin(\theta-\alpha)\}^{-1}$ to be expressed in simple exponential functions of h which can be readily integrated to give the result

$$t = \{ (\partial C_L / \partial \alpha) + (\eta/\alpha) (\partial C_L / \partial \eta) \} \times \alpha \{ (V_i - V)/g - 2H/V_i + 2H/V \} / C_D(\alpha) \cos(\theta-\alpha) \quad (30)$$

Equations (26) to (30) provide close approximations to glide path trajectories which are flown with angle of attack α sensibly constant such that the glide angle is not too steep in the sense that the approximation $\cos(\theta-\alpha) \cong 1$ is acceptable.

It can be seen from equation (26) that if changes in V^2 are ignored a maximum

value for the range $(X - X_1)$ occurs when a constant angle of attack is chosen to maximise $\alpha/C_D(\alpha)$. Ignoring changes in V^2 results in an optimum angle of attack which is independent of the altitude range. From equation (21) it is found that if α_0 is the value of α which maximises $\alpha/C_D(\alpha)$, then the optimal angle of attack is given by

$$\alpha_0^2 = \frac{C_{Do}}{(S/\pi e A S_w)(\partial C_L/\partial \alpha)^2} \quad (31)$$

The foregoing engineering approach shows that a close approximation to the glide path with maximum range occurs when the angle of attack is held at a constant value α_0 and hence, from equation (24), the corresponding constant elevator setting is

$$\eta_0 = -\alpha_0 (\partial C_m/\partial \alpha) / (\partial C_m/\partial \eta) \quad (32)$$

The optimum angle of attack is a function of the aerodynamic properties of the projectile and equations (27) and (29) show that the initial optimal velocity and glide path angle are dependent on α_0 and initial altitude h_1 . Thus for a selected value of h_1 , if the launch phase cannot consistently provide an initial mid-course velocity as high as the required optimal value, then α would have to be increased from the optimum to satisfy equation (27), and in consequence the range would be reduced. On the other hand if the launch phase could consistently provide an initial mid-course velocity in excess of the optimum, decreasing α below the optimum would again lead to reduced range provided the assumption that changes in V^2 were small still held. In this case some other strategy would be employed to retain potential energy until sufficient kinetic energy had been dissipated to slow the projectile down to the optimal velocity and then initiate the glide. It will be assumed that the launch phase can be designed such that the expected conditions at the commencement of mid-course flight are the optimal glide path values. The

function of the feedback control system actuating the elevators is then to minimise errors in position, at the end of mid-course flight, due to initial departures from optimal glide path trajectory parameters.

4. PERTURBED EQUATIONS OF MOTION

Departures from the optimal glide path parameters are now treated as first order perturbations about optimal values. A set of linear equations in these perturbed state variables can now be found from equations (6) to (11). The procedure is illustrated by taking equation (6) as an example. This equation is of the form

$$F_V(V, \alpha, \theta, h, \dot{V}, \eta, V_W) = 0,$$

Therefore $\delta F_V = 0$,

$$\begin{aligned} \text{i.e. } & (\partial F_V / \partial V)_0 V_1 + (\partial F_V / \partial \alpha)_0 \alpha_1 \\ & + (\partial F_V / \partial \theta)_0 \theta_1 + (\partial F_V / \partial h)_0 h_1 \\ & + (\partial F_V / \partial \dot{V})_0 \dot{V}_1 + (\partial F_V / \partial \eta)_0 \eta_1 + (\partial F_V / \partial V_W)_0 V_{W1} = 0 \end{aligned} \quad (33)$$

where subscript 0 means that partial derivatives are evaluated at optimal values. Carrying out this procedure for each equation from (6) to (11) yields a system of linear first order equations in

$$V_1, \alpha_1, \theta_1, q, h_1, \eta_1$$

which are the first order perturbations in

$$V, \alpha, \theta, \dot{\theta}, h, \eta, \text{ respectively.}$$

The resulting perturbation equations are now given

$$\dot{V}_1 = -(\rho_{ref}^{S/2m}) 2V_0 C_D(\alpha_0) V_1$$

$$\begin{aligned}
 & + \alpha_1 g \cos(\theta_0 - \alpha_0) \\
 & - \alpha_1 (\rho_{\text{ref}} S/2m) V_o^2 (\partial C_D / \partial \alpha)_o \\
 & - \theta_1 g \cos(\theta_0 - \alpha_0) \\
 & + (\rho_{\text{ref}} S/2m) (V_o^2/H) C_D(\alpha_0) h_1 \\
 & + V_w \cos \mu_w (\rho_{\text{ref}} S/2m) 2V_o C_D(\alpha_0) \cos(\theta_0 - \alpha_0) \\
 & + V_w \cos \mu_w (\rho_{\text{ref}} S/2m) V_o \sin(\theta_0 - \alpha_0) \\
 & \times \{ (\partial C_D / \partial \alpha)_o - C_L(\alpha_0) - \eta_o (\partial C_L / \partial \eta) \} \\
 & - V_w \sin \mu_w (\rho_{\text{ref}} S/2m) 2V_o C_D(\alpha_0) \sin(\theta_0 - \alpha_0) \\
 & + V_w \sin \mu_w (\rho_{\text{ref}} S/2m) V_o \cos(\theta_0 - \alpha_0) \\
 & \times \{ (\partial C_D / \partial \alpha)_o - C_L(\alpha_0) - \eta_o (\partial C_L / \partial \eta) \}
 \end{aligned} \tag{34}$$

$$\begin{aligned}
 \dot{\alpha}_1 & = -(gV_1/V_o^2) \cos(\theta_0 - \alpha_0) \\
 & - V_1 (\rho_{\text{ref}} S/2m) \{ C_L(\alpha_0) + \eta_o (\partial C_L / \partial \eta) \} \\
 & - (\alpha_1/V_o) (\rho_{\text{ref}} S/2m) V_o^2 (\partial C_L / \partial \alpha)_o \\
 & + (\alpha_1/V_o) g \sin(\theta_0 - \alpha_0) \\
 & - (\theta_1 g/V_o) \sin(\theta_0 - \alpha_0) + q \\
 & + (\rho_{\text{ref}} S/2m) (V_o h_1/H) \{ C_L(\alpha_0) + \eta_o (\partial C_L / \partial \eta) \} \\
 & - (\rho_{\text{ref}} S/2m) V_o (\partial C_L / \partial \eta) \eta_1 \\
 & + 2V_w \cos \mu_w (\rho_{\text{ref}} S/2m) \cos(\theta_0 - \alpha_0) \\
 & \times \{ C_L(\alpha_0) + \eta_o (\partial C_L / \partial \eta) \} \\
 & + V_w \cos \mu_w (\rho_{\text{ref}} S/2m) \sin(\theta_0 - \alpha_0)
 \end{aligned}$$

$$\begin{aligned}
 & \times \{ (\partial C_L / \partial \alpha)_o + C_D / (\alpha_o) \} \\
 & - 2V_w \sin \mu_w (\rho_{ref} S / 2m) \sin(\theta_o - \alpha_o) \\
 & \times \{ C_L(\alpha_o) + \eta_o (\partial C_L / \partial \eta) \} \\
 & + V_w \sin \mu_w (\rho_{ref} S / 2m) \cos(\theta_o - \alpha_o) \\
 & \times \{ (\partial C_L / \partial \alpha)_o + C_D(\alpha_o) \}
 \end{aligned} \tag{35}$$

$$\dot{\theta}_1 = q \tag{36}$$

$$\begin{aligned}
 \dot{q} = & -V_1 (\rho_{ref} S b^2 / 4BV_o) (\partial C_m / \partial \dot{\alpha})_o \\
 & \times (\rho_{ref} S / 2m) V_o^2 \{ C_L(\alpha_o) + \eta_o (\partial C_L / \partial \eta) \} \\
 & - V_1 (\partial C_m / \partial \dot{\alpha})_o \\
 & \times (\rho_{ref} S b^2 / 4BV_o) g \cos(\theta_o - \alpha_o) \\
 & + \alpha_1 (\rho_{ref} S b / 2B) V_o^2 (\partial C_m / \partial \alpha)_o \\
 & - \{ (\rho_{ref} S / 2m) V_o^2 (\partial C_L / \partial \alpha)_o - g \sin(\theta_o - \alpha_o) \} \\
 & \times \alpha_1 (\rho_{ref} S b^2 / 4B) (\partial C_m / \partial \dot{\alpha})_o \\
 & - \theta_1 (\rho_{ref} S b^2 / 4B) (\partial C_m / \partial \alpha)_o \\
 & \times g \sin(\theta_o - \alpha_o) \\
 & + q (\rho_{ref} S b^2 / 4B) V_o \\
 & \times \{ (\partial C_m / \partial q)_o + (\partial C_m / \partial \dot{\alpha})_o \} \\
 & - h_1 (\rho_{ref} S b^2 / 4B) (\partial C_m / \partial \dot{\alpha})_o \\
 & \times \{ \rho_{ref} S / 2m (V_o / H) (C_L(\alpha_o) + \eta_o (\partial C_L / \partial \eta)) \} \\
 & + \eta_1 (\rho_{ref} S b / 2B) V_o^2 (\partial C_m / \partial \eta)
 \end{aligned}$$

$$\begin{aligned}
 & +V_w \cos \mu_w (\rho_{ref} S b^2 / 4 B) \\
 & x(\partial C_m / \partial \dot{\alpha})_o (\dot{V}_o / V_o) \sin(\theta_o - \alpha_o) \\
 & -V_w \cos \mu_w (\rho_{ref} S b / 2 B) V_o (\partial C_m / \partial \alpha) \sin(\theta - \alpha) \\
 & +V_w \sin \mu_w (\rho_{ref} S b^2 / 4 B) \\
 & x(\partial C_m / \partial \dot{\alpha})_o (\dot{V}_o / V_o) \cos(\theta_o - \alpha_o) \\
 & -V_w \sin \mu_w (\rho_{ref} S b / 2 B) \\
 & x V_o (\partial C_m / \partial \alpha)_o \cos(\theta_o - \alpha_o) \\
 & -(\rho_{ref} S b^2 / 4 B) (\partial C_m / \partial \dot{\alpha})_o \\
 & x \sin(\theta_o - \alpha_o) d/dt(V_w \cos \mu_w) \\
 & -(\rho_{ref} S b^2 / 4 B) (\partial C_m / \partial \dot{\alpha})_o \\
 & x \cos(\theta_o - \alpha_o) d/dt(V_w \sin \mu_w)
 \end{aligned} \tag{37}$$

$$\begin{aligned}
 \dot{h}_1 = & V_1 \sin(\theta_o - \alpha_o) - \alpha_1 V_o \cos(\theta_o - \alpha_o) \\
 & + \theta V_o \cos(\theta_o - \alpha_o)
 \end{aligned} \tag{38}$$

Equations (34) to (38) are in a form amenable to application of linear optimal control theory.

5. LINEAR OPTIMAL CONTROL THEORY

Equations (34) to (38) can be written in the standard form

$$\dot{x} = Ax + b\eta_1 + Dw \tag{39}$$

where x is a 5- component state variable vector

A is a 5x5 system matrix

b is a 5- component control vector

η_1 is increment in elevator control angle

D is a 5x5 disturbance matrix
and w is a 5- component wind vector

In standard notation, x is the state variable column vector having components x_j , where corresponding to equations (34) to (38), $j=1,2,3,4,5$, such that

$$x_1 \equiv V, x_2 \equiv \alpha, x_3 \equiv \theta, x_4 \equiv q, x_5 \equiv h,$$

Optimal control theory is thoroughly covered in many texts.^{10,11,16} In reference 10 optimal feedback control is introduced through the Hamilton-Jacobi approach which is quite general and not restricted to linear systems. Theory of linear optimal systems is treated in great detail in reference 11 while reference 16 deals with optimisation generally. Because this thesis is restricted to linear optimal control of deterministic systems it is worthwhile demonstrating how readily solutions for such linear systems follow from the standard results of the calculus of variations. This leads directly to the optimal system description with the additional adjoint variables and to the alternative Riccati matrix equation. In the absence of random disturbances the deterministic problem is treated as follows. First an integral quadratic performance index of the form

$$J(t_f, t_i) = \int_{t_i}^{t_f} (x^T Q x + \eta_1^T P \eta_1) dt + x^T(t_f) S x(t_f) \quad (40)$$

is set up where Q, P, S are symmetric weighting matrices which are arbitrarily selected but subject to the conditions that P is position definite and Q and S are non-negative definite. The object is to find the functional form of the control angle increment η_1 which minimises J. This is, in effect, to determine a control setting which minimises the variance of perturbations in the state variables, subject to the constraints,

$$\dot{\mathbf{x}} = \mathbf{Ax} + \mathbf{b}\eta_1. \quad (41)$$

By writing equation (40) in the form

$$J(t_f, t_i) = \int_{t_i}^{t_f} (\mathbf{x}^T \mathbf{Q} \mathbf{x} + \eta_1^T \mathbf{P} \eta_1 + \dot{\mathbf{x}}^T \mathbf{S} \mathbf{x} + \mathbf{x}^T \mathbf{S} \dot{\mathbf{x}}) dt + \mathbf{x}^T(t_i) \mathbf{S} \mathbf{x}(t_i) \quad (42)$$

where $\mathbf{x}(t_f)$ is a constant, the problem can now be treated by the classical calculus of variations.⁽¹²⁾ To remove the constraints imposed by equation (41), the adjoint vector of Lagrange multipliers λ is introduced and the unconstrained functional

$$G = \mathbf{x}^T \mathbf{Q} \mathbf{x} + \eta_1^T \mathbf{P} \eta_1 + \dot{\mathbf{x}}^T \mathbf{S} \mathbf{x} + \mathbf{x}^T \mathbf{S} \dot{\mathbf{x}} + \lambda^T (\mathbf{Ax} + \mathbf{b}\eta_1 - \dot{\mathbf{x}})$$

is constructed, for which the Euler-Lagrange equations,

$$d/dt (\partial G / \partial \dot{\mathbf{x}}) - \partial G / \partial \mathbf{x} = 0,$$

where

$$\mathbf{x}^T = [\mathbf{x}^T, \lambda^T, \eta_1^T],$$

$$\text{become} \quad \dot{\mathbf{x}} = \mathbf{Ax} + \mathbf{b}\eta_1 \quad (43)$$

$$\dot{\mathbf{u}} = -\mathbf{Q}\mathbf{x} - \mathbf{A}^T \boldsymbol{\mu} \quad (44)$$

$$\eta_1 = -\mathbf{P}^{-1} \mathbf{b}^T \boldsymbol{\mu} \quad (45)$$

$$\lambda = 2\boldsymbol{\mu} \quad (46)$$

and the transversality condition¹² for free $x(t_f)$ and t_f gives

$$\mu(t_f) = Sx(t_f) \quad (47)$$

Substituting for η_1 in equations (43) from (45) gives,

$$\begin{bmatrix} \dot{x} \\ \dot{\mu} \end{bmatrix} = \begin{bmatrix} A & -bP^{-1}b^T \\ -Q & -A^T \end{bmatrix} \begin{bmatrix} x \\ \mu \end{bmatrix} \quad (48)$$

These equations could be solved for μ and hence from equation (45), η_1 would be known as a function of time. This is not the form of solution required for feedback control where η_1 is needed as a function of x . Equations (48) show that μ is a linear function of x and making the substitution

$$\mu = Rx \quad (49)$$

gives the matrix Riccati equation

$$\dot{R} + RA + A^TR - RbP^{-1}b^TR + Q = 0 \quad (50)$$

with $\eta_1 = -P^{-1}b^TRx \quad (51)$

which is now the required form for η_1 . The boundary condition for R is found from equations (47) and (49) to be

$$R(t_f) = S \quad (52)$$

Equation (50) can thus be solved for $R(t)$, $t_1 \leq t \leq t_f$, by allowing time to run backwards and solving for $R(\tau)$ where $\tau = t_f - t$. This is equivalent to solving

$$-\dot{R} + RA + A^T R - RbP^{-1}b^T R + Q = 0 \quad (53)$$

to find R as a function of τ subject to

$$R_{\tau=0} = S \quad (54)$$

Having solved for R, the feedback gain matrix K is defined as

$$K^T = P^{-1}b^T R \quad (55)$$

and hence from equation (51)

$$\eta_1 = -K^T x \quad (56)$$

Equation (56) implies that the greatest reduction in the variance of the perturbed state variables occurs when all the states are fed back.

Material from the cited literature which bears directly on linear optimal control design theory has been brought together in the sections which follow but with some additional details to emphasise the design techniques used in this thesis. Such details concern the properties of the Riccati matrix, its link with Liapunov theory, its asymptotic behaviour, and the reason why all state variables are fed back in the optimal case.

5.1 Properties of Riccati Matrix R

At this stage it is worth examining the properties of the Riccati matrix R a little further. Remembering that the weighting matrices Q, P, S, were chosen to be symmetric, then taking the transpose of equations (50) and (52) shows that R^T satisfies the same equation and boundary condition as R. Thus R is a symmetric matrix and instead of n^2 unknown elements there are $(n+1)n/2$.

5.1.1 Relationship between R and Integral Performance Index

It is also found that R provides a measure for the minimised performance index. This is readily shown by writing t for t_i in equation (40) and substituting the optimal value $-P^{-1}b^T R x$ for η_1 in equations (40) and (41), giving,

$$J(t_f, t) = \int_t^{t_f} x^T (Q + R b P^{-1} b^T R) x d\tau + x^T(t_f) S x(t_f) \quad (57)$$

$$\text{and} \quad \dot{x} = (A - b P^{-1} b^T R) x \quad (58)$$

Differentiating equation (57) with respect to t , gives

$$\dot{J}(t_f, t) = -x^T(t) (Q + R b P^{-1} b^T R) x(t) \quad (59)$$

Expressing $J(t_f, t)$ in the quadratic form

$$J(t_f, t) = x^T(t) C(t) x(t), \quad (60)$$

substituting into equation (59), and eliminating x through equation (58), yields

$$\dot{C} + CA + A^T C - R b P^{-1} b^T C + (R - C) b P^{-1} b^T R + Q = 0 \quad (61)$$

where the boundary condition

$$C(t_f) = S$$

follows from equations (57) and (60). Comparison of equations (61) and

(50) shows that

$$C = R$$

is a solution of equation (61) and hence from equation (60)

$$x^T(t) R(t) x(t) = J(t_f, t) \quad (62)$$

and thus R provides a measure for the minimised performance index.

5.1.2 Link between R and Liapunov Stability

The Riccati matrix R may also be used to check the stability of the optimised system through Liapunov's second method.⁽¹⁰⁾ The scalar function $J(t_f, t)$ can be regarded as a Liapunov function which assures stability for $J(t_f, t)$ positive definite and $\dot{J}(t_f, t)$ negative definite. When Q, P, and S are positive definite then $J(t_f, t)$ must be positive definite and from equation (59), the additional requirement that $(Q + RbP^{-1}b^TR)$ be positive definite assures that $\dot{J}(t_f, t)$ is negative definite.

5.1.3 Asymptotic behaviour of R

The asymptotic behaviour of R as $t_f \rightarrow \infty$ will now be examined. Substituting equation (56) into equations (40) and (41) gives

$$J(t_f, t_i) = \int_{t_i}^{t_f} x^T(Q + KPK^T)x dt + x^T(t_f)Sx(t_f) \quad (63)$$

$$\text{and} \quad \dot{x} = (A - bK^T)x \quad (64)$$

Thus if equation (64) represents a stable system, $x(t_f) \rightarrow 0$ as $t_f \rightarrow \infty$ and hence

$$J(t_f, t_i) \rightarrow \text{Constant as } t_f \rightarrow \infty.$$

Comparing this result with equation (62) shows that

$$R \rightarrow \text{constant as } t_f \rightarrow \infty$$

and hence $\dot{R} \rightarrow 0$.

This result shows that if equation (53) is used to solve for R in the case of the time-invariant, infinite upper limit, optimal system, and R approaches a finite limit for large t then the system must be stable. In this case equation (55) shows that the optimal feedback gain vector K is constant.

5.1.4 Time invariant, infinite upper limit performance integral

Another property of the Riccati matrix as determined from equation (50) is that it is independent of the values of the state variables and hence, from equation (55), so are values of the optimal feedback gains, K . This appears to be a consequence of the requirement that all state variables be fed back. A closer look at this situation can be had by rewriting equation (62) for the time-invariant system with infinite upper limit performance integral to give

$$\dot{x}^T(t)R x(t) = J(\infty, t) \quad (65)$$

In this case, where the feedback gain vector K is constant, the partial derivatives of $J(\infty, t)$ with respect to each component of K must be zero for a minimum value of performance index. This means that the partial derivatives of R on the left hand side of equation (65) with respect to the K components must all be zero if the minimum is to be independent of x , which evidently it is. Presumably then, if not all of the state

variables are fed back or if not all the feedback gains are regarded as free parameters, not all the partial derivatives of the elements of R can simultaneously be zero. Hence any sub optimal system based on incomplete state variable feedback must consider initial values of the state variables. This result is important because in many practical situations it is not feasible to feed back all the state variables and there is then a need to examine sub optimal systems. This problem will be discussed further in section 7.

5.1.5 Alternative to Riccati Matrix Solution

As an alternative to the Riccati matrix equation solution for the time-invariant infinite upper time limit optimal system, there is equation (48). This equation together with equation (64) provides some links between the eigenvalues of the closed loop system matrix and the elements of the weighting matrices P , Q , and the optimal feedback gain components of K . Equation (48) represents a system of order $2n$ but it is found from symmetry that the characteristic polynomial has only $n+1$ even powered terms. The characteristic equation in terms of the scalar parameter λ for this system is given by the determinantal equation

$$\begin{vmatrix} \lambda I_n - A & bP^{-1}b^T \\ Q & \lambda I_n + A^T \end{vmatrix} = 0 \quad (66)$$

where I_n denotes the unit matrix of order n . By virtue of the symmetry of Q and $bP^{-1}b^T$, the left hand side of equation (66) is found to be an even function of λ . This fact is readily established by substituting $-\lambda$ for λ in the determinant and interchanging rows and columns. Thus the characteristic polynomial of this optimal system is a polynomial in λ^2 of order n , and the eigenvalues occur in pairs, consisting of one positive and one negative value. For x to vanish as time becomes large

the eigenvalues with negative real parts are assigned to x and those with positive real parts to μ . The characteristic polynomial corresponding to the x eigenvalues is, from equation (64), the expansion of the determinant

$$\left| \lambda I_n - A + bK^T \right| ,$$

and is found to have coefficients which are linear in the components of K . This polynomial can also be constituted from the roots of equation (66) with the negative real parts. Equating corresponding coefficients in the two polynomials leads to a linear set of algebraic equations for determining values of the components of the optimal gain vector K . When direct algebraic factorisation of the characteristic polynomial of equation (66) into x and μ eigenvalue components is possible, direct algebraic relationships between the matrix elements of A, P, Q , and optimal gain components can be obtained. Having discovered that the coefficients of the characteristic polynomial in equation (64) are linear functions of the feedback gain components it is evident that if all the state variables are fed back there are sufficient free parameters to place the system poles in any desired positions.

5.1.6 Selection of Weighting Matrices

There now remains the question of how to choose the weighting matrices P, Q , and S . The ideal control system would immediately eliminate disturbances as they occurred but in doing so would require unlimited control power. To be realistic, finite errors due to disturbances must be allowed, so that control power demanded can be limited. The design aim then is to weight errors in the state variables as heavily as possible while constraining control power to a practical limit and at the same time ensuring that the assumed linear laws are not violated and the linearised theory rendered invalid. Dealing first with the

weighting matrix S , which because it penalises terminal errors, is used in designing missile terminal control systems and often leads to demands for rapid changes in feedback gains when homing in on a target. The weighting matrix Q is used to design systems which regulate perturbations in state variables throughout the whole trajectory. It is this sort of regulation which is sought in mid-course control of the gliding projectile with consequent relatively small changes in feedback gain. Thus in the mid-course control system design of this gliding projectile, S will be taken as zero. A very convenient way of dealing with Q is to try, by physical arguments, to find fixed ratios between its elements, and then to take some scalar multiple of Q as a variable parameter. Thus performance can be assessed against the variation of this one parameter. Unfortunately the method cannot be applied to this projectile because there are absolute limitations on angle of attack α and elevator control η . A feature of a high aspect ratio aircraft-like wing is that the variation in lift coefficient with angle of attack may be reliably regarded as linear up to the stall, but when stall does occur, the loss in lift is dramatically sudden. Thus perturbations in angle of attack α_1 must be constrained to lie between the steady value α_0 and the stall value. If large perturbations in α_1 are unavoidable it may be necessary to reduce α_0 and accept the accompanying reduction in range in return for improved accuracy. In similar fashion, η_1 is constrained to lie between η_0 and elevator deflection stall angle. With only one control variable, P is a scalar, and Q will have elements q_{ij} . On physical grounds, reasonable first guesses for P and Q are found by choosing acceptable maximum values for each state variable perturbation x_{im} , and elevator angle perturbation η_{1m} and putting $q_{ij} = 1/(x_{im}x_{jm})$, $P = 1/\eta_{1m}^2$. Using these values, the system equations can be solved and the maximum values of the critical state and control variables determined. Determination of weights can then proceed by an iterative procedure which increases state variable weights when full allowable

elevator deflection is not realised and vice versa.

6. CONTROL SYSTEM DESIGN

Using the physical properties of the gliding projectile given in Appendix I, values of the state variables V , α , θ , q , h , X , were computed for maximum range in undisturbed flight starting from an initial altitude of 4 km. This was accomplished by integrating equations (6) to (11) using the Differential Analysis R. Eplacement (DARE)⁽¹⁴⁾ simulation language on the University of Adelaide's CDC 6400 computer and later repeated with use of the Continuous System Modelling Program (CSMP) on the DRCS IBM 370 machine. The set of variables which maximise the range in undisturbed flight are distinguished by the subscript 0 while subscript i denotes initial condition. Initial values of V_0 and θ_0 are found from equations (27) and (29) while α_0 and η_0 are obtained from equations (31) and (32). For the undisturbed maximum range trajectory, equations (31) and (32) give

$$\alpha_0 = 0.17037 \text{ rad}$$

$$\eta_0 = -0.55370 \text{ rad}$$

and for $h_{oi} = 4000 \text{ m}$, equations (27) and (29) give

$$V_{oi} = 172.4 \text{ m s}^{-1}$$

$$\theta_{oi} = 0.05373 \text{ rad}$$

In addition, putting

$$q_{oi} = 0,$$

$$X_{oi} = 0$$

allows equations (6) to (11) to be integrated to obtain the 0 subscripted undisturbed maximum range state variables corresponding to the constant elevator setting η_0 . These results are plotted in figures 5 to 8, and for

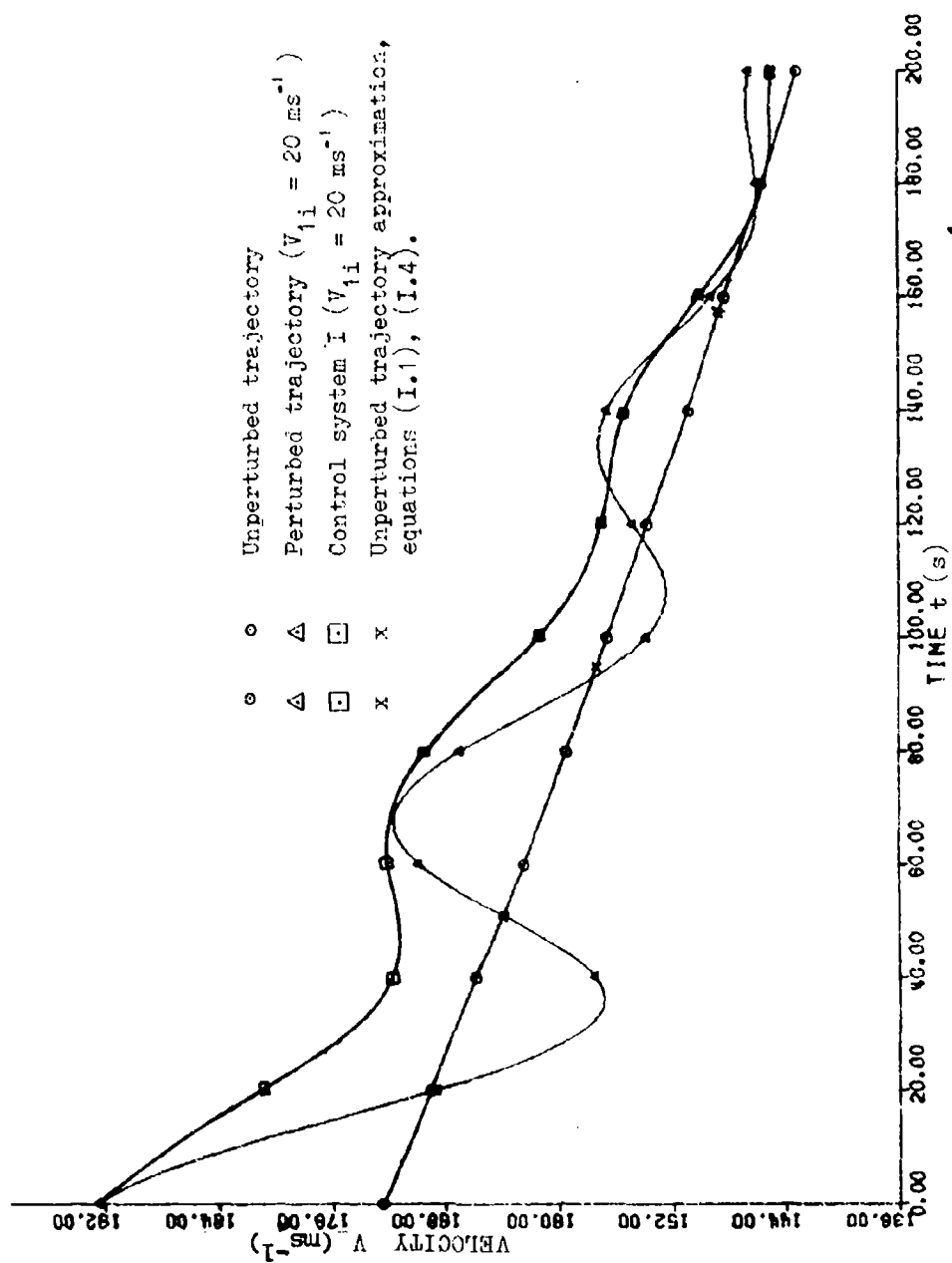


Figure 5. Velocity response to initial velocity perturbation 20 ms^{-1} for projectile with no control and control system I.

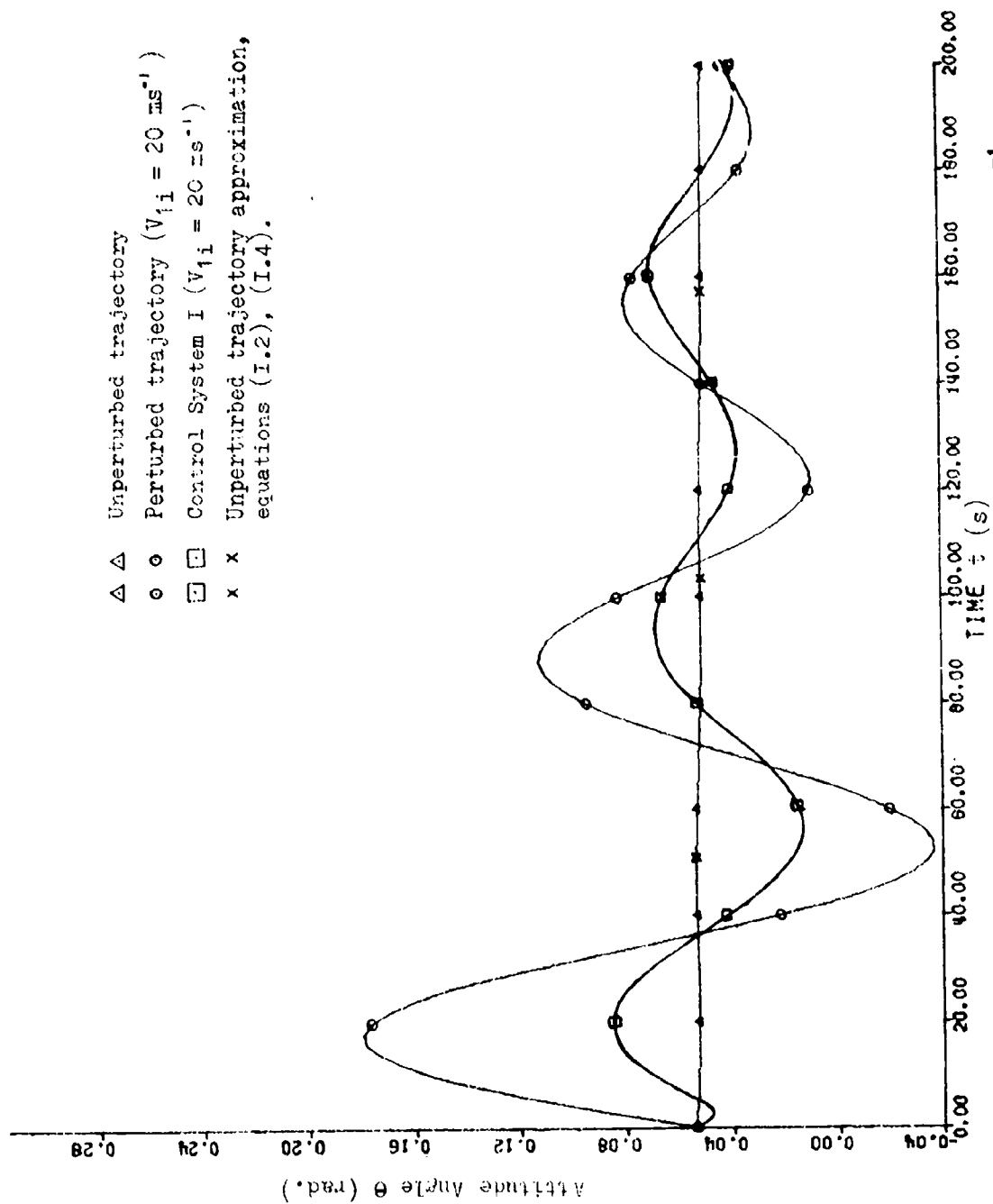


Figure 6. Attitude response to initial velocity perturbation 20 ms^{-1} for projectile with no control and control system I

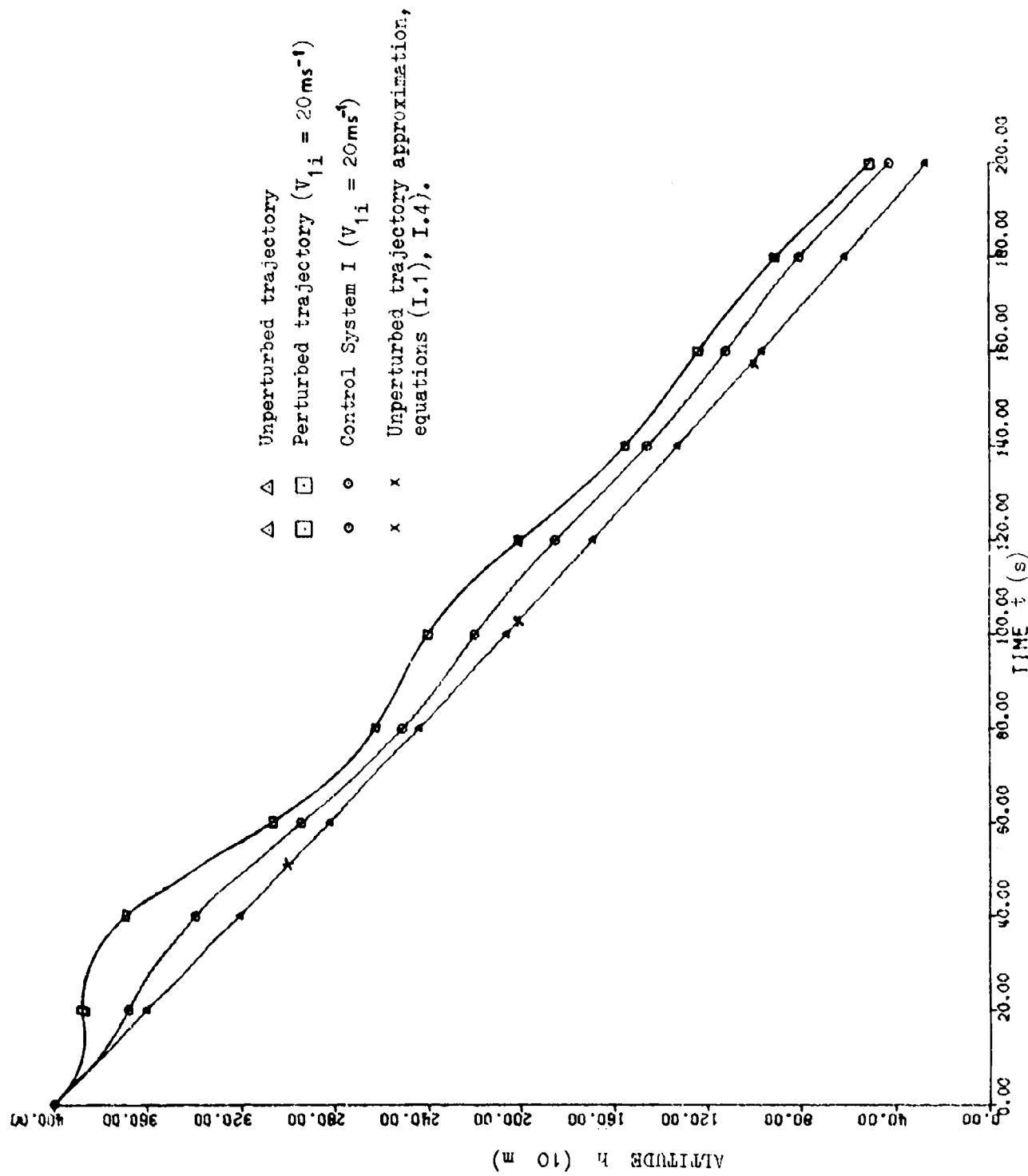


Figure 7. Altitude response to initial velocity perturbation 20 ms^{-1} for projectile with no control and control system I.

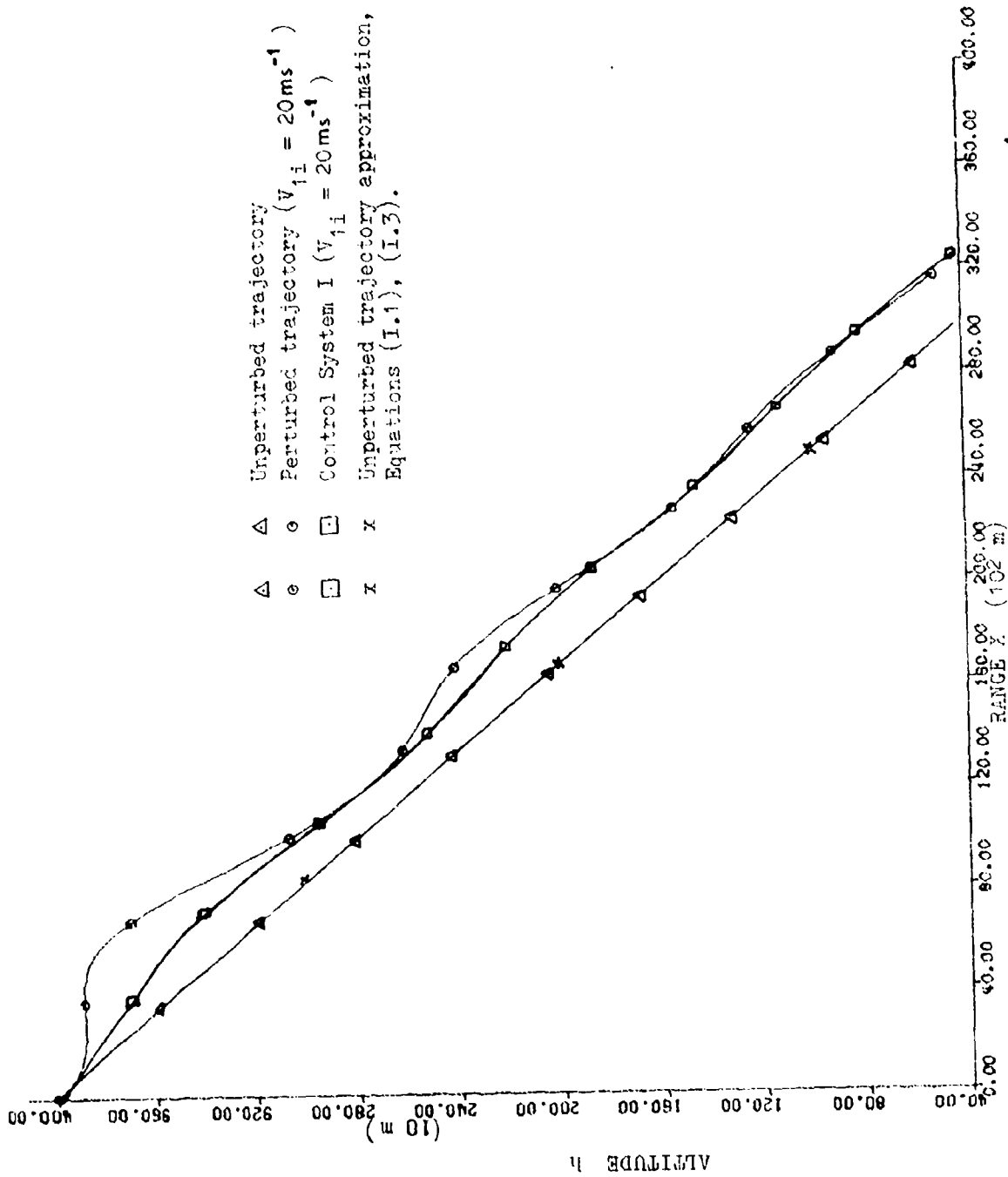


Figure 8. Positional response to initial velocity perturbation. 20 ms^{-1} for projectile with no control and control system I.

comparison, some spot values calculated from the approximations given by equations (26), (27), (29), (30), are superimposed and show close agreement. The 0 subscripted variables are the command values of the state variables that the control system must endeavor to achieve during disturbed flight. Such command values would need to be stored on-board in microprocessor memory and be made available for use by the control system. The accurate generation of command values from the simple relationships given by equations (26), (27), (29), (30) presents the possibility of designing a control system which can adapt to large errors in initial values of state variables through an on-board mini-computer together with memory. However, this paper is confined purely to feedback control with a preset store of command values. The state variable feedback scheme being considered is shown in figure 9, where the feedback gains K_V to K_h are determined by assigning weights to the five state variable and control variable perturbations appearing in the matrices Q and P of the integral performance index of equation (40). Before embarking on a design procedure it is necessary to check whether the desired linearised system needed is both controllable and observable. When some states are decoupled from the input, the system is not controllable and when there is decoupling between some of the states and the output, the system is not observable. Tests for controllability and observability are provided by the neat results of Kalman⁽¹⁵⁾. The result for the system given by equation (41) is that for controllability, the matrix whose n th column is given by $A^{n-1}b$ should be non-singular, where n is the order of the square matrix A . The controllability matrices for the values of A and b given in Appendix I were found to be non-singular.

6.1 Choice of Performance Index Weights and Determination of Feedback

The weighting of the state variables perturbations in the integral of the performance index will be chosen to be of the form

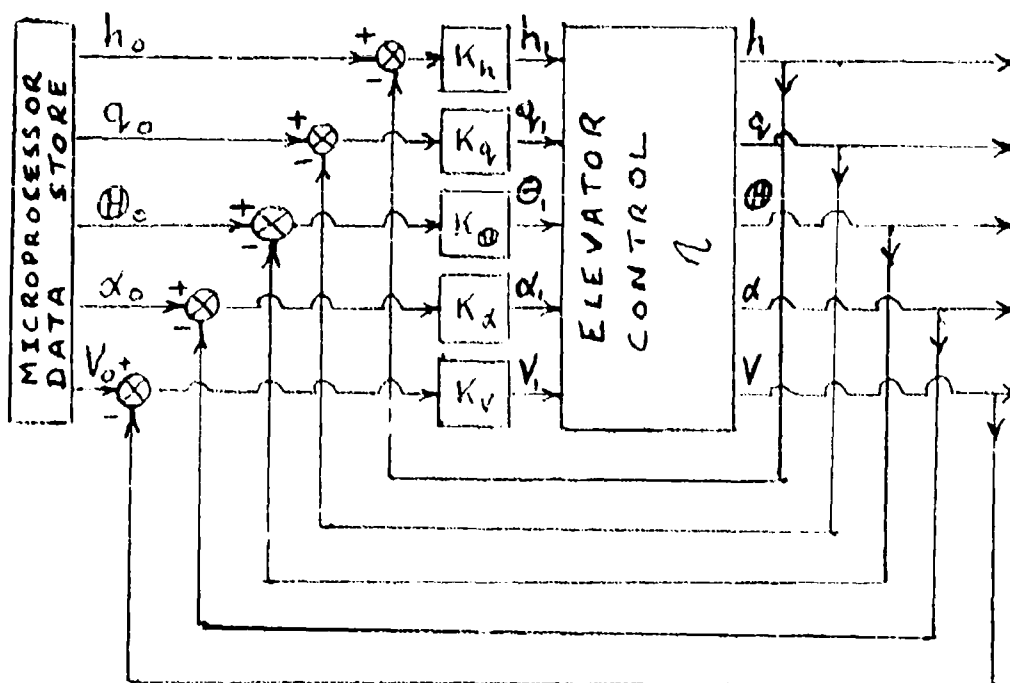


Figure 9. State Variable feedback scheme.

$$x^T Q x = \sum_{j=1}^n (x_j / x_{1w})^2$$

and the control weighting to be $(\eta_1 / \eta_{1w})^2$

Thus values of x_j , η_1 which exceed x_{1w} , η_{1w} will be heavily penalised. It will be assumed that initial errors of 20 m s^{-1} in velocity and 100 m in altitude may be encountered. As a first guess then, put

$$v_{1w} = 20 \text{ m s}^{-1}, h_{1w} = 100 \text{ m}$$

There seems to be no reason to limit the angular pitching rate q , hence this term will be omitted from the performance index. The question of maximum allowable angle of attack will now be considered. Maximum wing lift is dependent on Mach number, aspect ratio, and wing cross-section. Design handbooks such as references 7, 8 give values of maximum lift coefficient C_{LMAX} , for various Mach numbers and aspect ratios. For a wing of aspect ratio 7 at a Mach number of 0.5, which corresponds roughly to $v_{oi} = 172.4 \text{ m s}^{-1}$ at altitude $h_{oi} = 4 \text{ km}$, a C_{LMAX} of about 1.4, based on wing area, should be achievable. The maximum range flight at angle of attack $\alpha_0 = 0.17037$ radian requires C_L to be 1.16. This leaves a margin of about 0.035 radian or 2 degrees for control purposes. The constant elevator angle deflection for maximum range flight is -0.5537 radian so that if a maximum deflection of about 0.7 radian or 40 degrees is permitted a reasonable choice for η_{1w} is 0.1 radian. An initial guess for an attitude angle weight, θ_{1w} , can be obtained by considering the flight paths of figure 2. For 100 m error in altitude at the end of midcourse flight the corresponding mean flight path error is about $1/4$ degree and the change in line of sight angle to target is about 1 degree. Allowing 4 degrees of total seeker beam angle to accommodate final midcourse altitude errors requires a mean midcourse flight path error of $1/2$ degree. Thus as a first guess, θ_{1w} will be taken to be $1/2$ degree. Summarising, the weights on the

state and control variable perturbations were first taken to be

$$\begin{aligned}v_{1w} &= 20 \text{ m s}^{-1} \\ \alpha_{1w} &= 0.035 \text{ radian} \\ \theta_{1w} &= 0.0087 \text{ radian} \\ h_{1w} &= 100 \text{ m} \\ \eta_{1w} &= 0.1 \text{ radian.}\end{aligned}$$

The weighting matrices Q and P appearing in equations (40) and (53) are thus taken as

$$Q = \begin{bmatrix} 1/V_{1w}^2 & 0 & 0 & 0 & 0 \\ 0 & 1/\alpha_{1w}^2 & 0 & 0 & 0 \\ 0 & 0 & 1/\theta_{1w}^2 & 0 & 0 \\ 0 & 0 & 0 & 0 & 0 \\ 0 & 0 & 0 & 0 & 1/h_{1w}^2 \end{bmatrix} \quad (67)$$

and $P = 1/\eta_{1w}^2$.

The control system resulting from this choice of Q and P will be referred to as System 1. Substituting these values for Q and P into the Riccati matrix equation (55), together with values of A and b obtained from equations (34) to (38), allowed K to be determined and hence the optimal feedback gain vector K from equation (55). Because the Riccati matrix in this case is of order 5×5 and is symmetrical there are fifteen unknown elements r_{ij} to be solved for from the set of simultaneous equations

$$\begin{aligned}r_{ij} &= -\sum_{k=1}^5 r_{ij} a_{kj} + \sum_{k=1}^5 r_{kj} a_{ki} + q_{ij} \\ &\quad - \frac{1}{2} b_{1j}^2 r_{1j} + \frac{1}{2} b_{2j}^2 (r_{12} r_{4j} + r_{14} r_{2j}) + \frac{1}{4} b_{1j}^2 r_{14} r_{4j} \end{aligned} \quad (68)$$

where for $j=1, i = 1, 2, 3, 4, 5$

$$j=2, i = 3,4,5,6,$$

$$j=3, i = 3,4,5,$$

$$j=4, i = 4,5$$

$$j=5, i = 5.$$

and the q_{ij} are elements of Q . Solutions for the r_{ij} were computed from equations (68) using both the DARE and CSMP integration routines. Components of the time varying optimal gain vector K were then found from equation (55) and equation (56) gave the elevator deflection angle increment η_1 , which when added to η_0 , gives the value for η to be substituted into the trajectory equations (6) to (11). These equations were integrated for an initial velocity 20 m s^{-1} greater than the initial optimal value of $V_{oi} = 172.4 \text{ m s}^{-1}$. The resulting trajectories for V , θ , h , are shown in figures 5 to 8 where the optimal and no-feedback control trajectories are shown for comparison. These figures clearly reveal the low-damped oscillatory phugoid motion. From figures 7 and 8, the optimal flight path has an altitude of 1 km when the ground range is 25 km and the time taken for the projectile to reach this position is 158 s. The very marked effect that velocity perturbations have on attitude is indicated by figure 6, which shows that the initial velocity perturbation of 20 m s^{-1} induces an attitude oscillation of about 7 degrees amplitude initially in uncontrolled flight, decaying to 1.7 degrees at $t = 158 \text{ s}$. In controlled flight the maximum amplitude is 2.4 degrees, decaying to 0.7 degree. Figure 7 shows how the controlled flight improves the altitude variation with time in that the rate of descent is closer to the optimum than the uncontrolled flight. However, it is the positional accuracy which is important, and figure 8 reveals that the controlled flight shows no improvement over uncontrolled flight at a ground range of 25 km. The altitude error at 25 km ground range is about 300 m which would require a seeker beam angle of 6 degrees to accommodate, and to which must be added another 1.4 degrees for the attitude error. At this point, the question to

be investigated is whether this seeker beam angle requirement of 7.4 degrees to accommodate an initial velocity perturbation of 20 m s^{-1} can be reduced by improving the feedback control.

To this end, further changes in weighting values were made. Values of α_{1w} and η_{1w} were left unchanged because, in the trajectories just described, values of maximum angle of attack and elevator control deflection were considered to be marginally acceptable. The procedure was then to diminish the weights V_{1w} , θ_{1w} , h_{1w} , by a factor of two successively and to calculate trajectories for various combinations of these diminished weights and to note changes from optimal terminal conditions at $t = 158 \text{ s}$ in response to an initial velocity perturbation of 20 m s^{-1} . Because a check had shown that there was not a significant difference between trajectories calculated with time-varying optimal feedback gains and those calculated for constant feedback gains based on values of Riccati elements corresponding to $t=158 \text{ s}$ such constant gains were used in the trajectory selection procedure to reduce excessive computation. To assist in the selection process it is possible to compute and compare values of the performance index given by equation (40), for the various feedback gain vectors. This is achieved by solving equation (68) for the r_{ij} with the η_{1w}^2 term omitted and by substituting $a_{ij} - b_i K_j$ for a_{ij} and $q_{ij} + K_i K_j / \eta_{1w}^2$ for q_{ij} . The underlying philosophy behind this approach is that a tightening of the control over each state will bring each state close to the required optimal value at corresponding times and this should then also lead to acceptable position accuracy. However, attempts to exercise tight control over attitude and velocity simultaneously, revealed some adverse interaction and a closer examination of the physical reasons was demanded. This adverse interaction stems from trying to regulate velocity through elevator controls without significantly changing the projectile's attitude or flight path direction. To regulate a velocity in excess of the desired value, the elevators would be deflected so as to increase the angle of attack and hence increase the

induced drag. Thus, during a phugoid velocity cycle, the higher velocity part would be flown at higher than optimum angle of attack and the lower velocity part at lower angle of attack. In this way the mean drag force is increased, as is required, but so also is the mean lift force and it can be shown that the undamped amplitude of the phugoid flight path oscillation is approximately proportional to the square root of the lift coefficient C_L . This result is readily derived by solving the open loop part of the reduced system equations (II.35) for z_2 with $z_2=0$ and $z_1=v_{1i}$ at zero initial time. In this notation, z_1 is velocity perturbation V_1 and z_2 is the flight perturbation angle ψ_1 . It is found that the undamped amplitude of ψ_1 for the above initial conditions is proportional to $-a_{21}/\omega_{lp}$. From equation (35),

$$a_{21} \cong -(\rho ref S / 2m) C_L(\alpha_0) - (g/V_0^2) \cos(\theta_0 - \alpha_0) \quad (69)$$

when the contribution of elevator lift is ignored. Under optimal conditions, lift is approximately equal to weight and hence the magnitude of the two terms in equation (69) are roughly equal so that

$$a_{21} \cong -2(\rho ref S / 2m) C_L(\alpha_0).$$

Equation (II.32) shows that ω_{lp} is proportional to $(C_L(\alpha_0))^{1/2}$ and thus

$$-a_{21}/\omega_{lp} \text{ is approximately proportional to } (C_L(\alpha_0))^{1/2}.$$

Hence attempts to control velocity in this way tend to accentuate the phugoid oscillation initially by increasing the frequency and undamped amplitude of the flight path angle although damping is increased. This initial effect tends to increase the velocity direction error and although the velocity magnitude error may be reduced, a flight path positional error is still maintained.

Now consider what happens when the elevators act in the opposite manner so

that they reduce angle of attack in response to an increase in velocity. The tendency then is to reduce the phugoid frequency and undamped amplitude and although the velocity magnitude is not so well regulated, the flight path positional accuracy tends to improve. However, if this form of control is overdone in such a way that angle of attack is reduced too much in response to increased velocity, an instability will be reached when the glider will begin to nose dive at ever increasing velocity.

This interaction between velocity and attitude control of a glider highlights the difference between flight path control of a powered aircraft and a glider. On the powered aircraft, velocity regulation would be sought through feedback to engine throttle as well as to elevator controls.

Returning now to the search for more accurate trajectories by diminishing V_{1w} , θ_{1w} , h_{1w} , it was found, in accordance with the above considerations, that positional accuracy was not improved by reducing V_{1w} , but that improvement was gained by reducing θ_{1w} from 1/2 degree to 1/4 degree and h_{1w} from 100 m to 12.5 m. For the set of weights

$$V_{1w} = 20 \text{ m s}^{-1}$$

$$\alpha_{1w} = 0.035 \text{ radian}$$

$$\theta_{1w} = 0.00436 \text{ radian}$$

$$h_{1w} = 12.5 \text{ m}$$

$$\eta_{1w} = 0.1 \text{ radian}$$

equations (68) and (55) were again used to obtain an optimal time varying gain vector K . The components of K are plotted in figure 10. This figure shows the gain components to be virtually constant over most of the flight time and consequently trajectories were computed for these gains and for gains held constant at their initial values. These trajectories were sufficiently close to each other to indicate that constant feed back gains based on a constant initial-valued plant matrix A and control vector b were adequate for design purposes. This is a useful attribute of the optimal

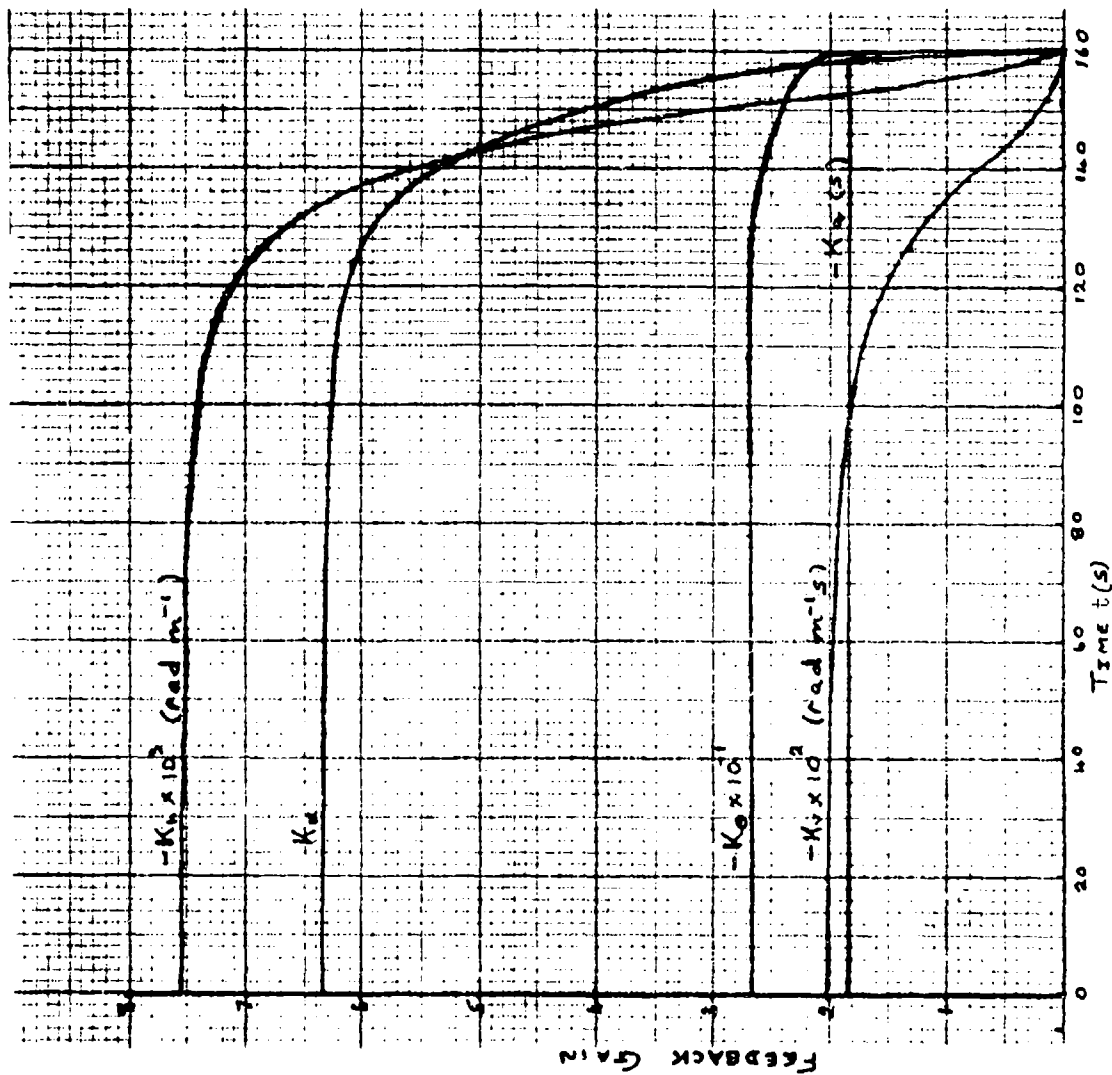


Figure 10. Optimal state feedback gains for control system II.

control approach in that it does indicate when a time-invariant system representation is a reasonable approximation for the determination of state feedback gain and thus when the extra complication of time varying gains can be dispensed with.

The values of feedback gains used in the constant gain trajectory computations are:-

$$K_V = -2.034 \times 10^{-2} \text{ radian m}^{-1} \text{ s}$$

$$K_\alpha = 6.335$$

$$K_\theta = -26.469$$

$$K_q = -1.867 \text{ s}$$

$$K_h = -7.566 \times 10^{-3} \text{ radian m}^{-1}$$

The control system using these values of feedback gain will be referred to as System II. Trajectories computed for this set of gains are shown in figures 11 to 16 for an initial velocity perturbation of 20 m s^{-1} . From figure 14 the altitude error at 25 km ground range is 200 m and from figure 12 the attitude error at $t = 158 \text{ s}$ is 0.45 degree. Thus the seeker beam angle needed to accommodate this error is 4.9 degree or 0.245 degree per m s^{-1} of initial velocity error. In figure 12 the oscillation in θ_0 is due to the magnified scale showing up round off error in the value used for V_{oi} and stresses the sensitivity of attitude angle to velocity perturbations. Figure 13 shows that the controlled rate of descent is indistinguishable from the optimal value, and the altitude error shown in figure 14 arises from the positive velocity increment shown in figure 11. In achieving this amount of control, figure 15 indicates a maximum angle of attack variation from optimum of 0.0322 radian or 1.84 degree and from figure 16 the maximum elevator deflection angle is 0.515 radian. Hence, in responding to an initial velocity error of 20 m s^{-1} the angle of attack is contained to within 2 degrees of the optimum value, as required, and the elevator deflection angle remains less than 0.7 radian. Another trajectory which

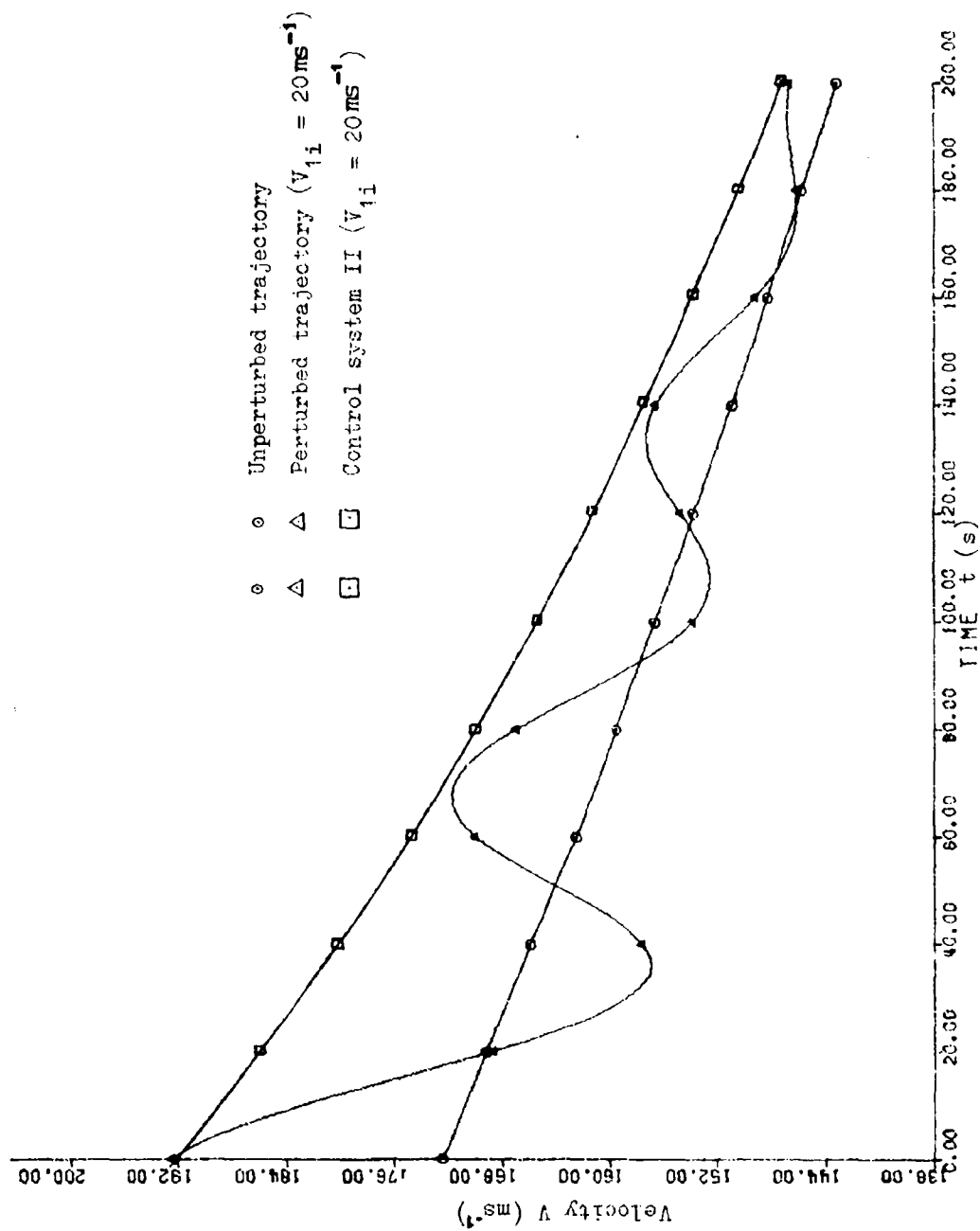


Figure 11. Velocity response to initial velocity perturbation 20 ms^{-1} for projectile with no control and control system II.

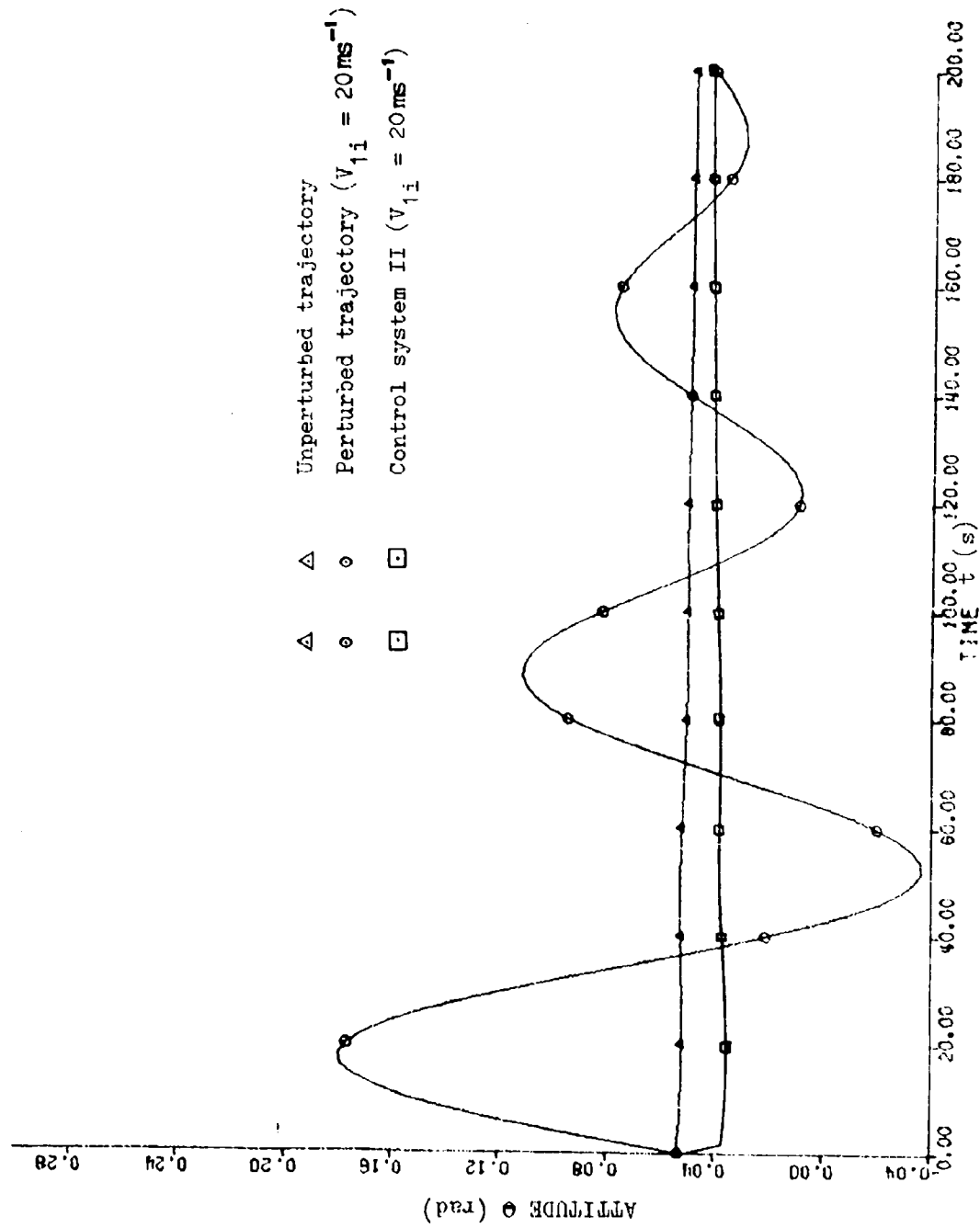


Figure 12. Attitude response to initial velocity perturbation 20 ms^{-1} for projectile with no control and control system II.

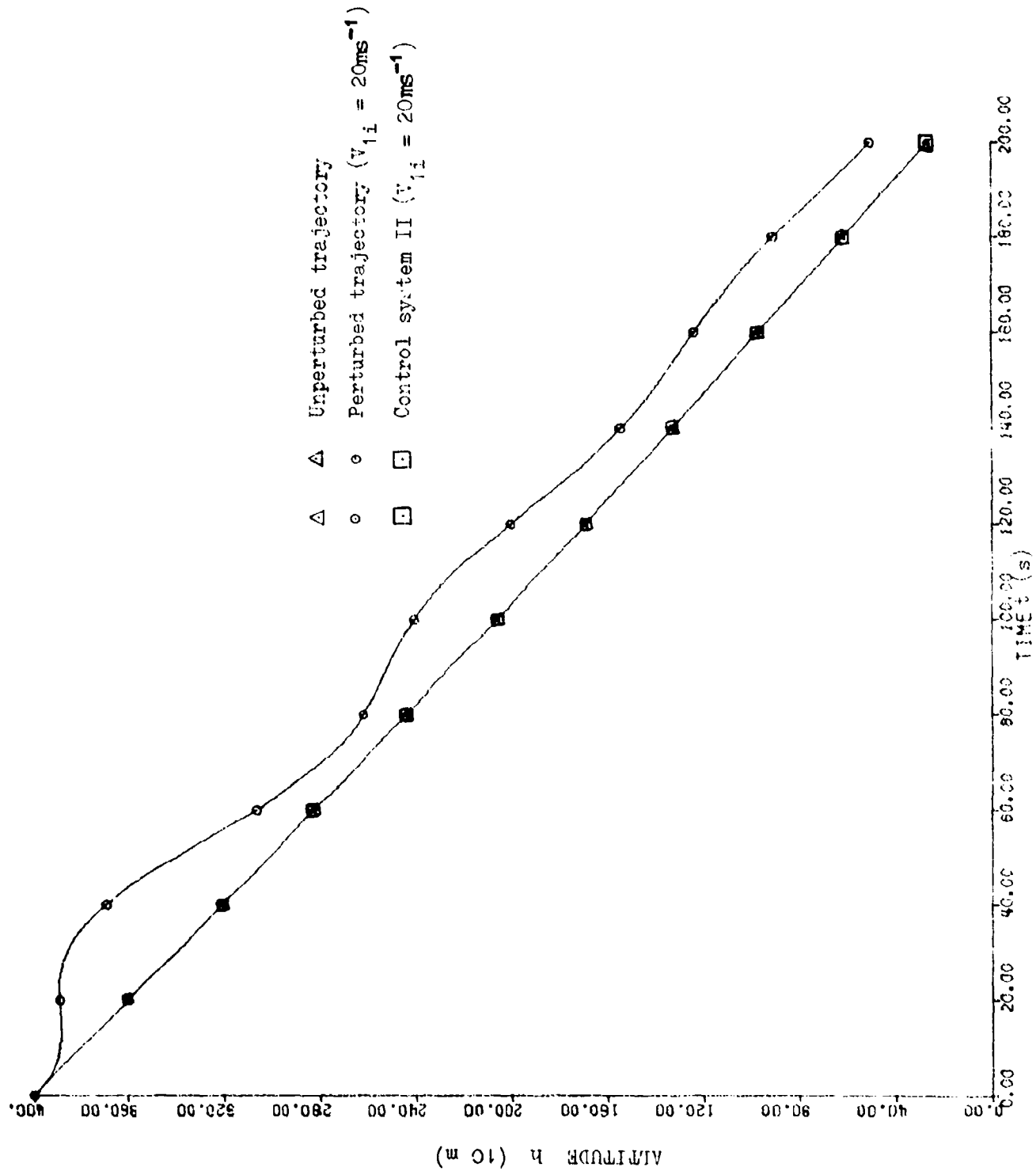


Figure 13. Altitude response to initial velocity perturbation 20 ms^{-1} for projectile with no control and control system II.

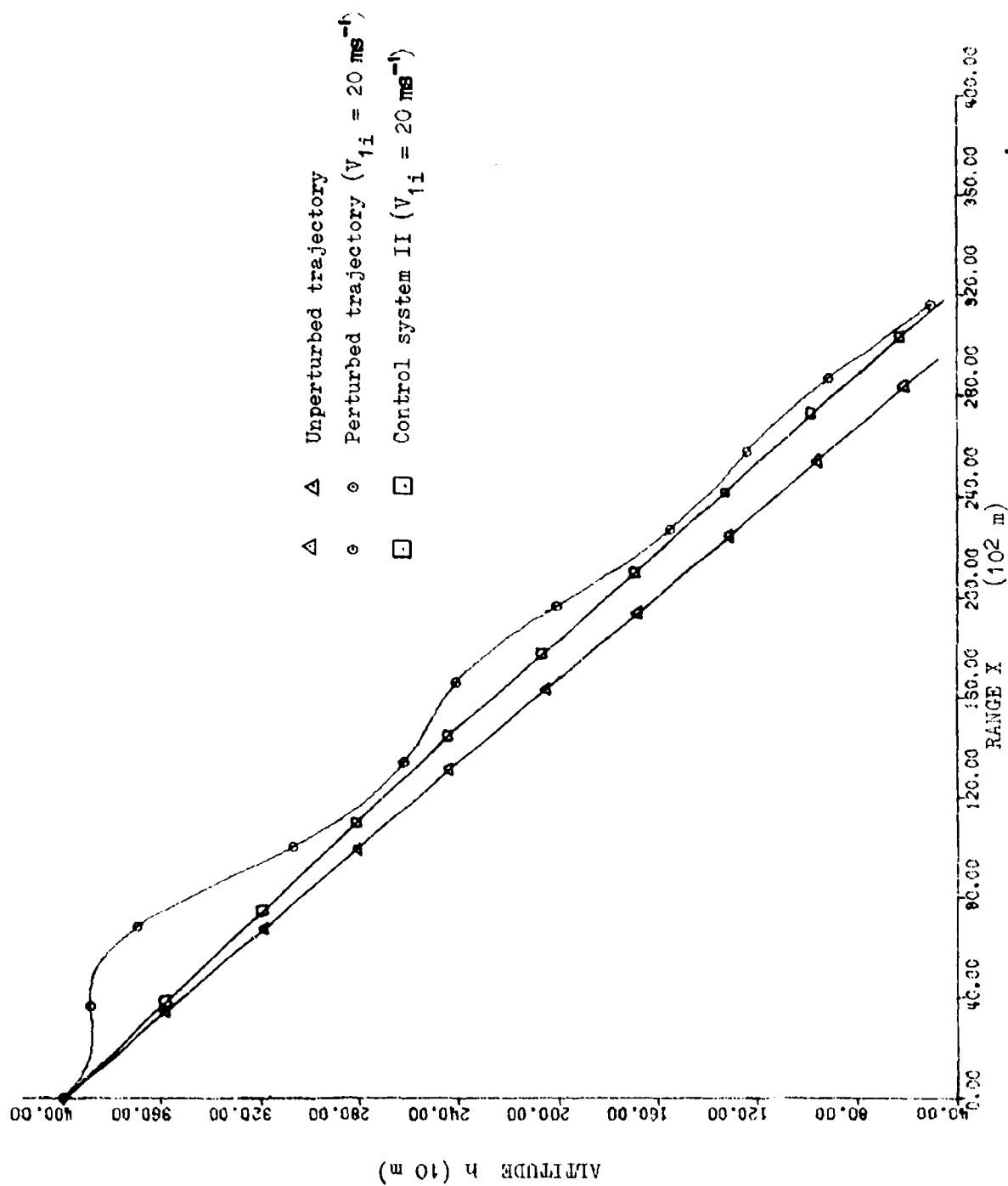


Figure 14. Positional response to initial velocity perturbation 20 ms^{-1} for projectile with no control and control system II.

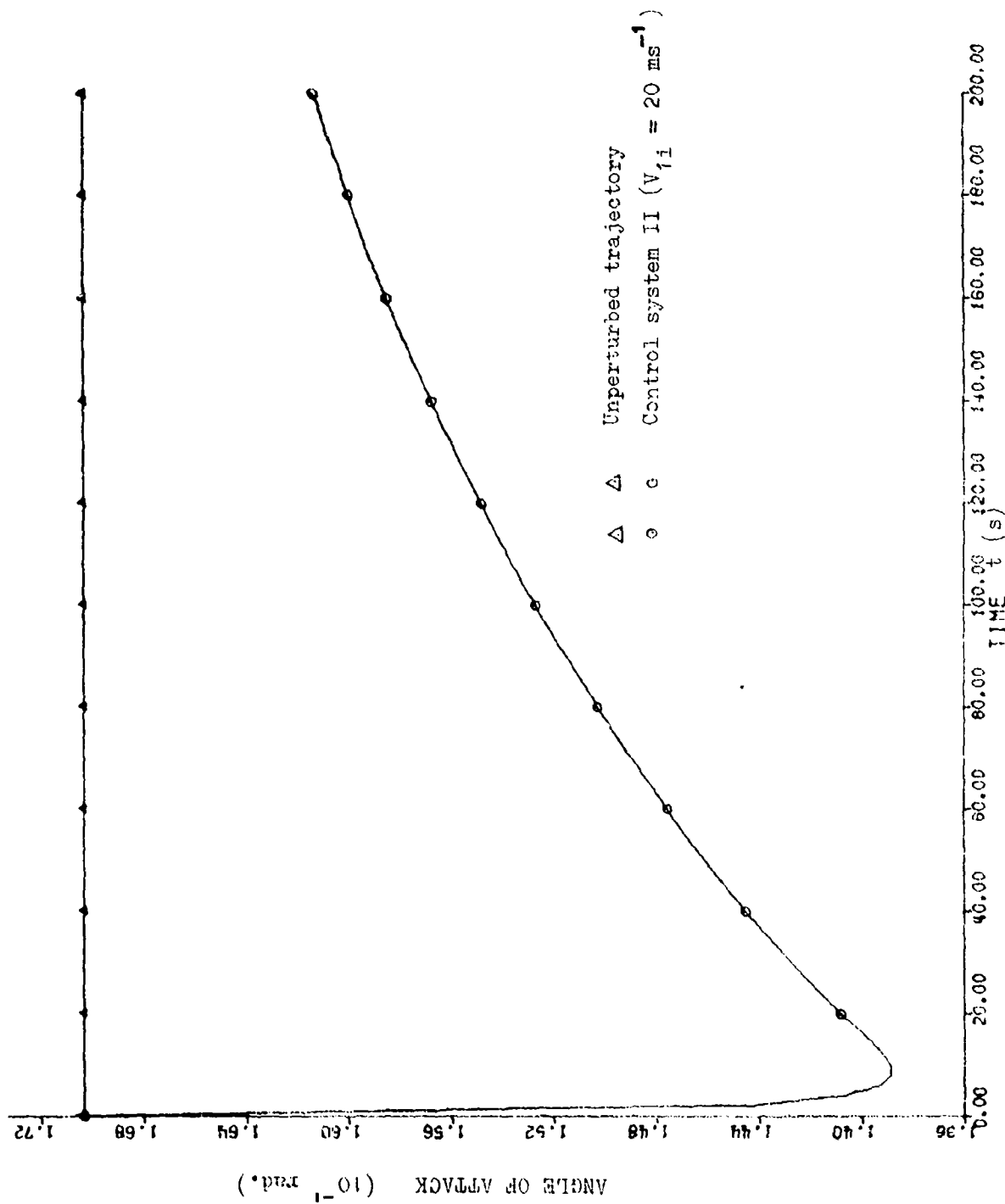


Figure 15. Angle of attack response to initial velocity perturbation 20 ms^{-1} for projectile with control system II.

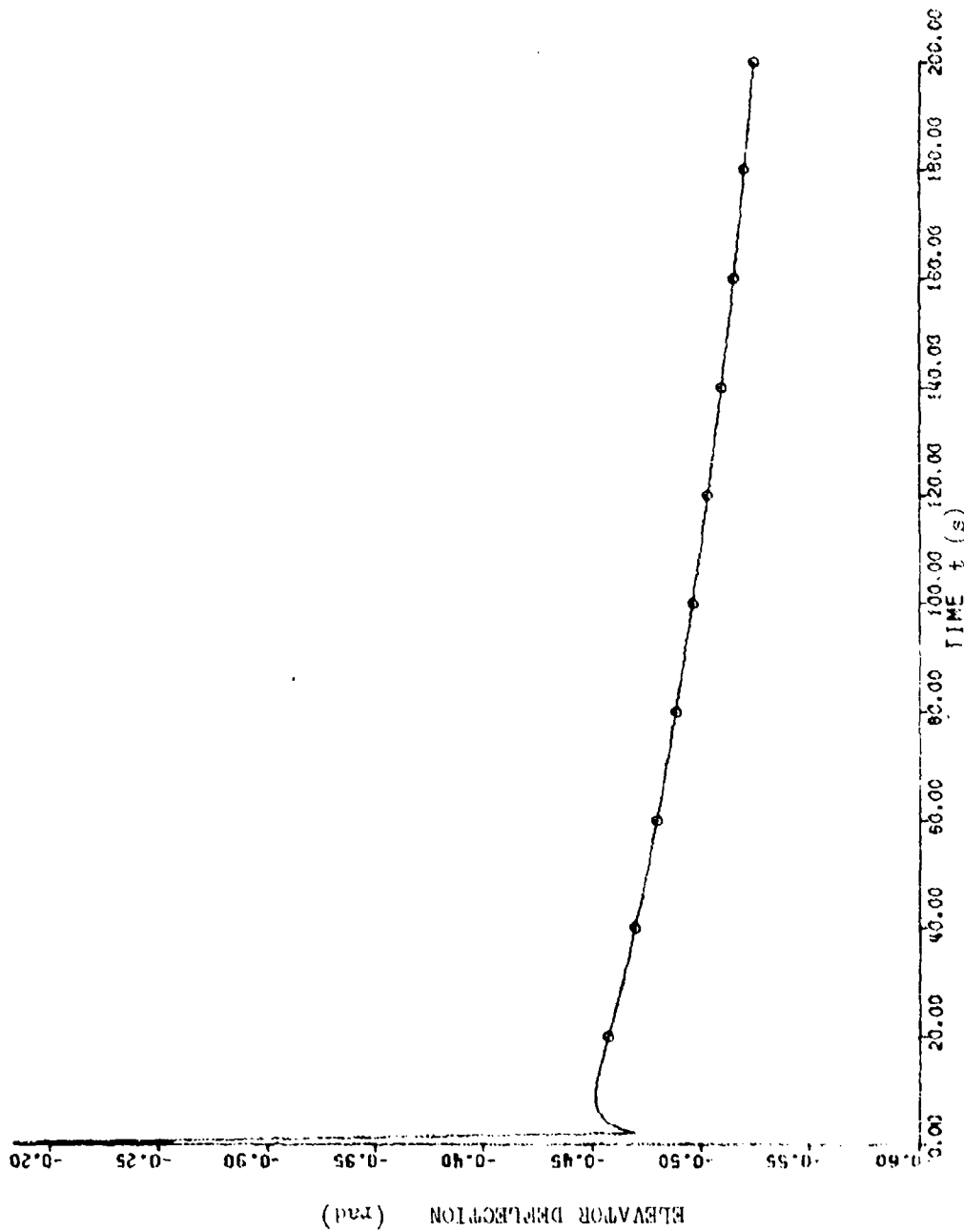


Figure 16. Elevator angle response to initial velocity perturbation 20 ms⁻¹ for projectile with control system II.

was computed for an initial altitude error of 100 m showed that this error had been halved by the end of midcourse flight.

To demonstrate the stability of this control system to in-flight disturbances, a series of random wind gusts was introduced along the trajectory having an initial velocity error of 20 m s^{-1} . Horizontal and vertical components of these gusts are shown in figures 17 and 18, and figure 19 shows them superimposed on projectile velocity. The gusts were of duration 5 s and had random directions and random magnitudes in the range 0 to 10 m s^{-1} . Responses to these gusts and to the initial velocity error of 20 m s^{-1} , of attitude, altitude, angle of attack, and elevator deflection angle, are shown in figures 19 to 24, and are all stable.

6.2 Integrity

There is now the question of the integrity of this control system II and the effect of the single failure of each state variable feedback will be examined. In a time-varying linear system one could compute the performance index by modifying the Riccati equation in the manner previously indicated in the search for a suitable weighting matrix Q . Such computations readily reveal a non-converging asymptotic behaviour when it exists and can thus be used to indicate stability or the lack of it. However in this instance where the system is well approximated by a time-invariant system it is easy to compute eigenvalues of closed-loop matrices formed from the difference between the initial-value plant matrix and the product of the initial-valued control vector and a constant feedback gain row vector which has each gain component made zero successively. Eigenvalues of the closed-loop system II having feedback failure of one state at a time are given in Table 1.

Table 1 shows that attitude feedback failure is completely destabilising. The main effect of each other failure is to greatly reduce short period damping. Trajectory computations for each failure, other than attitude,

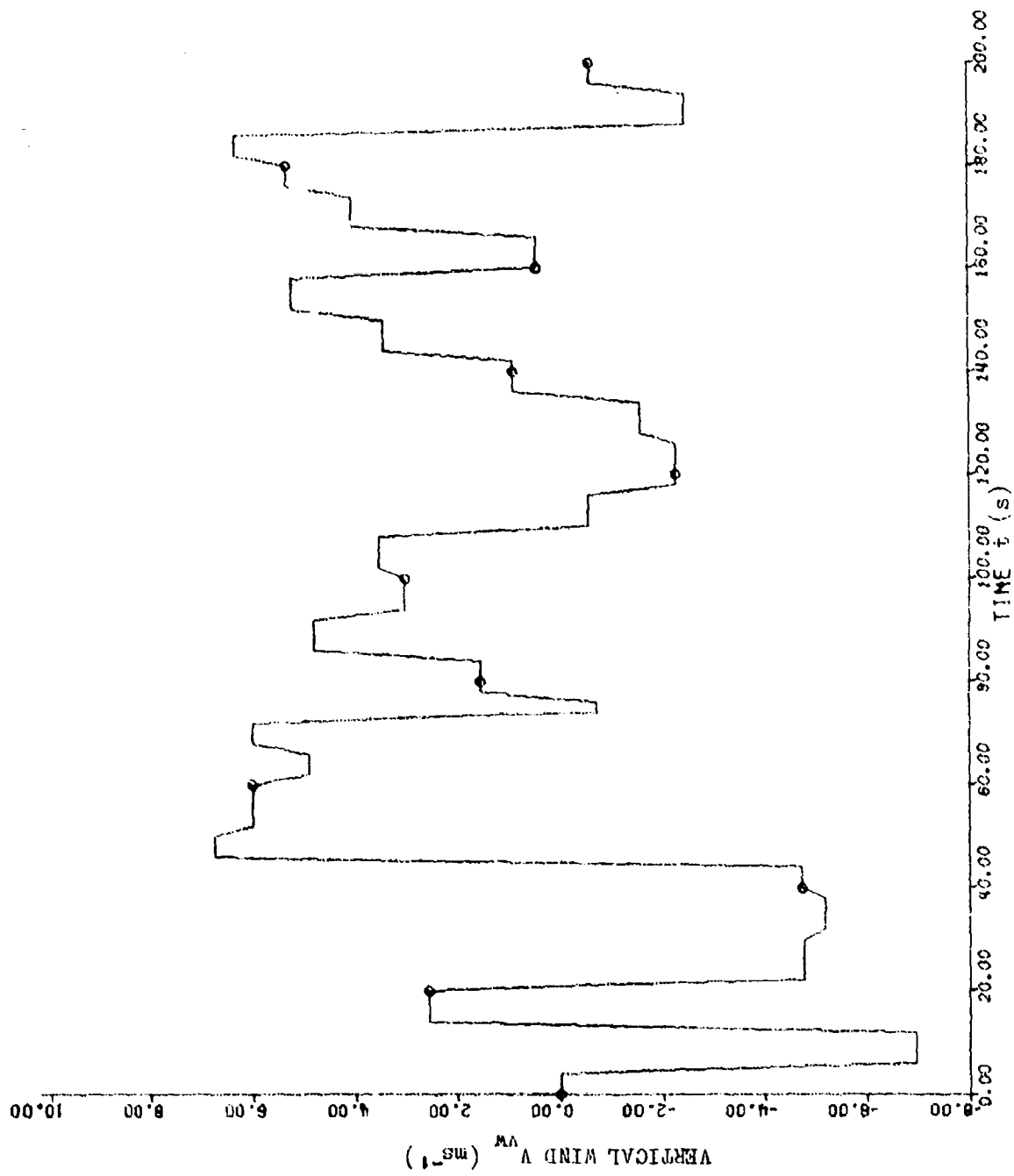


Figure 17. Random vertical wind gust sequence.

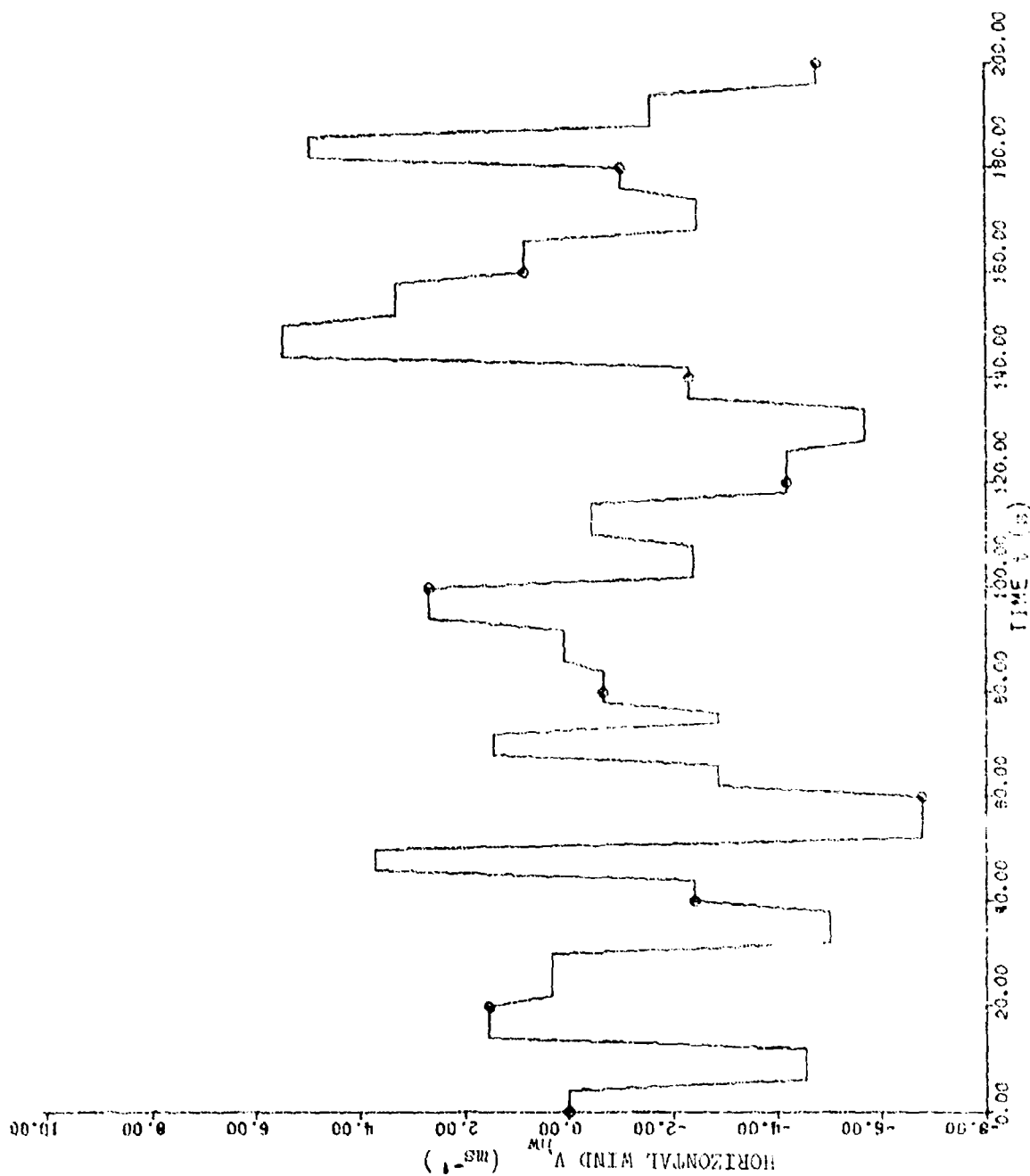


Figure 10. Random horizontal wind gust sequence.

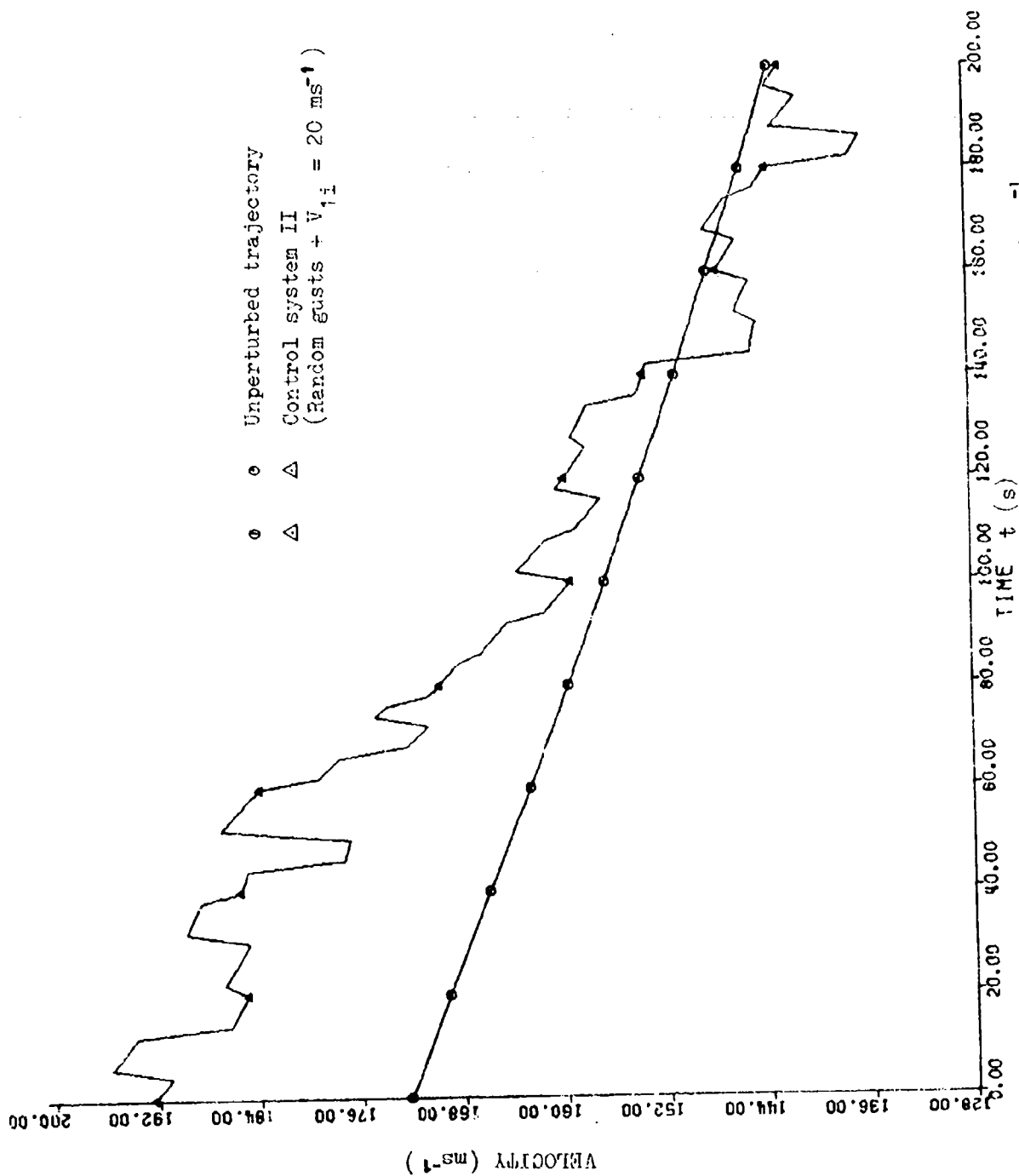


Figure 19. Velocity response to initial velocity perturbation 20 ms^{-1} and random gusts for projectile with control system II.

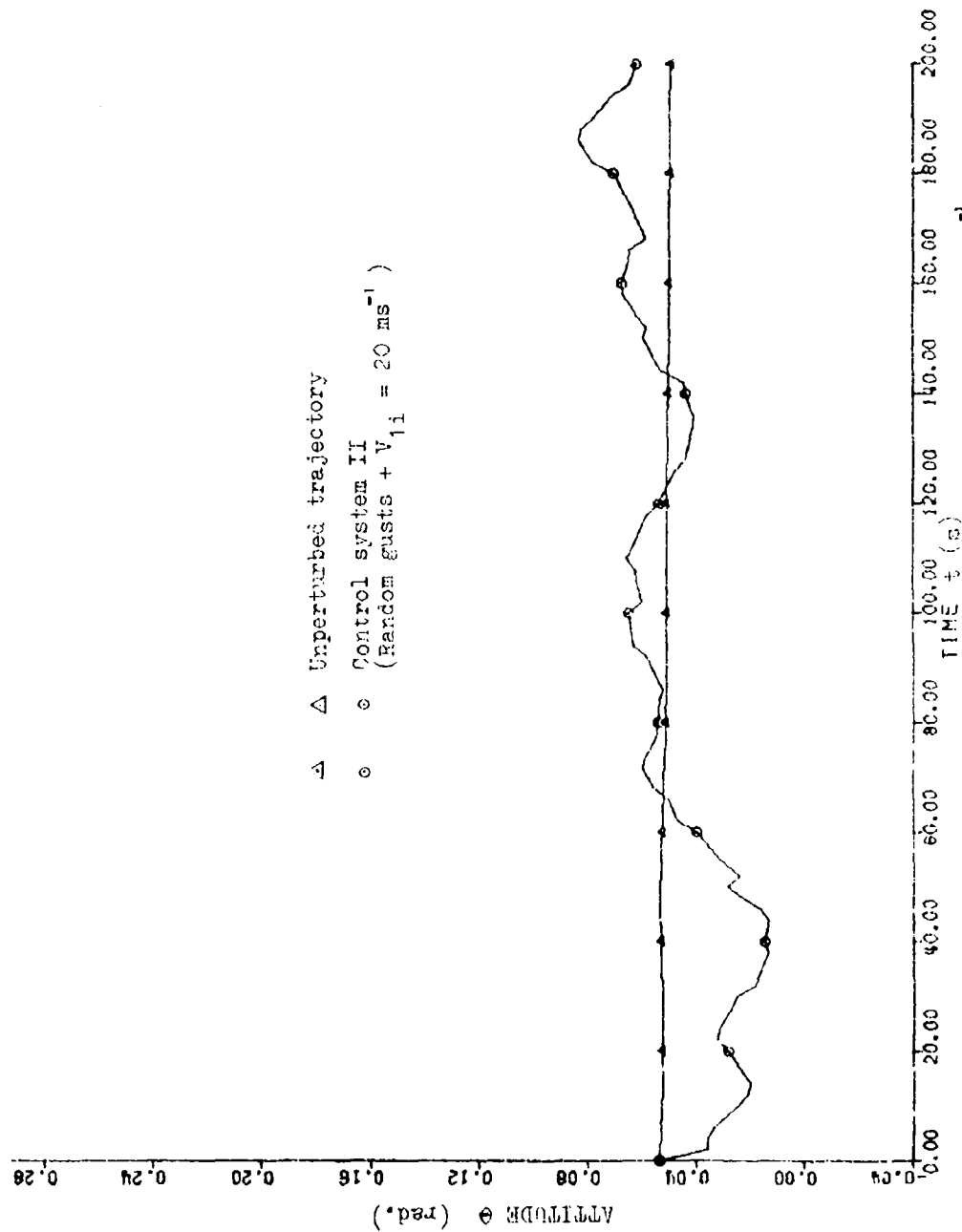


Figure 20. Altitude response to initial velocity perturbation 20 ms^{-1} and random gusts for projectile with control system II.

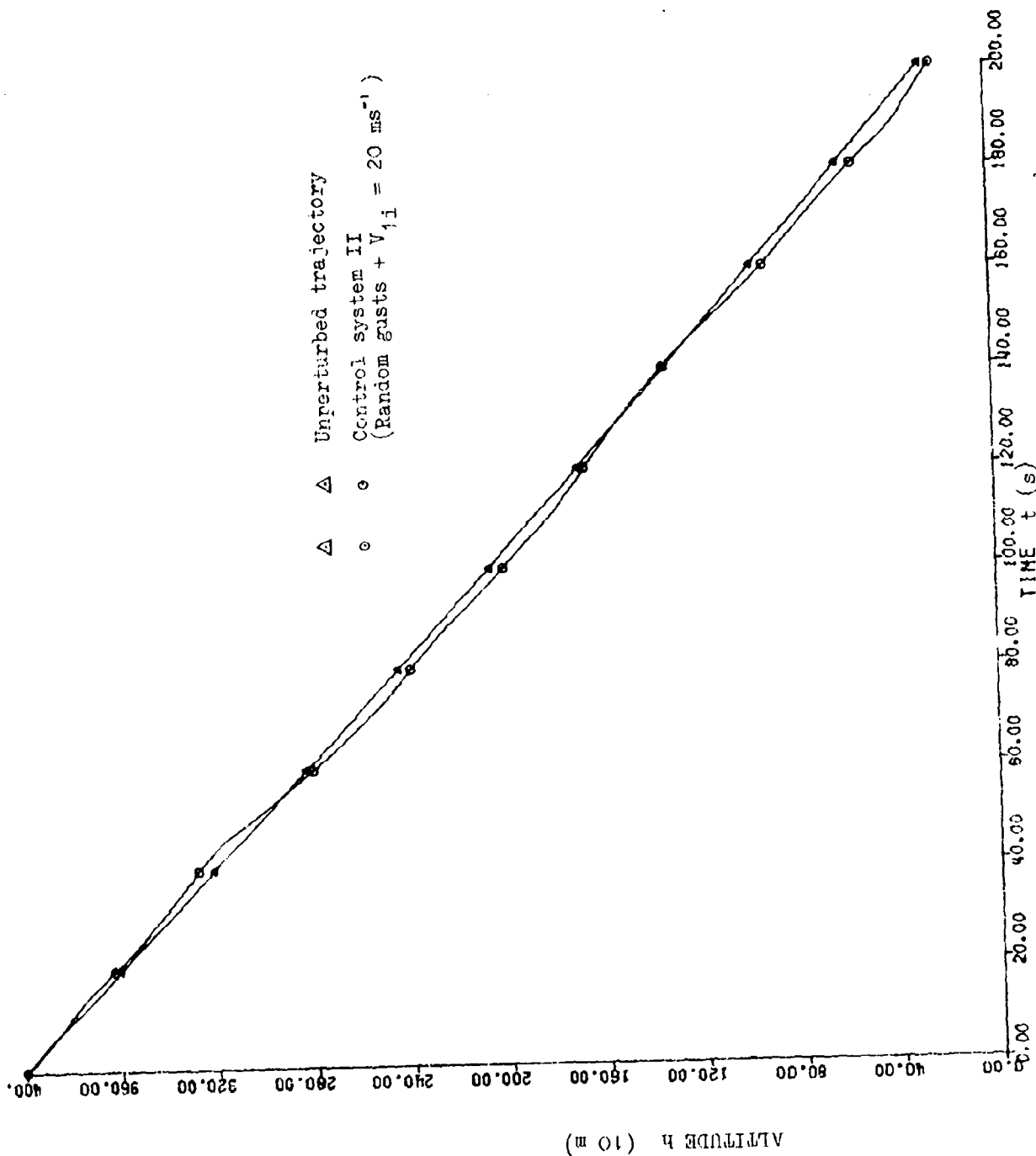


Figure 21. Altitude response to initial velocity perturbation 20 ms^{-1} and random gusts for projectile with control system II.

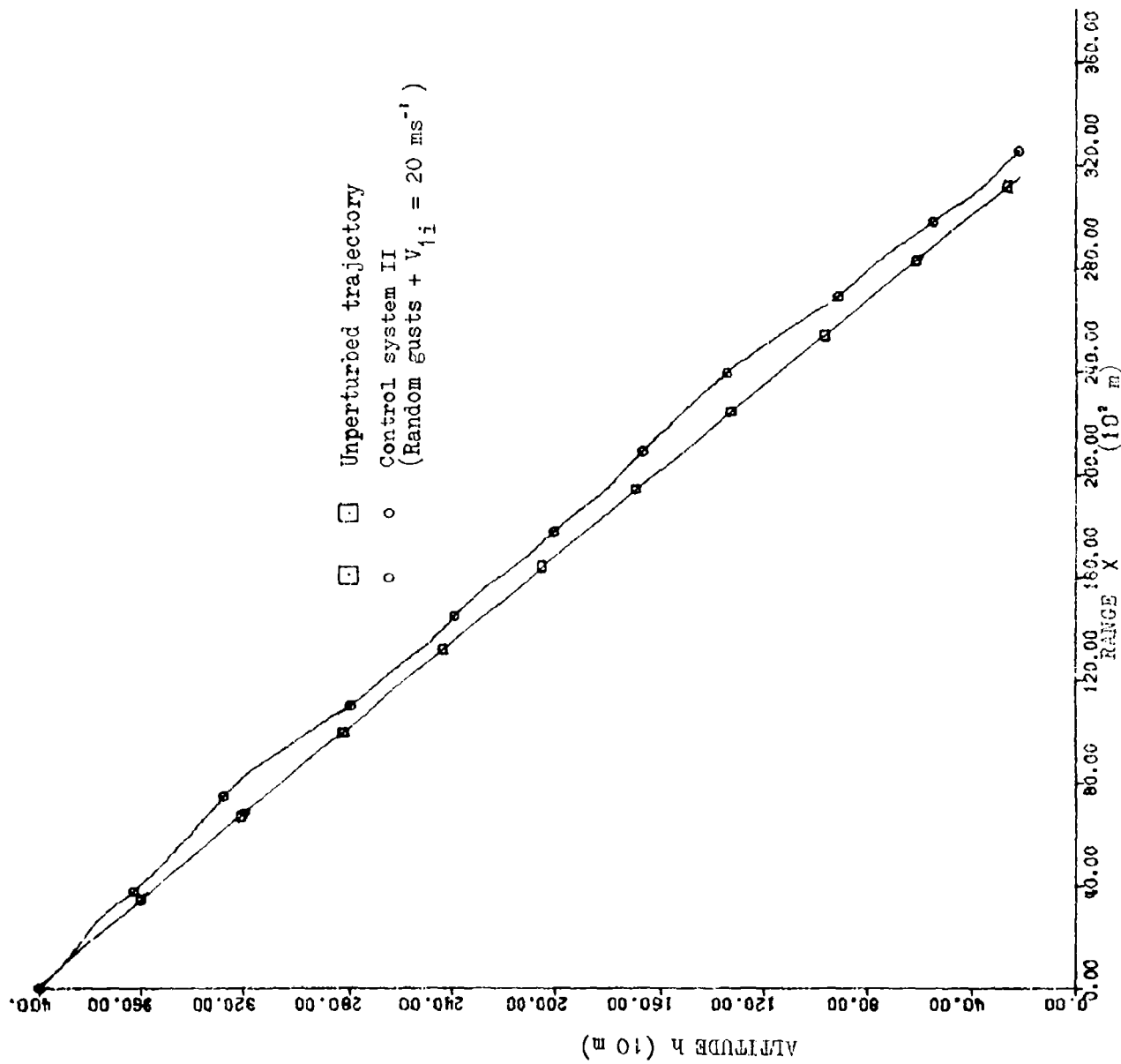


Figure 22. Positional response to initial velocity perturbation 20 ms^{-1} and random gusts for projectile with control system II.

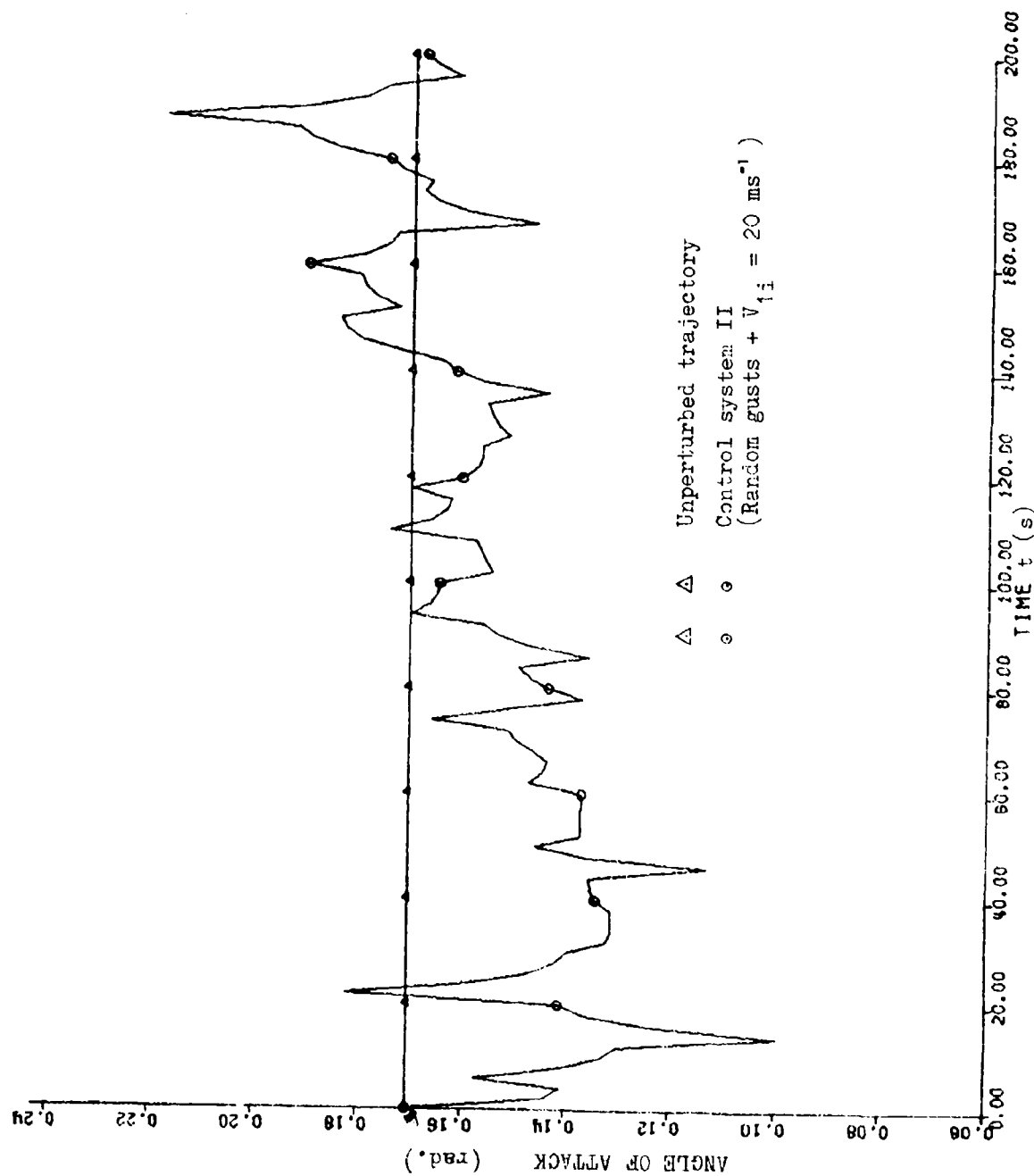


Figure 23. Angle of attack response to initial velocity perturbation 20 ms^{-1} and random gusts for projectile with control system II.

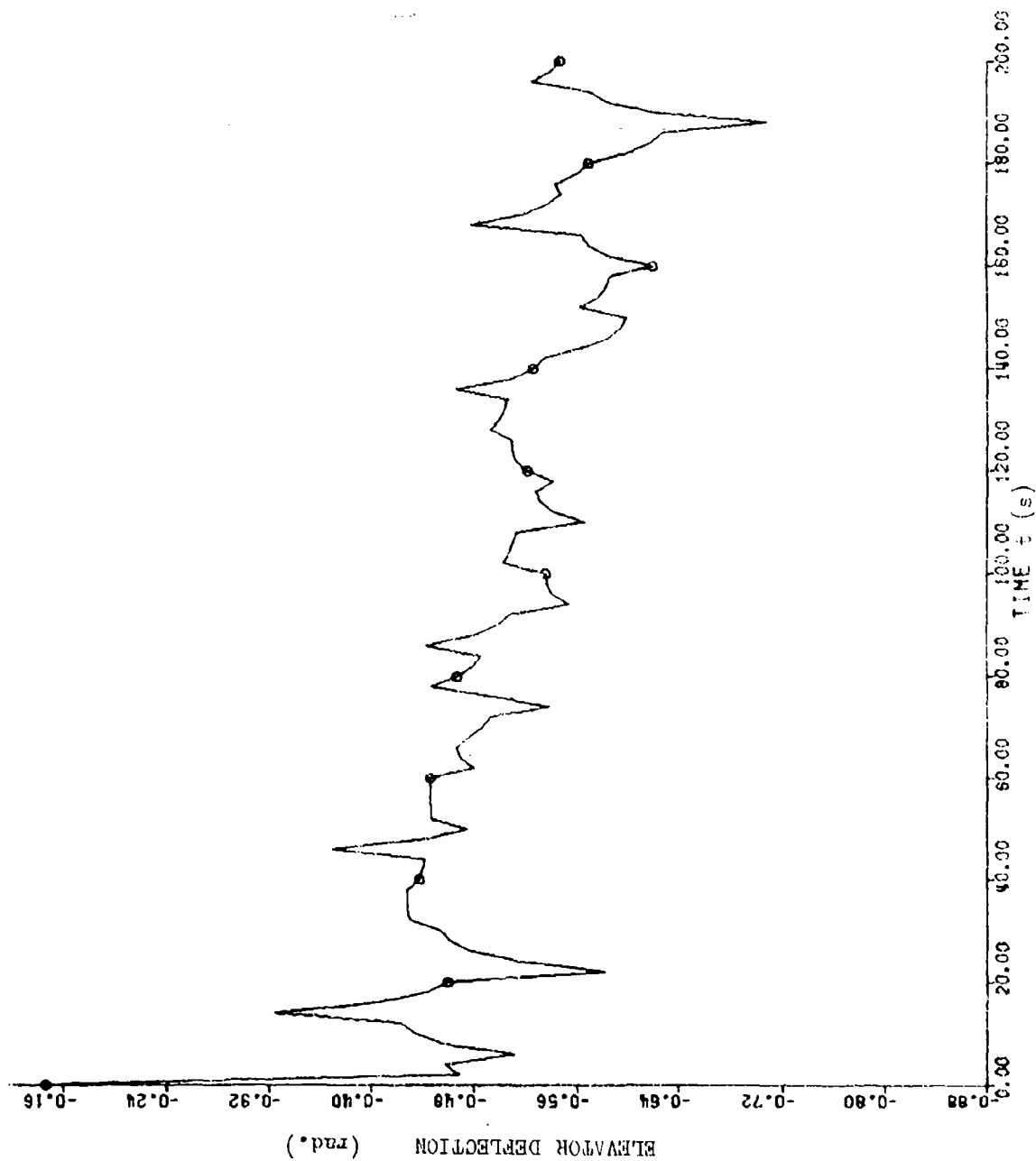


Figure 24. Elevator angle response to initial velocity perturbation. 20 ms⁻¹ and random noise for projectile with control system II.

TABLE 1. SYSTEM II POLES FOR EACH FEEDBACK FAILURE

Feedback Failure	None	Velocity	Angle of Attack	Attitude
System Poles s^{-1}	$-10.62 \pm 12.23i$	$-0.1102 \pm 16.22i$	$-0.2008 \pm 18.29i$	-6.1629
	-0.3174	-0.3148	-0.2250	5.618
	-0.06582	-0.07605	-0.08051	0.3062
	-0.006205	-0.005409	-0.005689	-0.3690
				-0.008212
Feedback Failure	Pitch Rate	Altitude	All	
System Poles s^{-1}	$-0.1135 \pm 16.22i$	$-0.1135 \pm 16.23i$	$-0.3456 \pm 6.045i$	
	-0.3178	-0.3774	$-0.01041 \pm 0.08546i$	
	-0.06555	-0.01051	-0.0008673	
	-0.006203	-0.001628		

confirmed that flight stability was maintained, except for pitch rate feedback failure in the face of velocity perturbations. For pitch rate feedback failure, angle of attack perturbations reached such large amplitude that for negative perturbations the lift became significantly less than the weight, causing the projectile to plunge downwards and further increase the velocity perturbation to values well outside the validity of the linear theory. Under these conditions, computations of the response to a 10 m s^{-1} initial velocity perturbation, showed that the projectile plunged downwards and made a 180 degree backward turn.

6.3 Implementation

This feedback system requires continuous measurement of the five state variables, velocity, angle of attack, attitude, pitching rate, and altitude. One could use a pitot tube for velocity, a yawmeter for angle of attack, a position gyroscope for attitude, and an altimeter for altitude. For pitching rate measurement there are rate gyroscopes, or an array of accelerometers, or coriolis devices using deflection of small gas jets or vibrating simply supported beams. A practical difficulty arises from the accuracy required for the initial setting value of a position gyroscope used to measure attitude. As mentioned previously, a $1/4$ degree error in flight path direction leads to a 100 m error in terminal altitude which in turn requires 2 degrees of seeker beam to see the target. If the projectile is launched from a moving platform such as an aircraft then an accuracy of a fraction of a degree in the initial gyroscope axis setting would not be achievable by simple means and attitude would not be available for mid course trajectory correction. When states are not available for measurement, the sophisticated solution is to use an on-board computer simulation of the plant behaviour to estimate the missing states from the measured ones. The way in which this is usually carried out is described with reference to figure 25. This figure shows the output from the part of the system under control to be the state vector x . When not all the components of x are available for measurement, the remaining ones may be represented by Fx where F is a matrix which, for example, would be a unitary matrix if all of x was available. Thus the signal which passes on into the estimating part of the scheme consists of the measurable parts of x contaminated by the measurement noise v . From this signal an estimate of the state vector, denoted by \hat{x} , is computed and fed back to the system controller. Clearly then, the function of the estimation process is to make \hat{x} approximate x as closely as possible. From figure 25 it is easily shown that

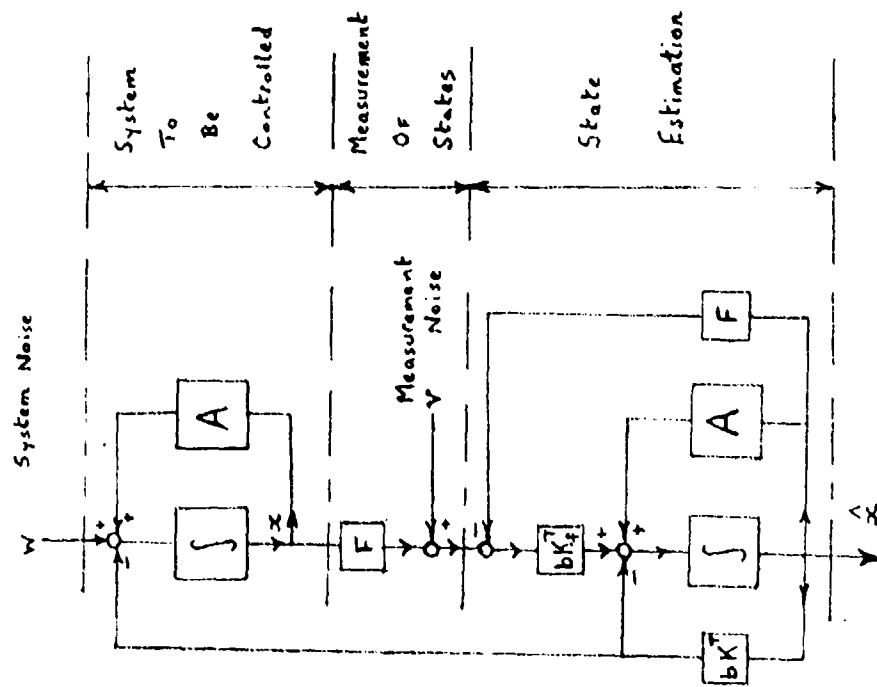


Figure 25. Scheme for estimation of feedback states from incomplete measurements.

$$\dot{\hat{x}} - \dot{\bar{x}} = (A - bK_f^T F)(\hat{x} - \bar{x}) - bK_f v + w \quad (70)$$

This equation shows that estimation performance depends on the choice of the gain vector K_f . For a time-invariant system, classical design techniques can be used to select K_f such that the estimation process is stable and such that a quick response minimises the difference between \hat{x} and \bar{x} . If the components of the noise vectors v and w are assumed to be white and Gaussian with zero mean values then a sophisticated method of determining K_f is available through use of Kalman filter theory, descriptions of which are to be found in references 11 and 16. The result of this theory is that the best estimate of x is given by \hat{x} when

$$K_f^T = P^{-1}FR \quad (71)$$

and R is the solution of the Riccati matrix equation (50), integrated forward in time, with the elements of the matrices Q and R now representing the power spectral densities of the components of the system noise vector w and the measurement noise vector v respectively.

Another approach to design when some states are not available and when the system is time-invariant is to investigate the use of compensating networks to achieve the closed loop transfer functions derived by optimal control theory for complete state feedback. Techniques for designing such compensating networks are discussed in references 10 and 17. However, the approach that will be considered in more detail in the next section is that of approximating the system to be controlled by one of reduced order.

7. SUB OPTIMAL CONTROL

In this section the possibility of sub optimal control is pursued because the lower performance from partial state feedback is compensated by design simplicity. The first method to be considered is that of representing the system by a reduced order mathematical model and using this model as the basis

for applying linear optimal control theory. Provided that this model is a close approximation, we might expect the design to be nearly optimal in the sense that the optimality will be almost independent of initial conditions.

7.1 Reduced Order Approximation

Reduced order approximations are likely to succeed when there is wide separation between system poles and the concept of fast and slow variables can be invoked. In dynamical problems this situation leads to the use of singular perturbation techniques which can be particularly useful in solving non linear equations. A discussion on the application of singular perturbation techniques to solution of aircraft performance problems is given in reference 18 where conditions for successful application are investigated. Typically, for conventional aircraft configurations, the phugoid and short period open loop modes can be separated, and the projectile considered here is no exception as is shown in Appendix II. However, in using this separation property to design closed loop control systems it is necessary to check the effect of loop closure on pole positions. At the end of Appendix II it is shown that the phugoid motion can be approximated by the second order system

$$\begin{aligned}\dot{z}_1 &= a_{11}z_1 + a_{13}z_2 + d_1\alpha_1 \\ \dot{z}_2 &= -a_{21}z_1 - a_{23}z_2 + d_2\alpha_1\end{aligned}\tag{72}$$

where $z_1 = V_1$

$z_2 = \theta - \alpha_1 = \psi_1$ the increment in flight path angle,

$$d_1 = a_{12} + a_{13}$$

$$d_2 = -(a_{22} + a_{23}),$$

the elements a_{ij} being those corresponding to the elements of the complete plant matrix A based on initial flight conditions. By putting

$$Q = \begin{bmatrix} 1/V_{1m}^2 & 0 \\ 0 & 1/\psi_{1m}^2 \end{bmatrix}$$

$$\text{and } P = 1/\alpha_{1m}^2$$

in equation (66), the characteristic equation for an optimally controlled system based on equations (72) and their adjoint set, becomes

$$\begin{vmatrix} \lambda - a_{11} & -a_{13} & d_1^2 \alpha_{1m}^2 & d_1 d_2 \alpha_{1m}^2 \\ a_{21} & \lambda + a_{23} & d_1 d_2 \alpha_{1m}^2 & d_2^2 \alpha_{1m}^2 \\ 1/V_{1m}^2 & 0 & \lambda + a_{11} & -a_{21} \\ 0 & 1/\psi_{1m}^2 & a_{13} & \lambda - a_{23} \end{vmatrix} = 0 \quad (73)$$

As pointed out previously in section 5.1.5, this characteristic polynomial is an even function of λ , having the form

$$\lambda^4 + c_1 \lambda^2 + c_3 = 0 \quad (74)$$

The roots of equation (74) are thus $\pm \lambda_1$ and $\pm \lambda_2$, where

$$\lambda_1 \lambda_2 = c_3^{1/2} \quad (75)$$

$$\text{and } \lambda_1^2 + \lambda_2^2 = -c_1 \quad (76)$$

Expanding the determinant in equation (73) gives

$$c_1 = -(a_{11}^2 + a_{23}^2 - 2a_{13}a_{21}) - d_1^2 \mu^2 - d_2^2 \nu^2 \quad (77)$$

$$c_3 = (a_{21}a_{13} - a_{11}a_{23})^2 + (a_{11}d_2 + a_{21}d_1)^2 \nu^2 + (a_{23}d_1 + a_{13}d_2)^2 \mu^2 \quad (78)$$

where $\mu = \alpha_{1m}/V_{1m}$

and $v = \alpha_{1m}/\psi_{1m}$.

The characteristic equation for an optimal system based on equations (72) alone is thus

$$\lambda^2 - (\lambda_1 + \lambda_2)\lambda + \lambda_1\lambda_2 = 0 \quad (79)$$

where λ_1, λ_2 are the roots of equation (74) with the negative real parts. Hence from equations (75) and (76)

$$2\lambda_1 = (-c_1 - 2c_3)^{1/2} - (-c_1 + 2c_3)^{1/2} \quad (80)$$

$$\text{and } 2\lambda_2 = -(-c_1 - 2c_3)^{1/2} - (-c_1 + 2c_3)^{1/2} \quad (81)$$

Equations (75) to (78) provide the links between the poles λ_1, λ_2 of the optimal system and the assigned weighting ratios μ, v .

Optimal feedback gains k_1 and k_2 can be related to the poles λ_1, λ_2 and weighting ratios μ, v by first substituting

$$\alpha_1 = -k_1 V_1 - k_2 \psi_1 \quad (82)$$

in equations (72) so that the characteristic equation becomes

$$\begin{aligned} \lambda^2 - (a_{11} - a_{33} - d_1 k_1 - d_2 k_2)\lambda \\ + (a_{21} a_{13} - a_{11} a_{23}) + k_1 (d_1 a_{23} + d_2 a_{13}) - k_2 (d_2 a_{11} + d_1 a_{21}) = 0 \end{aligned} \quad (83)$$

Equating coefficients in equations (79) and (83) and solving for k_1 and k_2 gives

$$k_1 = \frac{a_{11}(d_1 a_{21} + d_2 a_{11}) - a_{21}(d_1 a_{23} + d_2 a_{13})}{d_2(d_1 a_{23} + d_2 a_{13}) + d_1(d_2 a_{11} + d_1 a_{21})} - \frac{(\lambda_1 + \lambda_2)(d_1 a_{21} + d_2 a_{11}) + d_2 \lambda_1 \lambda_2}{d_2(d_1 a_{23} + d_2 a_{13}) + d_1(d_2 a_{11} + d_1 a_{21})} \quad (84)$$

and

$$k_2 = \frac{a_{13}(d_1 a_{21} + d_2 a_{11}) - a_{23}(d_1 a_{23} + d_2 a_{13})}{d_2(d_1 a_{23} + d_2 a_{13}) + d_1(d_2 a_{11} + d_1 a_{21})} - \frac{(\lambda_1 + \lambda_2)(d_1 a_{23} + d_2 a_{13}) - d_1 \lambda_1 \lambda_2}{d_2(d_1 a_{23} + d_2 a_{13}) + d_1(d_2 a_{11} + d_1 a_{21})} \quad (85)$$

Thus for the second order system given by equations (72), plots of optimal feedback gains k_1 and k_2 and of weight ratios μ and ν can be drawn in the λ plane from the relationships given by equations (77), (78), (80), (81), (84) and (85). Such plots are shown in figure 26 for the case when the characteristic equation for the closed loop system has a pair of complex conjugate roots. From equations (84) and (85) it is seen that when λ_1, λ_2 are complex conjugates of each other, the locii of k_1 and k_2 in the λ plane are concentric circular arcs. Putting $\lambda = \sigma + i\omega$, the centre of the k_1 circles is

$$\text{at } \sigma = (d_2 a_{11} + d_1 a_{21})/d_2$$

and of the k_2 circles

$$\text{at } \sigma = -(d_1 a_{23} + d_2 a_{13})/d_1$$

Figure 26 shows curves of constant values of μ along which ν varies. The largest value shown for μ is $\pi/450$ radian m^{-1}s which would correspond to $\alpha_{1m} \approx 2$ degrees and $V_{1m} \approx 5 \text{ m s}^{-1}$. From equations (77) and (78) it can be seen

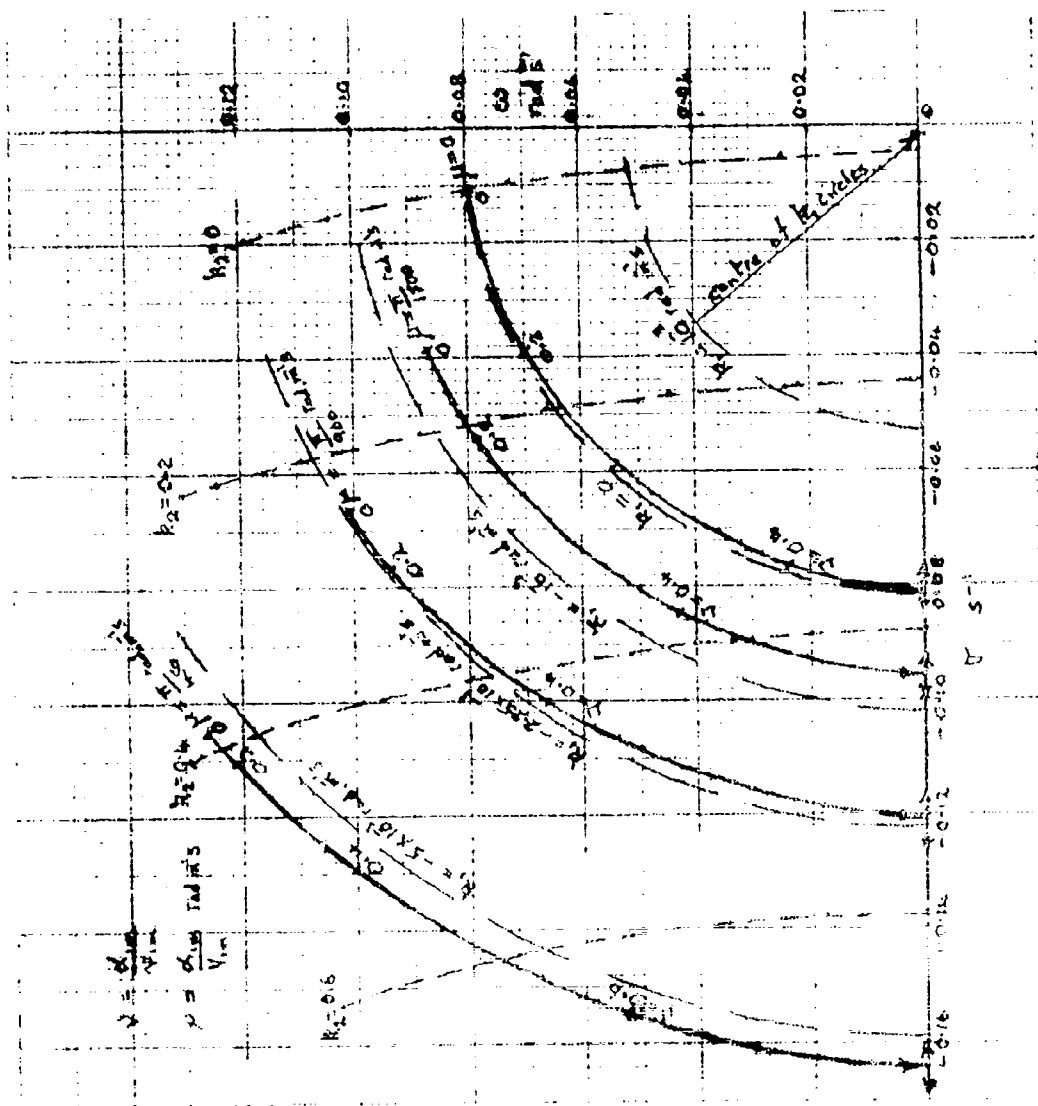


Figure 1. Plot of relative weights for complex poles.

that the roots of the open loop characteristic equation occur when $v=\mu=0$, and at that point on figure 26 the values of σ and ω are in close agreement to those given for the complete open loop system in Appendix I. As velocity weight is tightened, or, that is, V_{1m} is decreased and hence μ increased, figure 26 reveals that the phugoid becomes more oscillatory. This is because the system is trying to regulate velocity through the effect of angle of attack on drag. As attitude weight is tightened, that is as ψ_{1m} is made smaller, v increases and the system response eventually becomes aperiodic. In fact as $v \rightarrow \infty$, one root of the characteristic equation tends towards the centre of the k_1 circles and the other towards $-d_2 v$. Relaxing the velocity weight completely is represented by the $\mu=0$ curve in figure 26 and along this curve k_1 is positive, showing that when velocity is free to change, angle of attack is decreased when velocity perturbations are positive. Thus the physical features of the phugoid response are borne out in figure 26.

To relate the feedback gains k_1, k_2 of the reduced system to feedback gains in the full system, the assumption is made that α_1 is a fast variable and will respond instantly to elevator deflection so that the steady state relationship of equation (24) can be used to give

$$\begin{aligned}\eta_1 &= -\alpha_1 (\partial C_m / \partial \alpha) / (\partial C_m / \partial \eta) \\ &= -13\alpha_1 / 4, \text{ from Appendix I.}\end{aligned}$$

Thus, putting $\alpha_1 = -k_1 v_1 - k_2 \psi_1$

$$= -k_1 v_1 - k_2 \theta + k_2 \alpha_1,$$

leads to $K_1 = 13k_1/4, K_2 = -13k_2/4, K_3 = 13k_2/4,$

where K_1, K_2, K_3 are optimum zero operating on feedback of

v_1, α_1, θ to the elevators.

In order to restrict the total elevator deflection angle to less than 0.7 radian, the magnitude of k_1 must not exceed 2.25×10^{-3} radian $m^{-1}s$ to accommodate a maximum initial velocity error of $20 m s^{-1}$. Thus in figure 26 the choice of optimal feedback gains must be restricted to values lying in the region to the right of the $k_1 = -2.25 \times 10^{-3}$ radian $m^{-1}s$ circle, which is seen to be approximately given by $\mu = \pi/900$ radian $m^{-1}s$. This value of μ corresponds to $V_{1m} = 10 m s^{-1}$ for $\alpha_{1m} = 2$ degrees.

For aperiodic response when the two roots of the characteristic equation of the reduced system lie along the negative real axis the corresponding optimal feedback gains and weight ratios are plotted against the root closest to the origin and the plots are shown in figures 27 and 28. As v becomes large it is found that the root farthest from the origin on the negative real axis behaves as $-d_2 v$, k_1 approaches $-a_{21}/d_2 = 1.72 \times 10^{-3}$ radian $m^{-1}s$ and k_2 approaches v . Figure 28 shows that for the aperiodic response, k_2 is very close to its asymptotic value v . Thus for large values of v when one of the phugoid poles moves far away from the origin, the assumption that the phugoid poles and the short period poles are well separated, may be violated and a check on the stability of the complete closed loop system with feedback gains k_1 and k_2 should be made. This check showed that for values of v between 2 and 4, the feedback gains k_1 and k_2 caused undamping of the short period mode thus rendering the complete system unstable. The stability boundary corresponding to this undamping of the short period mode is shown in figures 27 and 28.

There now remains the problem of selecting a pair of feedback gains k_1 and k_2 , which reduces to choosing relative weights μ and v . In accordance with previous considerations that α_1 should be restricted to about 2 degrees and that the average error in flight path direction should be no more than $1/4$ degree, the values

$$\alpha_{1m} = \pi/90 \text{ radian}$$

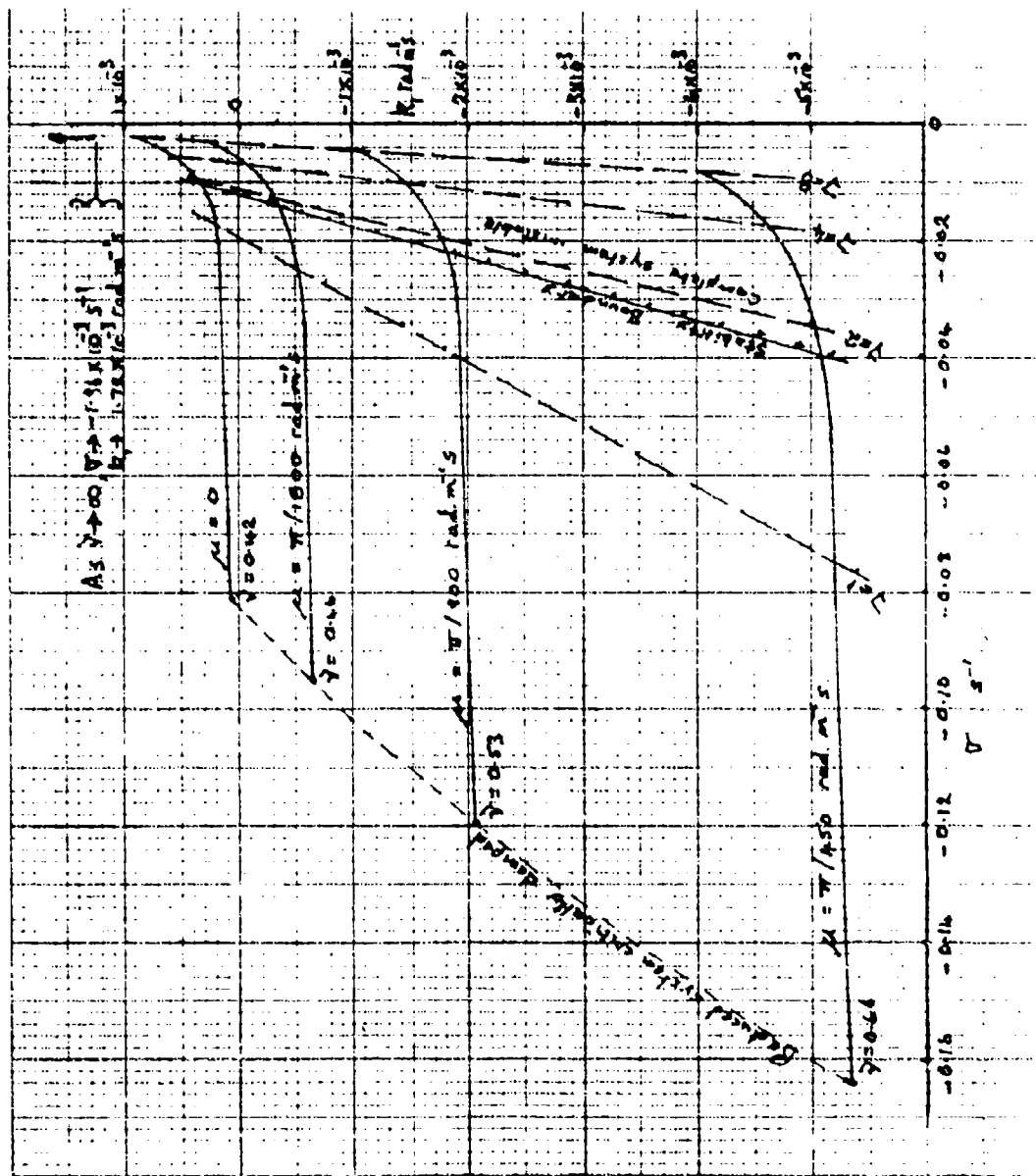


Figure 27. Optimal velocity feedback gain and relative weights for largest real poles of third order system.

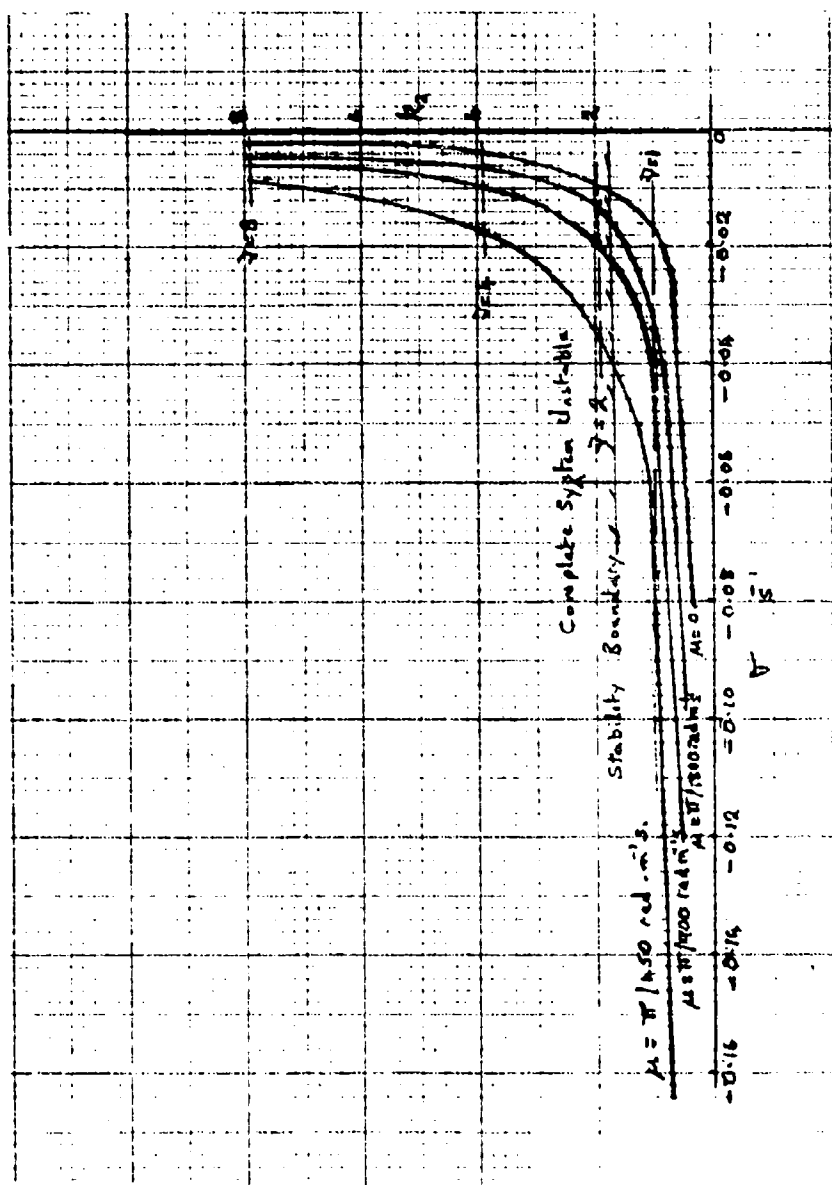


Figure 28. Optimal flight paths for single feedback gain and relative weights for largest real poles of reduced order system.

and $\psi_{1m} = \pi/720$ radian, are taken,
giving $v = 8$.

Because $V_{1m} = 20 \text{ m s}^{-1}$ was found to give the best results for the complete optimal control system, this value will be selected again, giving

$$\mu = \pi/1800 \text{ radian m}^{-1}\text{s}.$$

But, as shown in figures 27 and 28, the complete system is unstable for $v=8$, so some other criteria must be used for feedback gain selection. The approach used here is to search the stable regions of figures 27 and 28 for values of the weight ratios μ and v which minimise an integral performance index for the reduced system. In the general notation, the quadratic integral performance index based on the reduced system given by equations (72), is

$$J(t) = z^T R z$$

$$= \int_t^{\infty} \{ z^T Q z + \alpha_1^2 / \alpha_{1m}^2 \} dt \quad (86)$$

$$\text{where } R = \begin{bmatrix} r_{11} & r_{12} \\ r_{12} & r_{22} \end{bmatrix}$$

$$\text{and } Q = \begin{bmatrix} q_{11} & 0 \\ 0 & q_{22} \end{bmatrix}$$

For every pair of values of μ and v in the region searched there are a corresponding pair of feedback gains k_1 and k_2 . Using these feedback

gains, we can put

$$u_1 = -k_1 z_1 - k_2 z_2 \quad \text{in equation (86)}$$

and letting $t \rightarrow 0$ in the integral performance index, the Riccati equation for R reduces to a set of linear equations in the elements r_{ij} , given by

$$\begin{bmatrix} 2a_{11} & -2a_{21} & 0 \\ a_{13} & a_{11}a_{23} & -a_{21} \\ 0 & 2a_{13} & 2a_{23} \end{bmatrix} \begin{bmatrix} r_{11} \\ r_{12} \\ r_{22} \end{bmatrix} = \begin{bmatrix} k_1^2 - \alpha_{1m}^2 q_{11} \\ k_1 k_2 \\ k_2^2 - \alpha_{1m}^2 q_{22} \end{bmatrix} \quad (1/\alpha_{1m}^2) \quad (87)$$

In solving these equations, q_{11} and q_{22} are taken as the inverse squares of the maximum allowable values of V_1 and ψ_1 , which are

$$V_{1m} = 20 \text{ m s}^{-1}, \quad \psi_{1m} = 1/4 \text{ degree},$$

but k_1 and k_2 correspond to values of μ , v selected in the region being searched. When, as in previous considerations, only initial values of velocity perturbations are considered, then from equation (86)

$$J_{t \rightarrow 0} = r_{11} V_{1i}^2$$

and hence r_{11} can be used as a measure of performance index J. Such values of r_{11} were calculated along the curves of constant μ shown in figures 26, 27 and 28 except for $\mu = \pi/450$ radian m^{-1}s which requires too much control deflection. The lowest values of r_{11} were found to occur along $\mu=0$, decreasing monotonically from $v=0$ to a minimum between $v=2$ and $v=4$. Thus values of k_1 and k_2 are sought which correspond to a point on $\mu=0$ in figure 27, lying to the left of the stability boundary at a distance which ensures adequate damping of the short period mode. Trajectories were computed using the optimal feedback gains corresponding to $v=1, 1.4, 1.6$, and $\mu=0$. As expected, the greater the value of v the less the altitude error but the

lower the short period damping. The trajectory for $v=1$ showed no appreciable altitude correction, whereas trajectories for $v=1.4$ and 1.6 both showed about 50 m correction. Trajectories for $v=1.4$, which have more short period mode damping than those for $v=1.6$, are shown in figures 29, 30 and 31.

At this stage it is worth investigating how a similar approach, through use of the reduced order system, could be used to achieve a tighter regulation of velocity at the expense of flight path direction. This means choosing V_{lm} to be very small and ψ_{lm} to be large. In terms of relative weights, μ is to be as large as possible with v small. From figure 26, the largest value of μ which maintains angle of attack and elevator deflection to within acceptable limits for an initial velocity perturbation of 20 m s^{-1} , is $\mu=\pi/900 \text{ rad m}^{-1}\text{s}$. Equation (87) was again used to calculate r_{11} for the values of μ shown in figure 26, excepting again for $\pi/450 \text{ rad m}^{-1}\text{s}$, and values of v were selected to be 0, 0.2, 0.4. The minimum value for r_{11} occurred for $v=0.2$ and $\mu=\pi/900 \text{ rad m}^{-1}\text{s}$, for which the corresponding weights are $V_{lm}=10 \text{ m s}^{-1}$, $\psi_{lm}=10$ degrees, and $\alpha_{lm}=2$ degrees. Trajectories obtained for this tighter control of velocity are compared with the trajectories obtained for tight attitude control in figures 29, 30 and 31. Further comparisons of the response of these two kinds of control are shown in figures 32, 33 and 34, where angle of attack, velocity, and altitude are plotted for the first 20 s of flight, following an initial velocity perturbation of 20 m s^{-1} . Figures 32 and 33 show now velocity is decreased by increased incidence but, from figure 34, at the expense of increased attitude angle. The lower damping of the short period mode for the tightly controlled attitude case is evident from figure 32.

The tightly controlled velocity case is more appropriate for the gliding projectile because it suppresses attitude errors and provides some altitude correction. Only three states are fed back to the elevators, these are velocity, attitude, and angle of attack. The values of derived feedback

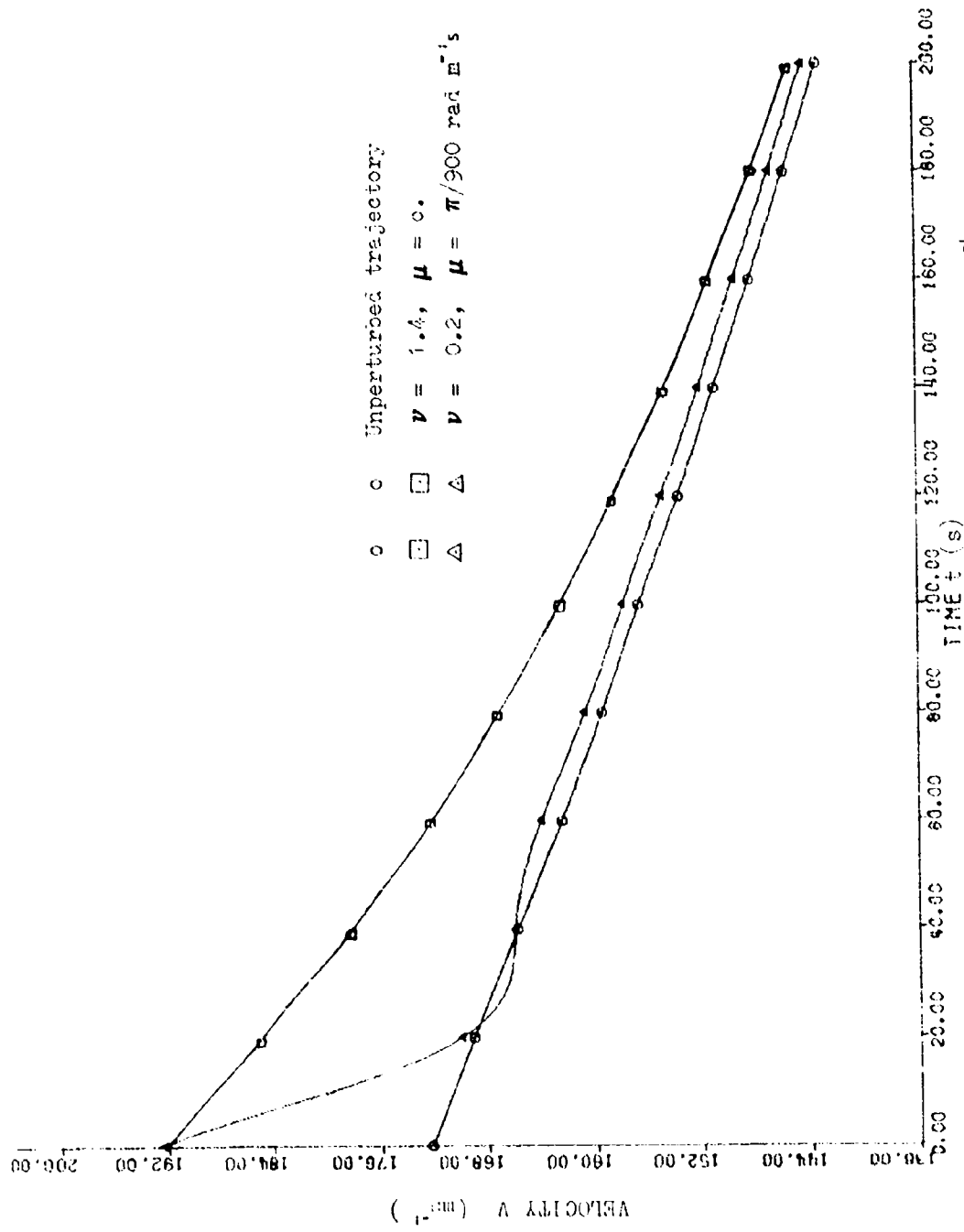


Figure 29. Velocity response to initial velocity perturbation 20 ms^{-1} for projectile with reduced order system control.

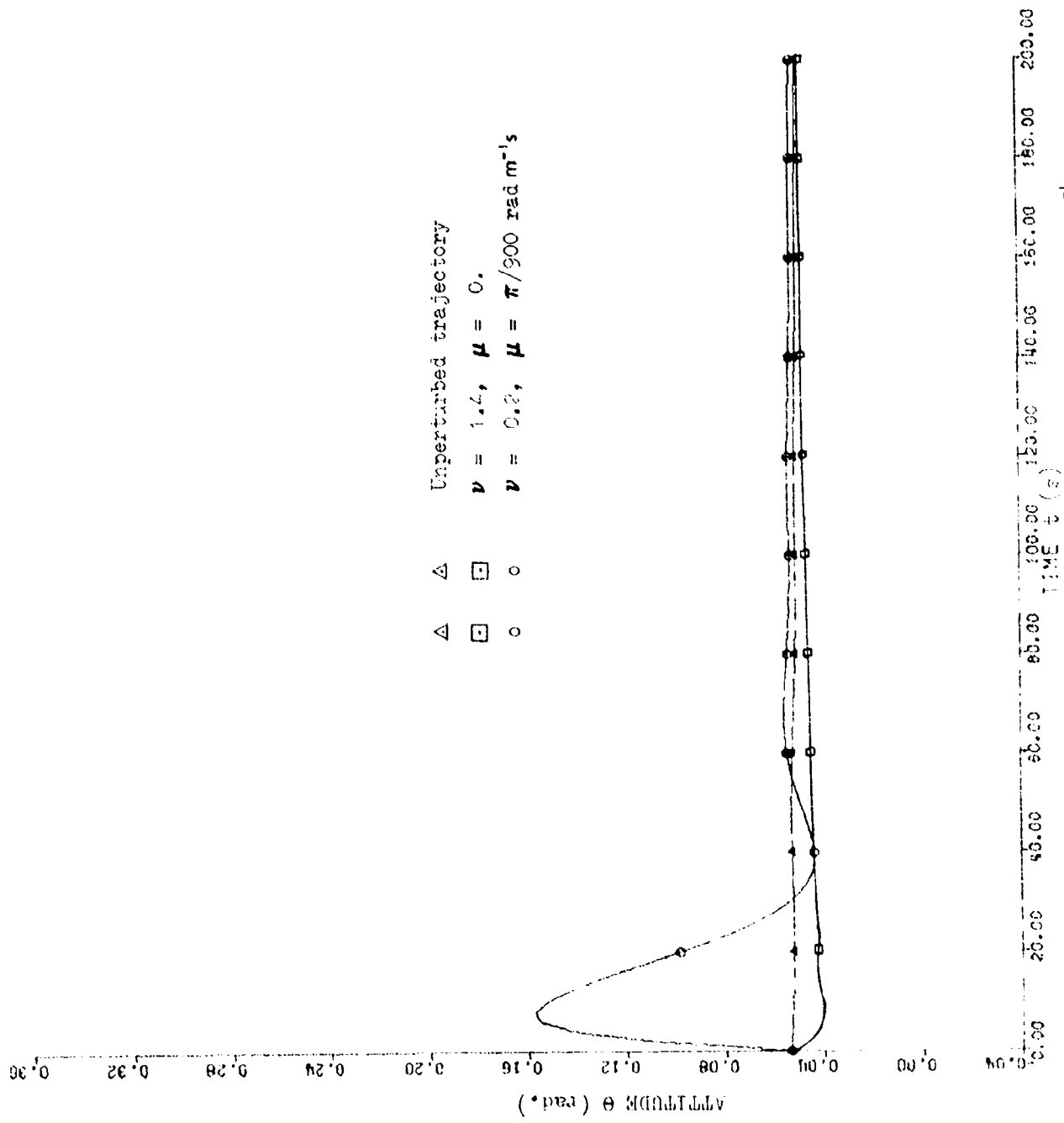
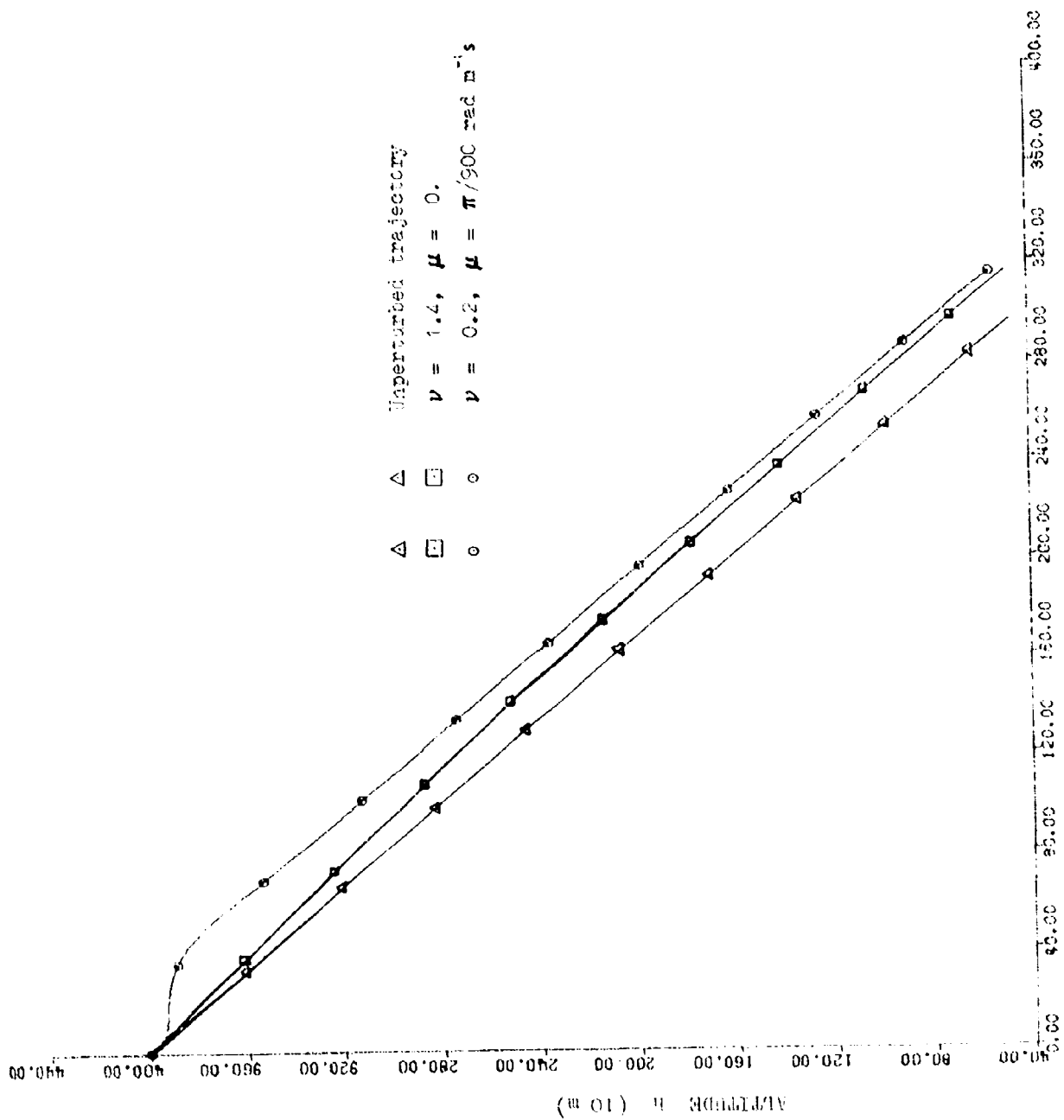


Figure 30. Attitude response to initial velocity perturbation 20 m/s for projectile with reduced order system control.



Δ Unperturbed trajectory
 \square $\nu = 1.4, \mu = 0.$
 \circ $\nu = 0.2, \mu = \pi/900 \text{ rad m}^{-1} \text{s}$

RANGE R (10^2 m)
 Figure 71. Positional response to initial velocity perturbation 20 ms⁻¹ for projectile with reduced order system control.

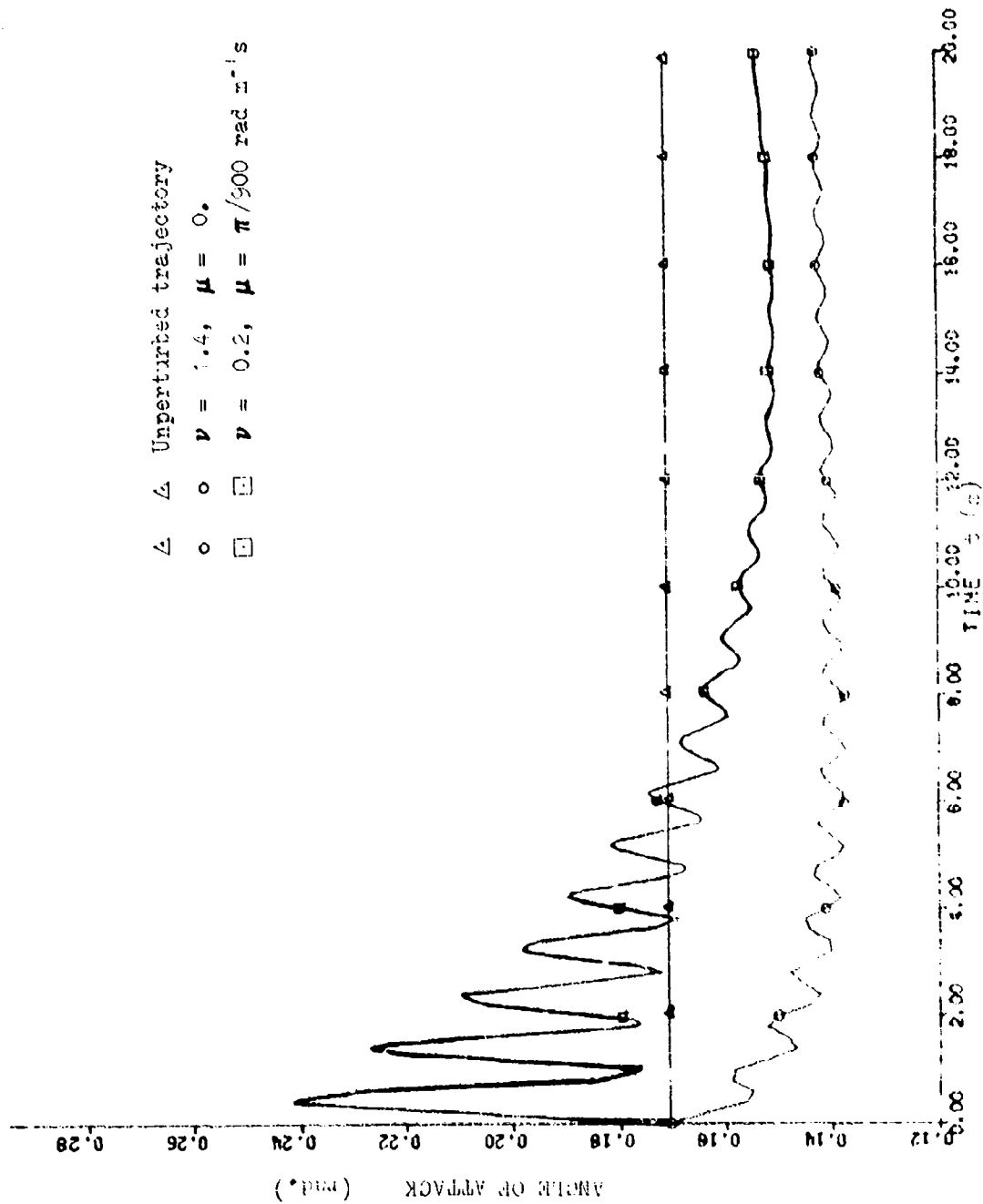


Figure 32. Initial angle of attack response to initial velocity perturbation 20 ms⁻¹ for projectile with velocity error control.

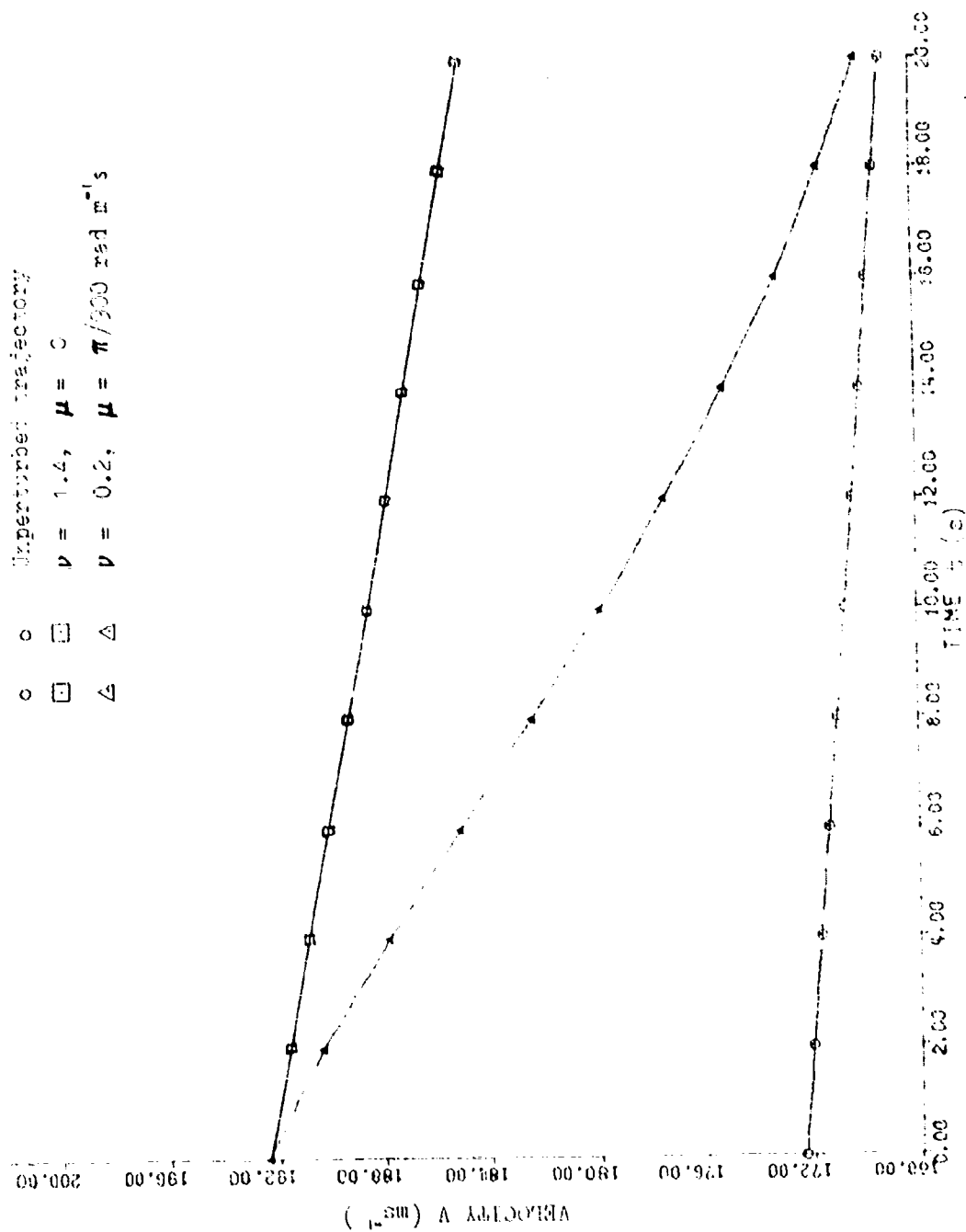


Figure 33. Initial velocity response to initial velocity perturbation 20 ms^{-1} for projectile with red on-order system control.

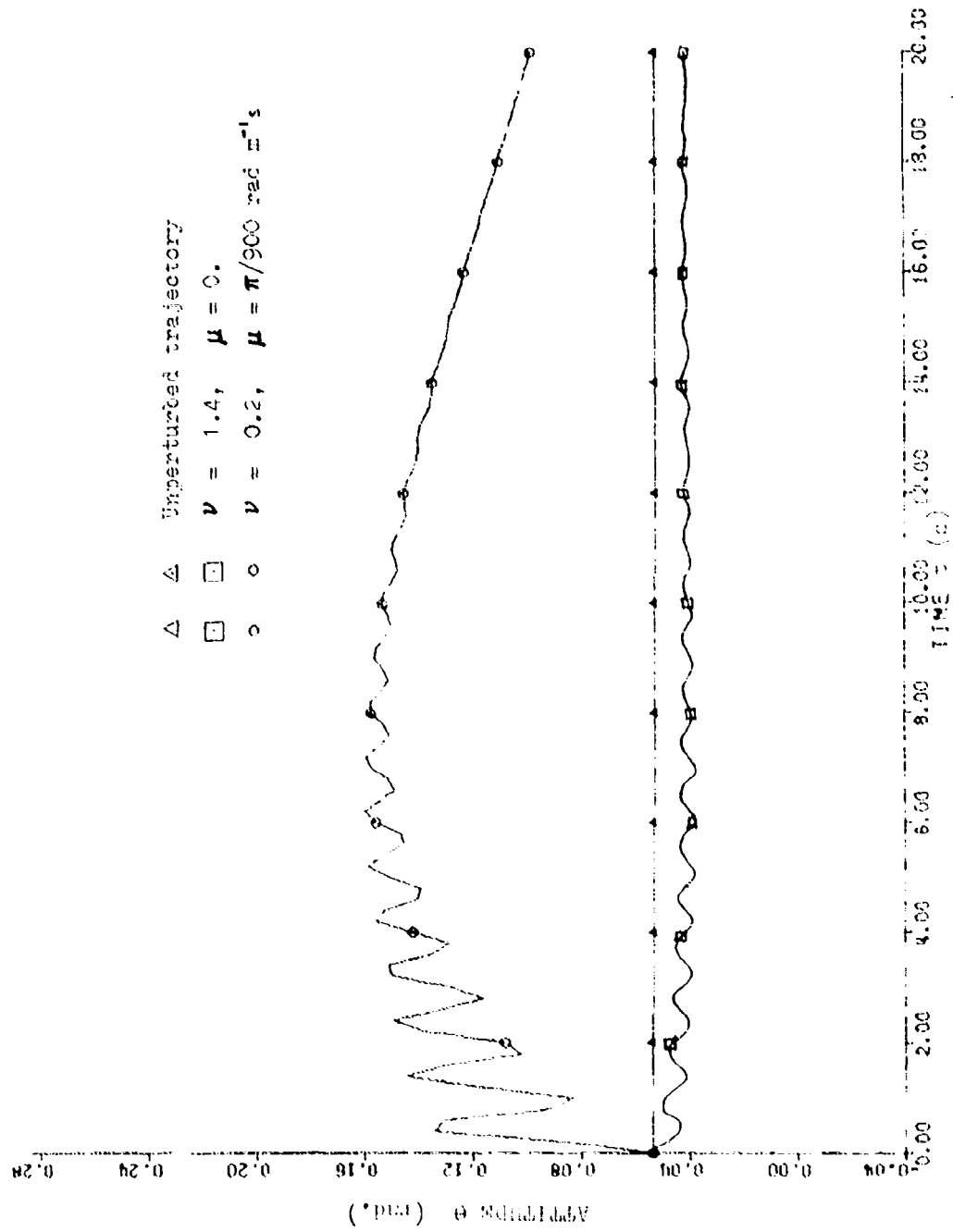


Figure 34. Initial altitude response to initial velocity perturbation, 20 ms⁻¹ for projectile with 20.341 degree system control.

gains are:-

$$K_V = -7.99 \times 10^{-4} \text{ radian m}^{-1}\text{s}$$

$$K_\alpha = 4.39$$

$$K_\theta = -4.39$$

From the computed trajectories, the errors at 25 km ground range resulting from an initial velocity perturbation of 20 m s^{-1} are 270 m in altitude and 0.12 degrees in attitude. These errors require a full beam angle of 5.6 degrees for seeing the target or 0.28 degree per m s^{-1} of initial velocity error. Maximum attitude error is 0.85 degree or 0.042 degree per m s^{-1} of initial velocity error. Improvement in altitude error is possible only at the expense of further undamping of the short period mode but this is undesirable. Stability was further checked by computing trajectories for flight with an initial velocity error of 20 m s^{-1} and with a series of random wind gusts having magnitudes in the range 0 to 10 m s^{-1} . These gusts are shown in figure 35 and the responses of angle of attack, attitude and altitude are shown in figures 36, 37 and 38. Figure 36 shows the relatively low damping of the short period mode as revealed by the angle of attack response to the first few random wind gusts. For these gusts, the angle of attack perturbation exceeds the maximum value limit of 2 degrees, reaching a maximum of 5.7 degrees at 13.5 s. This is not surprising since the system was designed to control velocity errors up to only 20 m s^{-1} within angle of attack perturbations of 2 degrees. As in the case of the full state feedback, failure of attitude feedback, undamps the short period mode, but is otherwise stable in the face of velocity, or angle of attack feedback failure.

This reduced order approach to optimal control system design resulted in relatively simple algebraic relationships between closed loop pole positions, optimal feedback gains, and state and control variable weights. The simpler model does provide insight into the physical behaviour of the

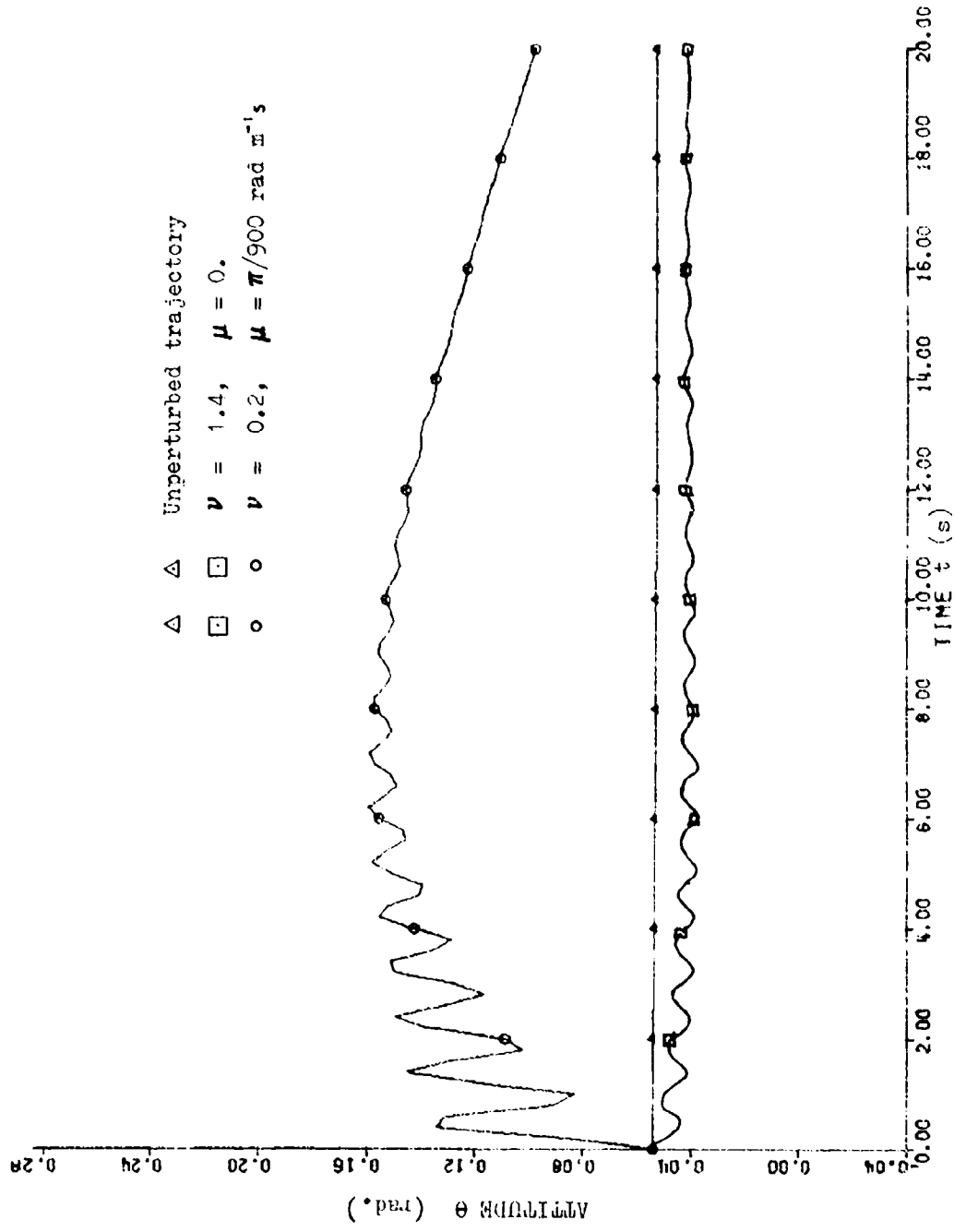


Figure 34. Initial attitude response to initial velocity perturbation 20 ms^{-1} for projectile with reduced order system control.

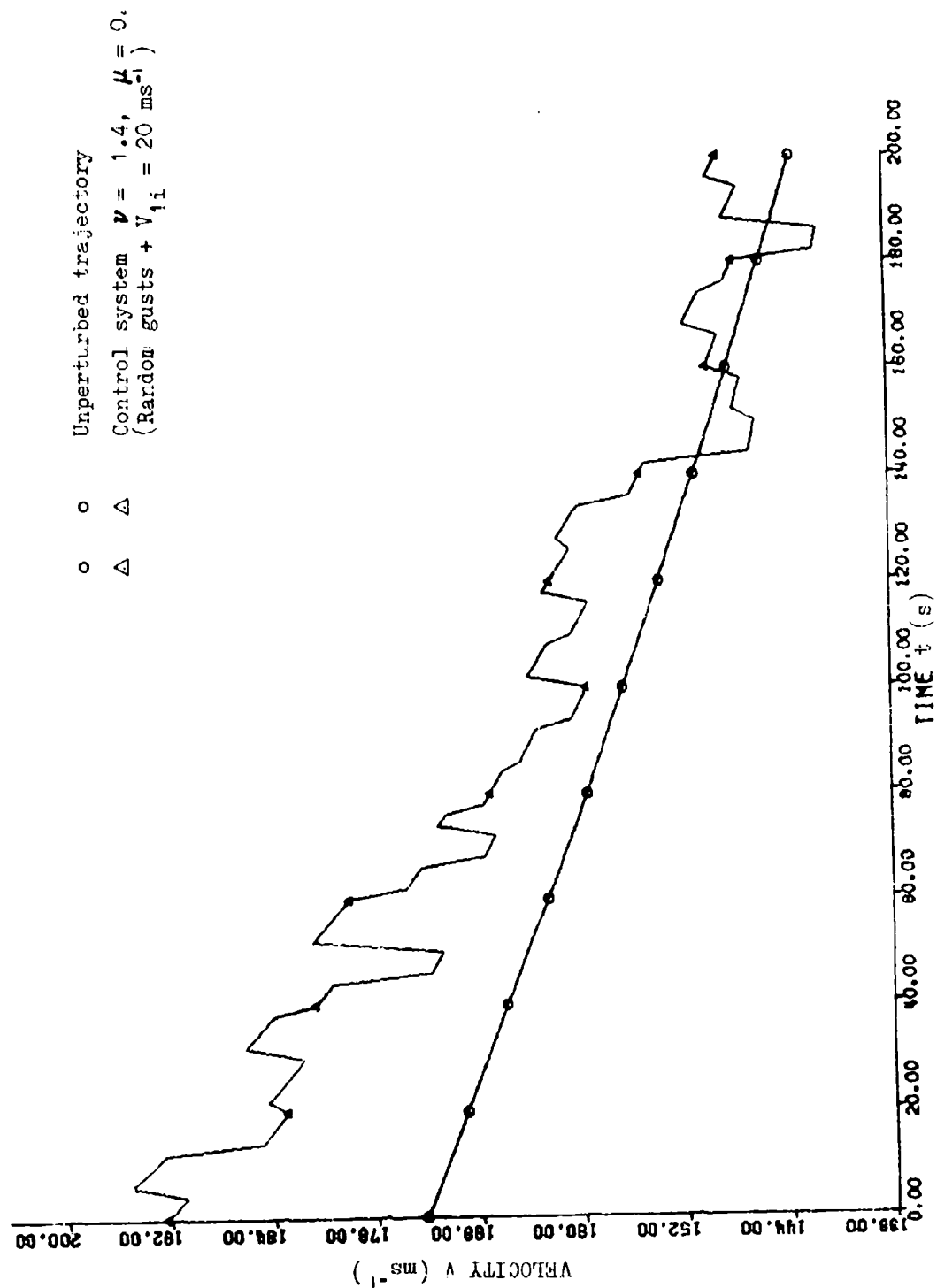


Figure 35. Velocity response to initial velocity perturbation 20 ms^{-1} and random gusts for projectile with reduced order control system.

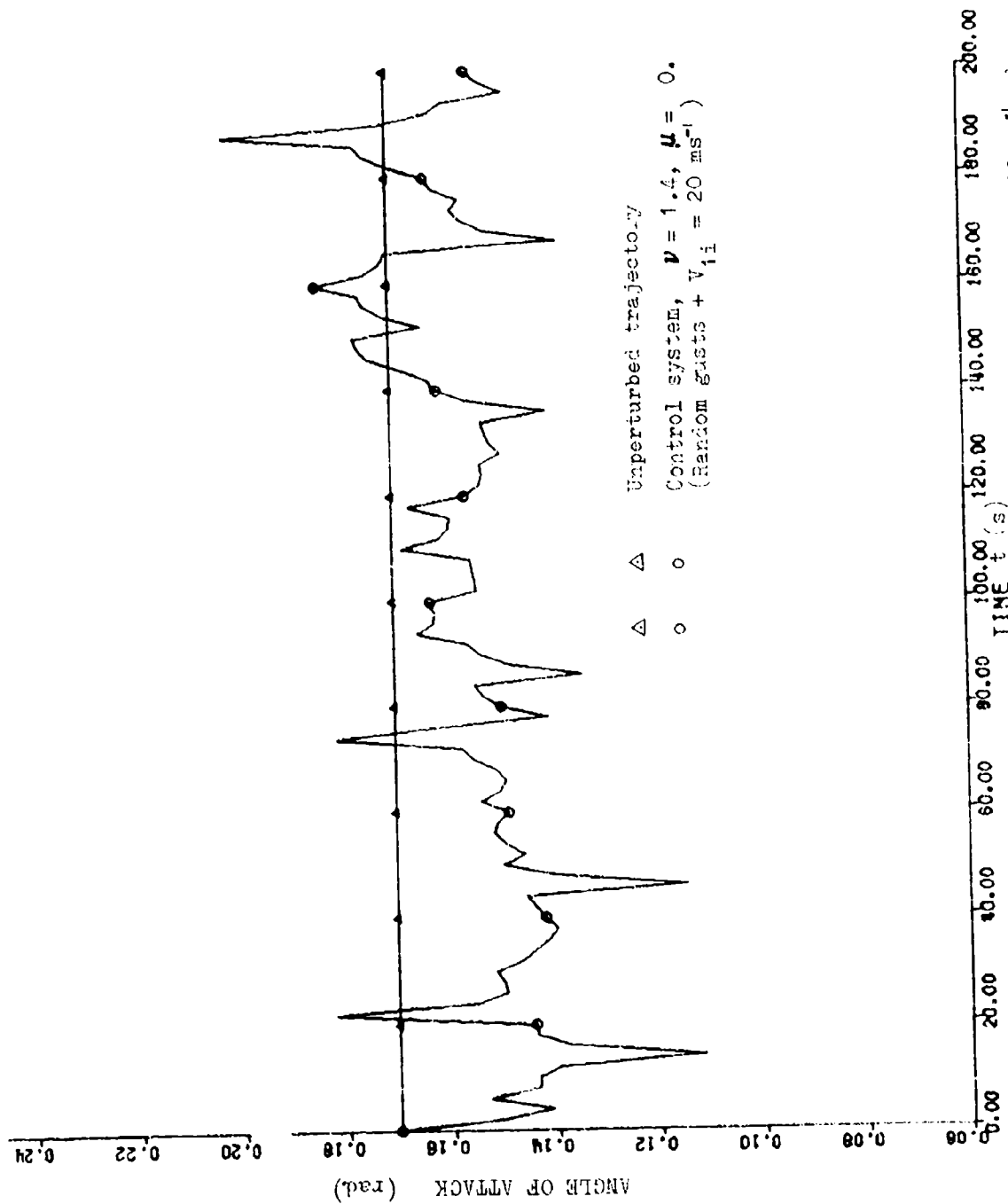


Figure 36. Angle of attack response to initial velocity perturbation 20 ms^{-1} and random gusts for projectile with reduced order control system.

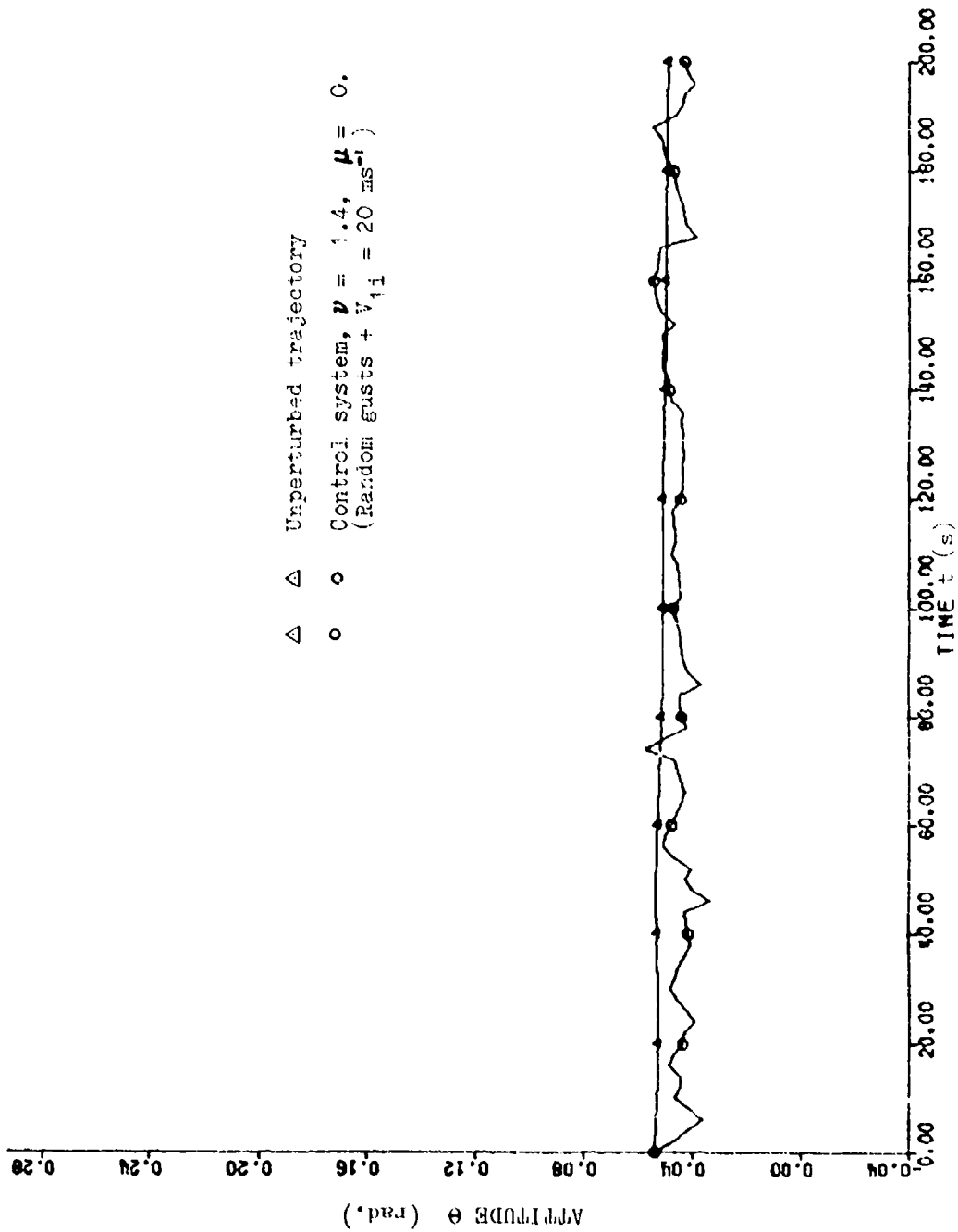


Figure 37. Altitude response to initial velocity perturbation 20 ms^{-1} and random gusts for projectile with reduced order control system.

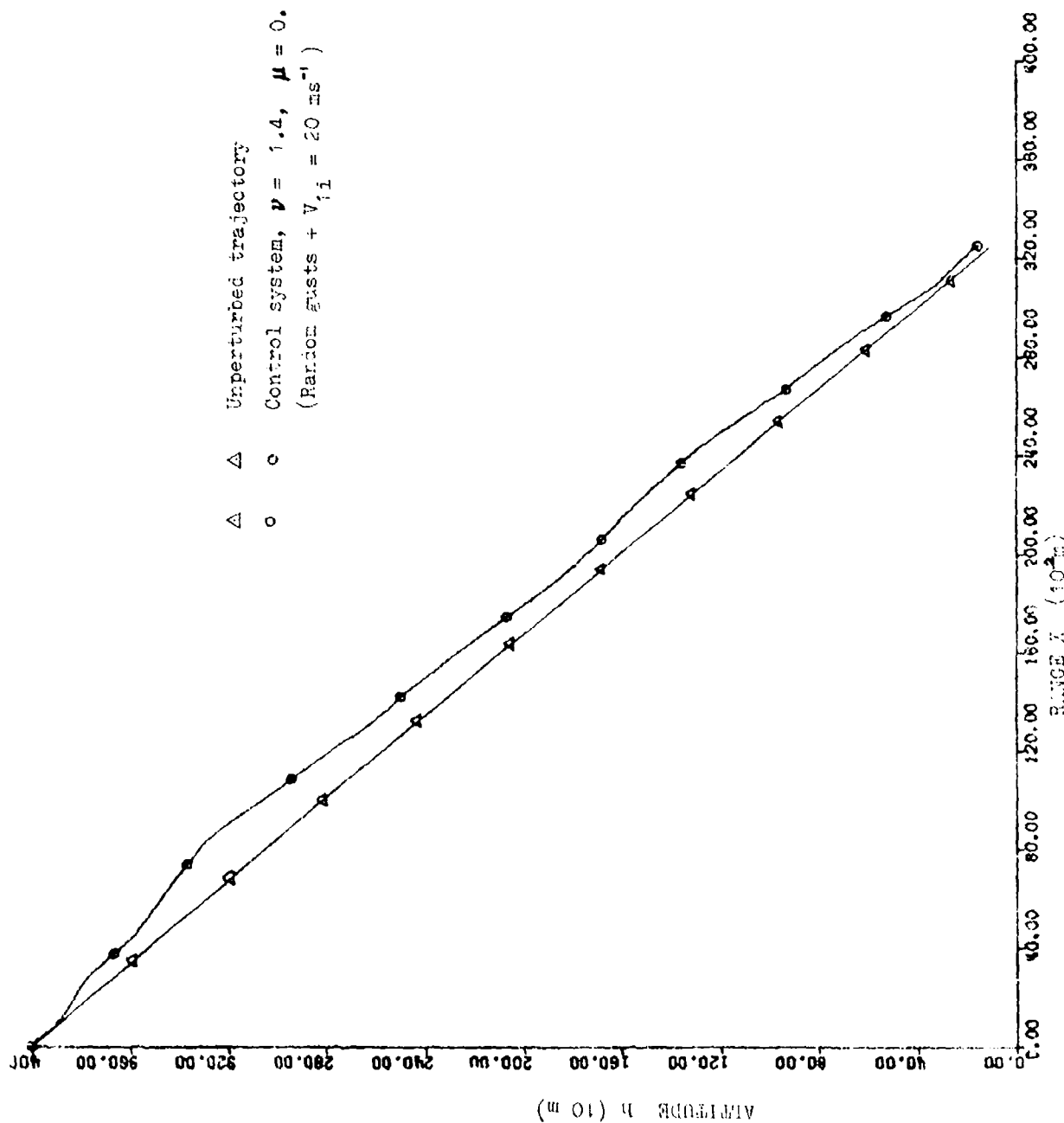


Figure 38. Positional response to initial velocity perturbation 20 ms^{-1} and random gusts for projectile with reduced order control system.

elevator-controlled glider, indicating the difficulties in obtaining altitude, attitude, and velocity regulation, simultaneously. Obviously the approach cannot safely be used in total isolation from the complete system as the discovery of short period mode instability has shown.

1.2 Single State Feedback

Because, as mentioned previously, there may be difficulty in setting initial attitude reference axes accurately enough, making in-flight attitude measurements too inaccurate for regulating gliding flight, it is of interest to discover what can be achieved by velocity feedback alone. In this section, the response of the complete system to initial velocity errors is considered when only velocity is fed back to the elevators. The search for a velocity feedback gain is first commenced through use of a modified form of equation (68) to compute Riccati elements. Using the same state variable weights as used in the final full state feedback system II design, a measure of the quadratic integral performance index, excluding the control contribution, is obtained by computing r_{11} from equation (68) with the quadratic term omitted and with a_{21} replaced by $a_{21} - b_2 K_1$ and a_{41} by $a_{41} - b_4 K_1$. In figure 39, r_{11} so obtained is plotted against K_1 and a minimum is seen to occur at $K_1 = -6 \times 10^{-3}$ radian $m^{-1}s$. When K_1 is negative the elevators reduce angle of attack for positive velocity perturbations. As discovered previously this type of response leads to the best altitude correction but can lead to irrecoverable downward plunging flight if K_1 is not carefully selected. This tendency is reflected in figure 39 where a rapid rise in r_{11} is shown for K_1 approaching -7×10^{-3} radian $m^{-1}s$. However, for $K_1 = -6 \times 10^{-3}$ radian $m^{-1}s$, the short period mode damping was too low and the computed trajectory showed instability. Backing off from this minimum value of K_1 to a value of -5×10^{-3} radian $m^{-1}s$ produced a stable trajectory with a low-damped oscillatory response in the phugoid mode. Plots of velocity, attitude, altitude and angle of attack response to an initial velocity perturbation of $20 m s^{-1}$ are shown in figures 40, 41, 42

and 43. These figures show a low-damped oscillatory response having an amplitude in attitude perturbation of about 2 degrees, and in altitude perturbation of about 270 m. Maximum angle of attack perturbation is about 1.8 degrees. Figures 40 and 43 show how angle of attack decreases for positive velocity perturbation. It is of interest to compare these trajectory results with trajectories obtained for a positive value of K_1 when angle of attack increases with positive velocity perturbation. For the purpose of comparison, trajectories for $K_1 = 5 \times 10^{-3}$ radian $m^{-1}s$ are also shown in figures 40 to 43. These trajectories show that amplitudes of initial phugoid response are increased but so is the damping. The settling time for this sort of control is small enough to effectively remove initial perturbations in velocity and attitude by the end of midcourse flight, but its accentuated attitude response to in-flight velocity disturbances renders it unsuitable as a midcourse controller.

The controller with $K_1 = -5 \times 10^{-3}$ radian $m^{-1}s$ has attitude and altitude responses to velocity perturbations which have smaller values than the uncontrolled system and hence this sort of controller could find application in mid-course flight. However, the feedback gain for this controller is not fully optimal, having been selected to minimise the response to initial velocity perturbations only. Nevertheless, a result given in reference 10, could find application in providing information on how such a sub optimal system would respond to a general set of initial conditions. The result referred to, uses the fact that the ratio of two quadratic forms, each having the same number of variables, has turning points for finite values of the variables provided that none of the square terms disappear from the denominator. Thus, for the ratio $x^T R x / x^T Q x$, where Q must be positive definite, it is shown in reference 10 that the maximum value of this ratio is the maximum eigenvalue of $Q^{-1}R$. To see how this result can be applied to a control system we return to equations (39) and (40) and exclude wind disturbances and the final state weighting matrix S .

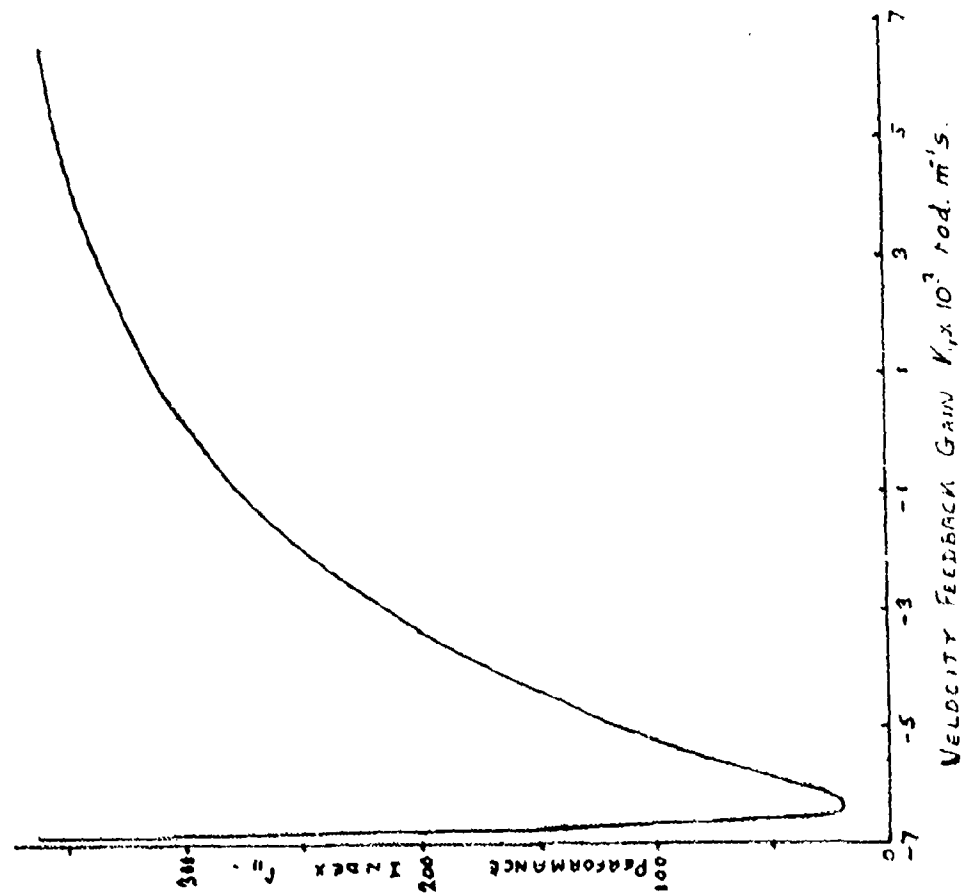


Figure 39. Performance index for feedback of velocity only.

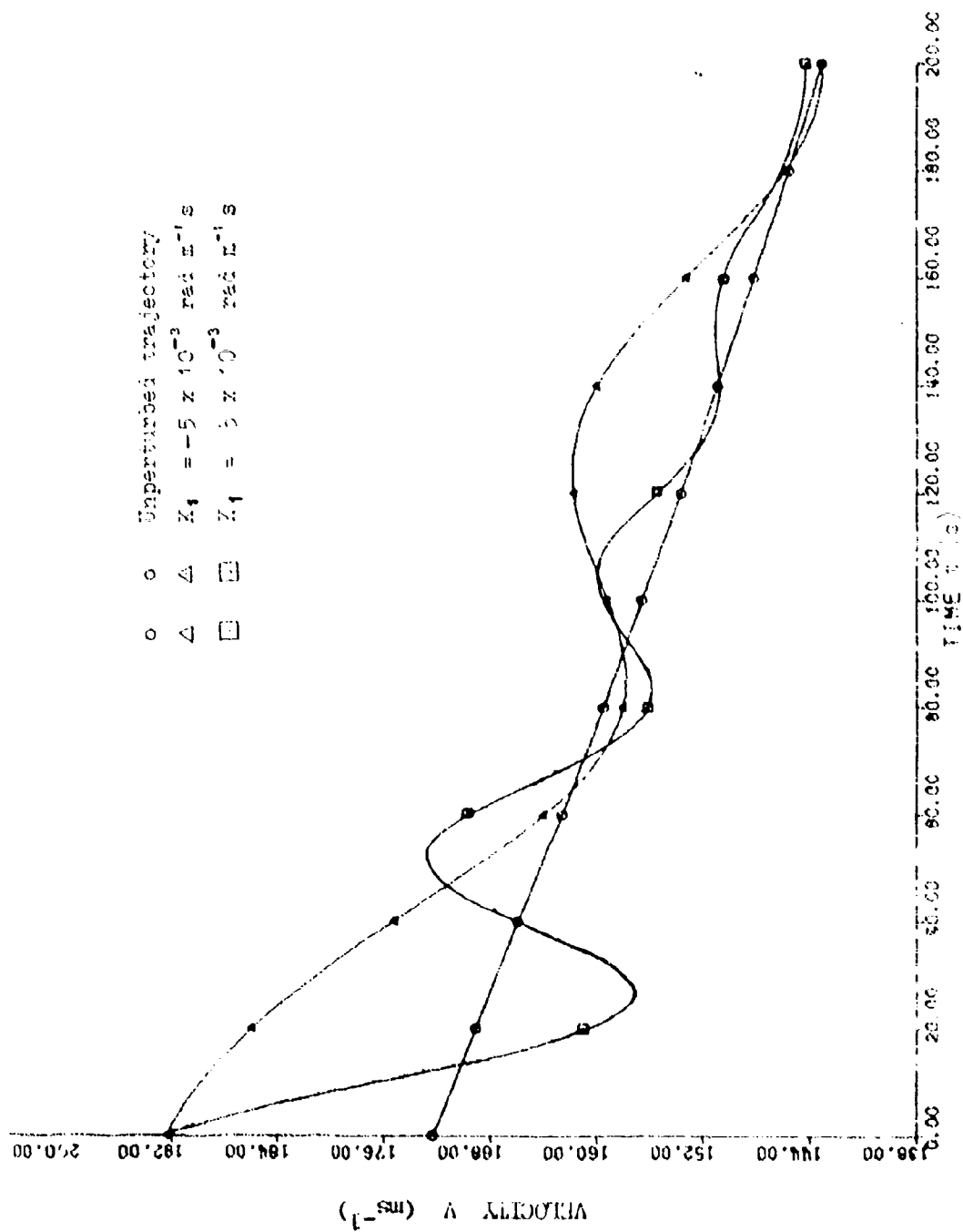


Figure 10. Velocity response to initial velocity perturbation $\pm 10 \text{ m/s}$ for projectile with velocity feedback control only.

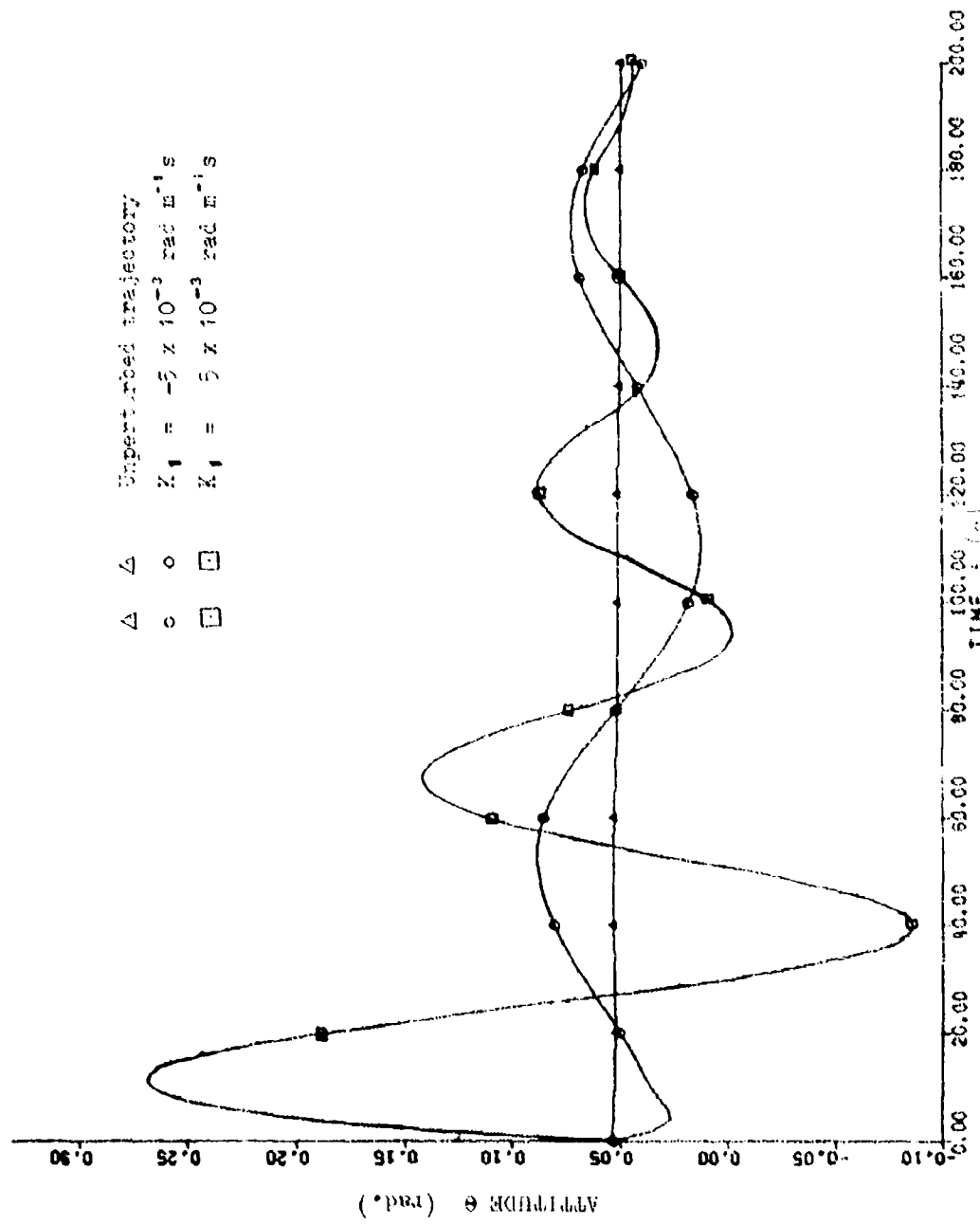


Figure 41. Response response to initial velocity perturbation 20 m s^{-1} for projectile with velocity 100 m s^{-1} only.

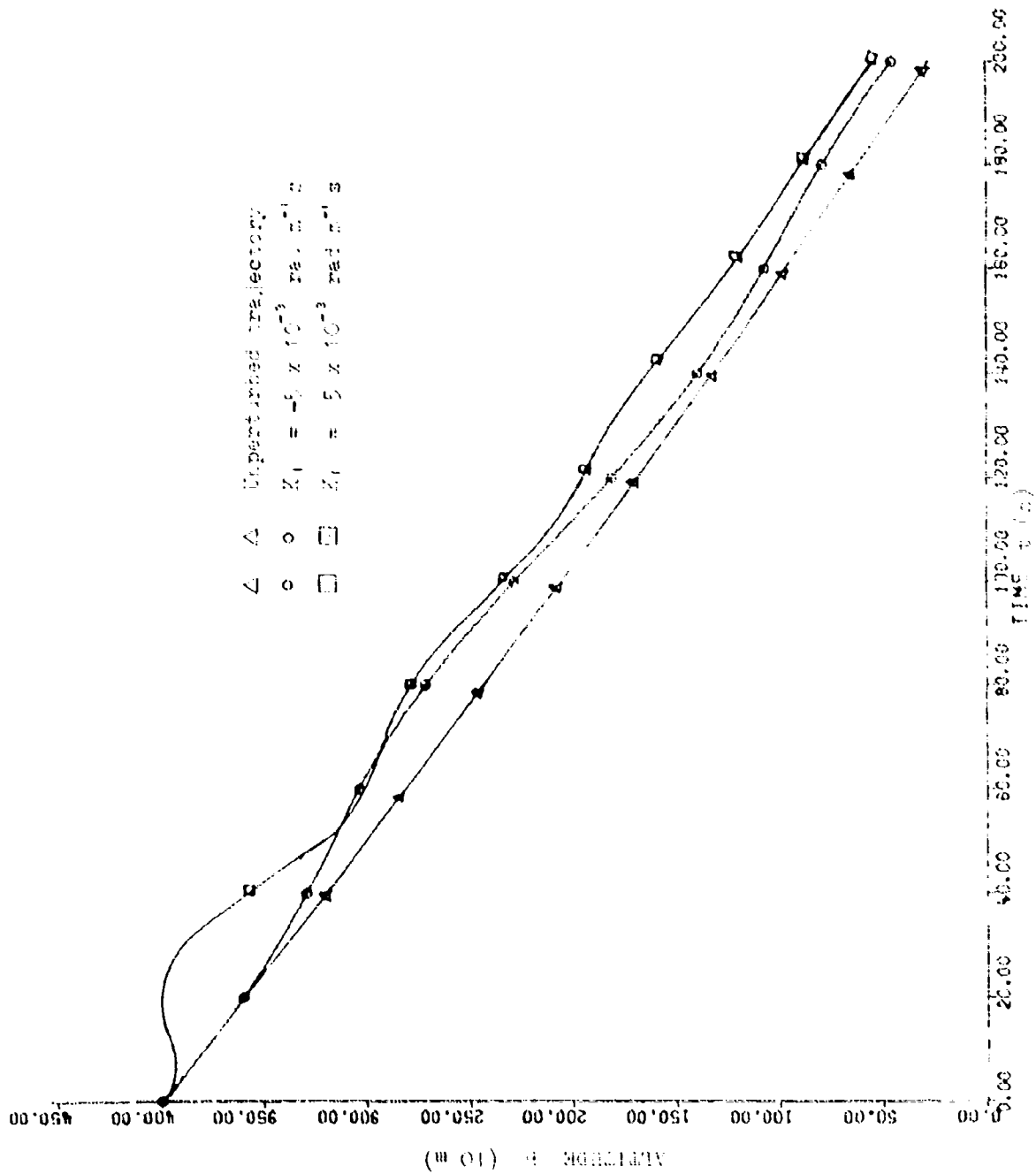


Figure 42. Altitude response to initial velocity perturbation of 5 m/s for projectile with velocity feedback control only.

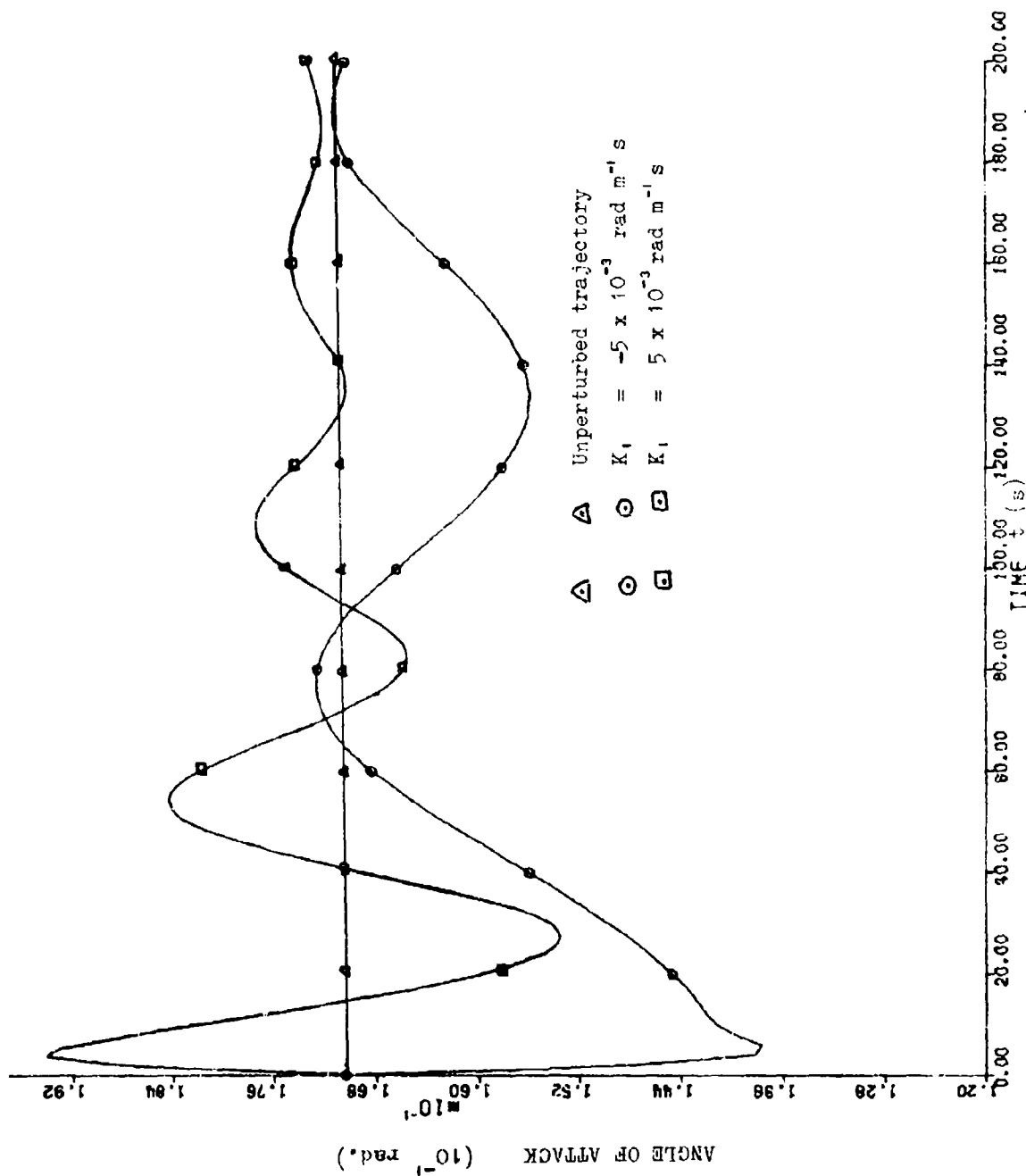


Figure 43. Angle of attack response to initial velocity perturbation 20 ms^{-1} for projectile with velocity feedback control only.

Putting $\eta_1 = -K^T x$, where K is now any gain vector which does not destabilise the closed loop system, we have

$$\dot{x} = A_1 x \quad (88)$$

$$\begin{aligned} \text{and } J_1(x, t) &= \int_t^{t_f} x^T(\tau) Q_1 x(\tau) d\tau \\ &= x^T(t) R_1 x(t), \end{aligned} \quad (89)$$

$$\begin{aligned} \text{where } A_1 &= A - bK^T \\ Q_1 &= Q + KPK^T \\ \text{and } t_f &\text{ is constant} \end{aligned}$$

Following reference 10,

$$\begin{aligned} (dJ_1/dt)/J_1 &= -(x^T Q_1 x)/(x^T R_1 x) \\ &\leq -T, \end{aligned} \quad (90)$$

where T is the maximum eigenvalue of $Q_1^{-1} R_1$. Integrating both sides of inequality (90) leads to the inequality

$$t \leq -T \log_e \{J_1(x, t)/J_1(x_0)\} \quad (91)$$

The usefulness of this result depends on the value of the upper bound T which has been derived. It should be noted that the choice of Q_1 for determining T is arbitrary, apart from the requirement that Q_1 be positive definite. When Q_1 is positive non-negative, the maximum eigenvalue of $Q_1^{-1} R_1$ becomes infinite, rendering (91) a useless piece of information. From equations (88) and (89), R_1 corresponding to arbitrary Q_1 can be found

from the matrix equation

$$\dot{R}_1 + A_1^T R_1 + R_1 A_1 + Q_1 = 0. \quad (92)$$

Suppose now that we have a system with known closed loop behaviour, perhaps an optimal system with full state feedback. Let the known value for the performance index of this system at time t_f be $J(x(t_f))$. Now change the feedback gain vector K to another set of values such that closed loop stability is maintained. So doing, establishes A_1 . Suppose further, that a reasonable value of T has been found by selecting arbitrary Q_1 and solving equation (92) for R_1 , then inequality (91) can be used as a basis for finding an upper bound for the time the changed system would take to bring the performance index $J(x(t))$ to some fixed value $J(x(t_f))$. To use inequality (91) we need to know the maximum value of $J_1(x, t)$ which just fits inside $J(x(t_f))$. The mathematical problem then is to find the maximum for $J_1(x, (t)) = x^T R_1 x$ subject to the constraint

$$\begin{aligned} J(x, (t)) &= x^T R x \\ &= J(x(t_f)), \text{ a known constant.} \end{aligned}$$

This is achieved by introducing a Lagrange multiplier λ and seeking the turning points of the auxiliary function

$$J_1(x(t)) - \lambda \{J(x(t)) - J(x(t_f))\}$$

which occur when

$$\partial J_1 / \partial x - \lambda \partial J / \partial x = 0,$$

$$\text{or, that is when } 2R_1 x - 2\lambda R x = 0, \quad (93)$$

which shows that λ is an eigenvalue of $R^{-1}R_1$.

Pre-multiplying equation (93) throughout by x^T , shows that

$$J_1 - \lambda J = 0,$$

and thus if J_{1m} is the maximum value of J_1 which just fits inside $J(x(t_f))$

$$J_{1m} = \lambda J(x(t_f))$$

where λ is the minimum eigenvalue of $R^{-1}R_1$,

and from inequality (91),

$$t \leq -T \log_e \{ \lambda J(x(t_f)) / J_1(x_0) \} \quad (94)$$

where t is the time taken for the modified system to bring the performance index J of the initial system from $J(x(0))$ to $J(x(t_f))$. Inequality (94) thus affords some means of comparison between settling time for a given optimal control system with complete state feedback and the stable system with the same plant matrix but with arbitrarily selected feedback gains.

8. DISCUSSION AND RESULTS

Linear optimal control theory has been used to determine the state variable feedback which best regulates mid course flight of a gliding aircraft-like projectile with elevator controls. A set of differential equations in perturbations of the state and control variables about the desired operating conditions for the projectile have been derived. These equations provided the linear mathematical model necessary for application of optimal control theory to determining feedback gains. The desired operating condition was the trajectory resulting from the constant elevator setting for which the horizontal range over an altitude drop from 4 to 1 km was maximised.

In gliding trajectories, aerodynamic lift and weight are approximately equal and opposite and characteristically, conditions change slowly along the flight path. Consequently it was discovered that a time-invariant system model was

adequate for feedback control design. Because lift depends on the square of velocity, perturbations in velocity can easily destroy the balance between lift and weight causing the projectile to rise or fall about the desired flight path. To control these excursions about the desired flight path, the elevator controls modify the aerodynamic lift by causing changes in angle of attack. Because at a fixed horizontal range from its point of launch, the projectile's seeker beam must be able to capture the target it is also important to restrict angular excursions in attitude of the beam axis about its direction on the desired trajectory.

The physics of regulating altitude and attitude in response to velocity perturbations through use of feedback to elevator controls has been considered. It has been discovered that there are three extreme ways in which elevator controls can react. Firstly, velocity can be controlled by bringing about changes in altitude. For example, if velocity is too high, the elevator controls could cause the projectile to climb until velocity falls to the value where lift just balances the weight and flight would then proceed at an altitude consistently higher than the desired value, but desired values of attitude and velocity would be maintained. The second way in which elevators can react is to cause a decrease in angle of attack in response to increased velocity and vice versa. This action reduces the increase in lift due to increase in velocity and hence tends to reduce displacements normal to the desired flight path and, at the same time, also tends to maintain the desired attitude. Reducing angle of attack in response to higher velocity and vice versa leads to a lower mean drag than that for the uncontrolled flight at constant angle of attack. The resulting motion is oscillatory and the lower mean drag means that damping is lower than in uncontrolled flight. If this type of control is overdone so that the lift, in response to increased velocity, becomes less than the weight, then the flight path will take a downward plunge attempting to perform a 180 degrees backward turn. This behaviour could not be predicted by the linearised mathematical model. The

third type of elevator control occurs when the angle of attack is caused to increase in response to increased velocity and vice versa. This results in increased mean drag which attempts to reduce velocity to the desired value. The increased differential between lift and weight initially tends to increase displacements normal to the desired flight path and the resulting motion is highly oscillatory with greater amplitude and damping than in uncontrolled flight. The oscillatory nature of the response can preserve some accuracy in altitude.

These observations on the three extreme types of response lead to the following conclusions. Of the three states, velocity, attitude, and altitude, it is possible to regulate any two at the expense of the third using elevator controls, but not all three at once. The control system design method used, effectively mixes the three different types of response in proportions dependent upon the weights selected for the state variable perturbations in the integral quadratic performance index. It is not possible to obtain continuously improving flight regulation from feedback gains obtained by simultaneously increasing the weighting of all state perturbations in the performance index. Because altitude and attitude are the important parameters in meeting accuracy requirements of the mid course trajectory, velocity was not heavily weighted.

Three control systems have been considered. In the first system all five states are fed back to the elevators. In the second system, based on a reduced order mathematical model, only three states are fed back. Thirdly, a system which fed back only velocity to the elevators was considered and in this case the performance index was based on velocity perturbations only. Features of the three system are given in Table 2 below.

Comparative performance of these systems is given in Table 3 below

In these three systems, elevator deflection angles are less than 0.7 radian and angle of attack variations do not exceed 2 degrees in response to velocity perturbations of up to 20 m s^{-1} . All three systems were found to be stable in

TABLE 2. COMPARATIVE FEATURES OF 3 FEEDBACK CONTROL SYSTEMS

System	States fed back to elevators	Feedback gains	Pole Positions s^{-1}
1) Full State Feedback (System II)	Velocity Angle of attack Attitude Pitch rate Altitude	$K_v = -2.034 \times 10^{-2} \text{ rad m}^{-1} \text{ s}$ $K_\alpha = 6.335$ $K_q = -1.867 \text{ s}$ $K_\theta = -26.47$ $K_h = -7.566 \times 10^{-3} \text{ rad m}^{-1}$	$-10.62 \pm 12.23i$ -0.3174 -0.0682 -0.006205
2) Reduced Order Model	Velocity Angle of attack Attitude	$K_v = -7.99 \times 10^{-4} \text{ rad m}^{-1} \text{ s}$ $K_\alpha = 4.385$ $K_\theta = -4.385$	$-0.052 \pm 6.05i$ -0.5198 -0.01144 -0.001085
3) Velocity Feedback Only	Velocity	$K_v = -5 \times 10^{-3} \text{ rad m}^{-1} \text{ s}$	$-0.3511 \pm 6.046i$ $-0.0042 \pm 0.05233i$ -0.002297
4) No Feedback			$-0.3456 \pm 6.045i$ $-0.01041 \pm 0.08546i$ -0.008673

the face of successive random wind gusts having magnitudes in the range 0 to 10 m s^{-1} . It was found that time-invariant models of system behaviour were adequate for determination of feedback. Consequently, the full state feedback

TABLE 3. COMPARATIVE PERFORMANCE OF 3 FEEDBACK CONTROL SYSTEMS

System	Maximum amplitude of response to unit velocity perturbation		Amplitude of response at end of midcourse flight to unit initial velocity perturbation		Total seeker beam angle required per unit initial velocity perturbation
	Altitude	Attitude	Altitude	Attitude	
1) Full State feedback (11)	10m/ms^{-1}	$0.05^{\circ}/\text{ms}^{-1}$	10m/ms^{-1}	$0.022^{\circ}/\text{ms}^{-1}$	$0.24^{\circ}/\text{ms}^{-1}$
2) Reduced order model	13.5m/ms^{-1}	$0.04^{\circ}/\text{ms}^{-1}$	13.5m/ms^{-1}	$0.006^{\circ}/\text{ms}^{-1}$	$0.28^{\circ}/\text{ms}^{-1}$
3) Velocity feedback alone	20m/ms^{-1}	$0.10^{\circ}/\text{ms}^{-1}$	15m/ms^{-1}	$0.063^{\circ}/\text{ms}^{-1}$	$0.43^{\circ}/\text{ms}^{-1}$
4) No feedback	24m/ms^{-1}	$0.37^{\circ}/\text{ms}^{-1}$	15m/ms^{-1}	$0.086^{\circ}/\text{ms}^{-1}$	$0.47^{\circ}/\text{ms}^{-1}$

system could be synthesised by compensating networks, designed by classical methods, when not all states are available for measurement. The system based on a reduced order model performs very well in suppressing attitude response to velocity perturbations and, from Table 3, this is reflected in the seeker beam angle size needed. However, Table 2 shows the short period mode to be very lightly damped and the persistence of short period oscillations may be undesirable. The velocity alone feedback system achieves a moderate suppression of attitude response but is not effective in altitude control. This is because the altitude control being sought is control with respect to horizontal range and not time. With the full feedback control system, the correction of altitude as a function of time is excellent for the trajectory with an initial velocity perturbation. However, as previously pointed out, for elevator controls, regulation of altitude and attitude with time can only be carried out when velocity regulation is slackened. Thus the rate of descent may be excellently regulated but the perturbation in the horizontal component of the initial velocity will tend to persist, leading to a

persistent altitude error with horizontal range.

The full state feedback system induces well damped responses to disturbances, and effectively halves the seeker beam angle that an uncontrolled projectile would require. The performance of this system indicates the measure of error suppression obtainable when angle of attack variations are limited to 2 degrees about the operating value and elevator deflection is limited to 0.7 radian. When initial trajectory errors cannot be confined within acceptable limits a different strategy in selecting a mean flight path is called for. To meet a wide range of initial trajectory errors it may be necessary to arrange automatic on-board selection of compensating fixed elevator settings. The penalty for this, is that in addition to the requirements of the feedback control system, more on-board computer memory is needed together with elevator setting algorithms.

LIST OF SYMBOLS

A	Plant matrix
B	Moment of inertia of projectile in pitching plane about axis through centre of gravity
C_D	Drag coefficient
C_{D0}	Drag coefficient at zero angle of attack
C_L	Lift coefficient
C_m	Pitching moment coefficient
D	Aerodynamic drag, or in equation (39), a disturbance matrix
F	Unmeasurable state selection matrix
G	Unconstrained functional
H	Scale height for exponential atmospheric density approximation
I	Unit matrix
J	Integral quadratic performance index
K	Feedback gain vector
K_f	Feedback gain vector used in estimation process to minimise $(x-\hat{x})$
L	Lift force on projectile
L_c	Lift contribution from controls
M	Pitching moment about centre of gravity of projectile
P	Control variables weighting matrix
Q	State variables weighting matrix
R	Riccati matrix
S	Reference area for aerodynamic coefficients, or in equation (40), a final state weighting matrix
T	Upper bound of settling time for a dynamical system
$s/(\pi EAS_w)$	Induced drag factor
\bar{V}	Velocity vector
V	Velocity magnitude
X	Horizontal range variable
a_{ij}	Element of the plant matrix A

b	Control vector
b_2, b_4	Components of control vector b
d_1, d_2	Components of control vector for reduced order system
g	Gravitational constant, 9.8 m s^{-2}
h	Altitude
i_e	Unit vector in horizontal downrange direction
j	Unit vector in horizontal direction normal to i_e
k_e	Unit vector direction vertically downwards
k_1	Velocity feedback gain in reduced order system
k_2	Flight path angle feedback gain in reduced order system
k	Integer
m	Mass of projectile
\hat{n}	Unit vector normal to flight path forming right hand set with \hat{i}, \hat{j}
q	Angular pitching rate
r_{ij}	Element of Riccati matrix R
t	Time
\hat{t}	Unit vector in a forwards direction tangential to flight path
v	Measurement noise vector
w	System noise vector
x	State variable vector
\hat{x}	Estimate of x
z	State variable vector for reduced order system
θ	Angle between longitudinal axis of glider and horizontal
α	Angle of attack
η	Elevator deflection angle
θ_1	Perturbation in θ
λ	Variable used in characteristic polynomials or Lagrange multiplier
μ	Relative velocity weight for reduced order system
μ_w	Angle between atmospheric wind and the horizontal
v	Relative flight path angle weight for reduced order system
ρ	Atmospheric density

ρ_{ref}	Constant reference atmospheric density corresponding to scale height H
σ	Real part of complex root of characteristic equation
ω	Imaginary part of complex root of characteristic equation
τ	Dummy time variable
ψ	Flight path direction angle ($\theta - \alpha$)

Superscripts

T	Transposed matrix
---	-------------------

Subscripts

0	Unperturbed or optimal trajectory conditions
1	Perturbed trajectory conditions
i, j, k	Integers
m	Denotes maximum value of a variable for weight selection purposes
i	Initial value at $t=0$
f	At final value of time
w	Wind
hw	Horizontal wind
vw	Vertical wind
R	Relative wind
V	Velocity
α	Angle of attack
θ	Attitude
q	Pitching rate
h	Altitude

REFERENCES

1. Edmunds, J.M.: Cambridge Linear Analysis and Design Programs, Second Version. Cambridge University Engineering Dept. CUED/F-CAMS/TR 198, 1980.
2. Daly, K.C., and P. Katzberg: The Classical Design Suite, Department of Computing and Control, Imperial College, London SW7, Publication No.73/18 (Program Description), June, 1973.
3. Melsa, J.L. and S.K. Jones: Computer Programs for Computational Assistance in the Study of Linear Control Theory. McGraw-Hill, 2nd Edition, 1973.
4. Etkin, B.: Dynamics of Flight - Stability and Control. John Wiley and Sons, New York, 1959.
5. Kolk, W.R.: Modern Flight Dynamics. Prentice Hall Pub. Co., 1961.
6. Neumark, S.: The Disturbed Longitudinal Motion on an Uncontrolled Aircraft and of an Aircraft with Automatic Control: Royal Aircraft Establishment, U.K. RAE Report Aero 1793, 1943.
7. DATCOM: USAF Stability and Control DATCOM. McDonnell Douglas Corp., September 1970.
8. ESDU: Engineering Sciences Data Unit - Aerodynamics Sub-section. (Formerly Data Sheets of Royal Aeronautical Society)
9. Miele, A.: Flight Mechanics: Theory of Flight Paths. Addison-Wesley

Publishing Co., Inc. Reading, Mass., Vol.1, 1962.

10. Schultz, D.G. and J.L. Melsa: State Functions and Linear Control Systems
McGraw-Hill, 1967.
11. Kwakernaak, H. and R. Sivan: Linear Optimal Control Systems. Wiley-
Interscience, 1972.
12. Elsgole, L.E.: Calculus of Variations. Pergamon Press, 1961.
13. Lanczos, C.: Applied Analysis. Prentice-Hall, 1956.
14. Korn, G.A. and J.V. Wait: Digital Continuous System Simulation.
Prentice-Hall Inc., 1978.
15. Kreindler, E. and P.E. Sarachik: On the Concepts of Controllability and
Observability of Linear Systems, IEEE Trans. Autom. Control,
Vol.AC-9, No.2, pp.129-136, April 1964.
16. Bryson, A.E. and Y.C. Ho: Applied Optimal Control. John Wiley, 1975.
17. Truxal, J.G.: Automatic Feedback Control System Synthesis. McGraw-Hill,
1955.
18. Shinar, J. and A. Merari: Aircraft Performance Optimization by Forced
Singular Perturbation: Technion-Israel Institute of Technology,
Dept. of Aeronautical Engineering, TAE No.412, June 1980.

APPENDIX 1

PROJECTILE MASS AND AERODYNAMIC PROPERTIES

Mass	m	$= 280 \text{ kg}$
Pitching moment of inertia	B	$= 73 \text{ kg m}^2$
Reference area	S	$= 0.06 \text{ m}^2$
Reference length	b	$= 0.28 \text{ m}$
Wing aspect ratio		$= 7$
Wing area		$= 0.9 \text{ m}^2$
Induced drag factor	$S/\pi e A S_w$	$= 1.378 \times 10^{-2}$
	g	$= 9.8 \text{ m s}^{-1}$
Sea level air density	ρ_{ref}	$= 1.228 \text{ kg m}^{-3}$
Air density at altitude h ,	ρ	$= \rho_{\text{ref}} \exp(-h/H)$, where $H=10^4\text{m}$
	$\rho_{\text{ref}} S/2m$	$= 1.3157 \times 10^{-4} \text{ m}^{-1}$
	$\rho_{\text{ref}} S b/2B$	$= 1.4130 \times 10^{-4} \text{ m}^{-2}$
	$\rho_{\text{ref}} S b^2/4B$	$= 1.9783 \times 10^{-5} \text{ m}^{-1}$

Aerodynamic Force Coefficients

$$C_{D0} = 0.25$$

$$(\rho_{\text{ref}} S/2m) C_{D0} = 3.2893 \times 10^{-5} \text{ m}^{-1}$$

$$\partial C_L / \partial \alpha = 25$$

$$(\rho_{\text{ref}} S/2m) \partial C_L / \partial \alpha = 3.2893 \times 10^{-3} \text{ m}^{-1}$$

$$\partial C_L / \partial \eta = 1$$

$$(S/\pi \epsilon A S_w) (\partial C_L / \partial \alpha)^2 = 8.612$$

$$C_D(\alpha) = C_{D0} + S/\pi \epsilon A S_w (\partial C_L / \partial \alpha)^2 \alpha^2$$

$$\partial C_D = (2S/\pi \epsilon A S_w) (\partial C_L / \partial \alpha)^2 \alpha$$

Aerodynamic Moment Coefficients

$$\partial C_m / \partial \alpha = -13$$

$$(\rho_{\text{ref}} S b/2B) \partial C_m / \partial \alpha = -1.837 \times 10^{-3} \text{ m}^{-2}$$

$$\partial C_m / \partial q = -112$$

$$(\rho_{\text{ref}} S b^2/4B) \partial C_m / \partial q = -2.2156 \times 10^{-3} \text{ m}^{-1}$$

$$\partial C_m / \partial \dot{\alpha} = -24$$

$$(\rho_{ref}^{Sb^2/4B}) \partial C_m / \partial e = -4.7478 \times 10^{-4} m^{-1}$$

$$\partial C_m / \partial \eta = -4$$

$$(\rho_{ref}^{Sb/2B}) \partial C_m / \partial \eta = -5.652 \times 10^{-4} m^{-2}$$

Optimal Glide Path Parameters

From equation (31), $\alpha_o = 0.17037 \text{ rad} = 9.76 \text{ degrees}$

and from equation (27), $V_o = 141.14 \exp(h/2H) m s^{-1}$,
with $\cos(\theta_o - \alpha_o) \approx 1$. (1.1)

Maximum value of Lift/Drag

$$= \frac{\alpha_o (\partial C_L / \partial \alpha)}{C_{Do} + \alpha_o^2 (\partial C_L / \partial \alpha)^2 S / \pi e A S_w}$$

$$+ \frac{\eta_o (\partial C_L / \partial \eta)}{C_{Do} + \alpha_o^2 (\partial C_L / \partial \alpha)^2 S / \pi e A S_w}$$

$= 7.411$ for $\alpha_o = 0.17037 \text{ rad}$
and $\eta_o = -0.5537 \text{ rad}$.

From equation (29), $\tan(\theta_o - \alpha_o) = -1.3224 / \{(V_o^2 / 2H)\}$ (1.2)

From equation (27), range $X_o = 7.411 \{(V_{oi}^2 - V_o^2 / 19.6) + (h_{oi} - h_o)\} m$ (1.3)

and from equation (30), time t

$$= 7.411 [\{(V_{oi} - V_o) / 9.8\} + 2H \{(1/V_o) - (1/V_{oi})\}] \quad (1.4)$$

Also, equation (28) gives $V_o = (V_o^2/2H)\sin(\theta_o - \alpha_o)$ (1.5)

h_i	$= 4 \times 10^3 \text{ m}$	h_f	$= 10^3 \text{ m}$
V_{oi}	$= 172.4 \text{ m s}^{-1}$	V_{of}	$= 148.4 \text{ m s}^{-1}$
$\theta_{oi} - \alpha_{oi}$	$= -0.11664 \text{ rad}$	$\theta_{of} - \alpha_{of}$	$= -0.12072 \text{ rad}$
θ_{oi}	$= 0.05373 \text{ rad}$	θ_{of}	$= 0.04965 \text{ rad}$
X_{oi}	$= 0$	X_{of}	$= 25,144 \text{ m}$
t_i	$= 0$	t_f	$= 157.2 \text{ s}$
\dot{V}_{oi}	$= -0.1729 \text{ m s}^{-2}$	\dot{V}_{of}	$= -0.1326 \text{ m s}^{-2}$

Values of elements a_{ij} of plant matrix A as given by equations (34) to (39) for initial flight conditions ($h_i = 4 \times 10^3 \text{ m}$)

i+	1	2	3	4	5
j					
↓					
1	-0.0152 s^{-1}	2.041 ms^{-2}	-9.733 ms^{-2}	0	0.000131 ts^{-2}
2	$-0.00065429 \text{ m}^{-1}$	-0.38673 s^{-1}	0.0066153 s^{-1}	1	$0.000006 \text{ m}^{-1} \text{ s}^{-1}$
3	0	0	0	1	0

4	$0.000036\text{m}^{-1}\text{s}^{-1}$	-36.554s^{-2}	-0.00036296s^{-2}	-0.3109s^{-1}	0
5	-0.11638	-171.23ms^{-1}	171.23m s^{-1}	0	0

Values of elements a_{ij} of plant matrix A as given by equations (34) to (39) for final flight conditions ($h_f=10^3\text{m}$)

i→	1	2	3	4	5
j					
↓					
1	-0.0177s^{-1}	2.0352ms^{-2}	-9.7287ms^{-2}	0	0.0001311s^{-2}
2	-0.00076863m^{-1}	-0.44963s^{-1}	0.0079527s^{-1}	1	$0.000008\text{m}^{-1}\text{s}^{-1}$
3	0	0	0	1	0
4	$0.000049\text{m}^{-1}\text{s}^{-1}$	-36.575s^{-2}	-0.00050701s^{-2}	-0.3613s^{-1}	0
5	-0.12043	-147.32ms^{-1}	147.32ms^{-1}	0	0

Values of components b_i of control vector b as given by equations (34) to (39) for initial flight conditions ($h_i=4 \times 10^3\text{m}$)

$$b_1 = b_3 = b_5 = 0$$

$$b_2 = -1.52 \times 10^{-2} \text{ s}^{-1}, \quad b_4 = -1.126 \times 10^1 \text{ s}^{-2}$$

Values of components of b for final flight conditions ($h_f=10^3\text{m}$)

$$b_1 = b_3 = b_5 = 0$$

$$b_2 = -1.7662 \times 10^{-2} \text{ s}^{-1}, \quad b_4 = -1.126 \times 10^1 \text{ s}^{-2}.$$

APPENDIX 11

CHARACTERISTIC EQUATION AND SOLUTION

In this appendix the characteristic equation corresponding to equation (39), with coefficients assumed to be time-invariant, is solved by an approximate method so that the dynamical behaviour of the glider can be related to its aerodynamic and mass properties. By comparing the magnitude of the most significant elements a_{ij} of the plant matrix A, given in Appendix I for initial and final values of flight, it can be seen that the assumption of time invariance is reasonable. This situation is brought about because the aerodynamic coefficients have been assumed to have constant values over the speed range and in gliding flight the dynamic pressure, given by $\rho V^2/2$, is then approximately constant. The Mach number range based on optimal glide path conditions varies from 0.53 initially to 0.44 finally, which is well outside the transonic range, so that the assumption of constant aerodynamic coefficients is reasonable.

It is evident from the very small values of the elements in the fifth column of the plant matrices given in Appendix I that the state variables are only weakly dependent upon altitude. Hence for open loop analysis, at least, it is reasonable to consider only the fourth order system obtained by taking the elements in the fifth column of A to be zero. If the roots of this fourth order equation are $\lambda_1, \lambda_2, \lambda_3, \lambda_4$, then the fifth root corresponding to the complete quintic is approximated by

$$\lambda_5 = |A|/\lambda_1\lambda_2\lambda_3\lambda_4 \quad (11.1)$$

where $|A|$ is the determinant of the complete A matrix. In considering the system given by equation (39) it is worth including feedback of all the state variables excluding altitude. Thus equation (39) will be treated as the system

$$\dot{x} = \begin{bmatrix} a_{11} & a_{12} & a_{13} & a_{14} \\ . & . & . & . \\ . & . & . & . \\ a_{41} & a_{42} & a_{43} & a_{44} \end{bmatrix} x - \begin{bmatrix} b_1 \\ b_2 \\ b_3 \\ b_4 \end{bmatrix} [K_1 K_2 K_3 K_4] x \quad (11.2)$$

$$\text{or } \dot{x} = Cx \quad (11.3)$$

where the elements of the matrix C are given by

$$c_{ij} = a_{ij} - b_i K_j. \quad (11.4)$$

The characteristic polynomial corresponding to the system given by equation (11.3) is found by expanding the determinant

for $|\lambda I_4 - C|$ in the form

$$\lambda^4 + C_0 \lambda^3 + C_1 \lambda^2 + C_2 \lambda + C_3,$$

where it is found that

$$C_0 = -(a_{11} + a_{22} + a_{44}) + b_2 K_2 + b_4 K_4 \quad (11.5)$$

$$C_1 = a_{11}(a_{22} + a_{44}) - a_{22}a_{44} - a_{24}a_{42} - a_{12}a_{21} - a_{43}$$

$$+ b_2 K_1 a_{12} - K_2(a_{11}b_2 + a_{44}b_2 - a_{24}b_4) + b_4 K_{13}$$

$$- K_4(a_{11}b_4 + a_{22}b_4 - a_{42}b_2) \quad (11.6)$$

$$C_2 = a_{11}a_{24}a_{42} - a_{11}a_{22}a_{42} + a_{12}a_{21}a_{44} - a_{12}a_{41}a_{24}$$

$$+ a_{42}a_{22} - a_{42}a_{23}$$

$$\begin{aligned}
 & -K_1(a_{12}a_{44}b_2 - a_{12}a_{24}b_4 - a_{13}b_4) \\
 & -K_2(a_{11}a_{24}b_4 - a_{11}a_{44}b_2 + a_{43}b_2 - a_{23}b_4) \\
 & -K_3(a_{11}b_4 - a_{42}b_2 + a_{22}b_4) \\
 & -K_4(a_{11}a_{42}b_2 - a_{11}a_{22}b_4 + a_{12}^2b_4 - a_{12}a_{41}b_2)
 \end{aligned} \tag{11.7}$$

$$\begin{aligned}
 C_3 = & a_{11}a_{23}a_{42} - a_{11}a_{22}a_{43} + a_{12}a_{21}a_{43} - a_{12}a_{41}a_{23} \\
 & + a_{13}a_{41}a_{22} - a_{13}a_{42}a_{21}
 \end{aligned} \tag{11.8}$$

$$\begin{aligned}
 & -K_1(a_{12}a_{43}b_2 - a_{12}a_{23}b_4 + a_{13}a_{22}b_4 - a_{13}a_{42}b_2) \\
 & -K_2(a_{11}a_{23}b_4 - a_{11}a_{43}b_2 + a_{13}a_{41}b_2 - a_{13}a_{21}b_4) \\
 & -K_3(a_{11}a_{42}b_2 - a_{11}a_{22}b_4 + a_{12}a_{21}b_4 - a_{12}a_{41}b_2)
 \end{aligned}$$

By carrying out an order of magnitude analysis of these expressions for the C_i coefficients from the values of a_{ij} given in Appendix I it is possible to simplify the results as follows:-

$$C_0 = -(a_{22} + a_{44}) + b_2K_2 + b_4K_4 \tag{11.9}$$

$$\begin{aligned}
 C_1 = & -a_{42} + b_2K_1a_{12} + b_4K_2 + b_4K_3 \\
 & -K_4\{b_4(a_{11} + a_{22}) - b_2a_{42}\}
 \end{aligned} \tag{11.10}$$

$$C_2 = a_{42}(a_{11} - a_{23}) + K_1b_4(a_{13} + a_{12}) - K_2b_4(a_{11} - a_{23})$$

$$\begin{aligned}
 & -K_3\{b_4(a_{11}+a_{22})-a_{42}b_2\} \\
 & -K_4\{b_4(a_{12}a_{21}-a_{11}a_{22})+b_2a_{11}a_{42}\}
 \end{aligned} \tag{11.11}$$

$$C_3 = a_{11}a_{23}a_{42}-a_{13}a_{21}a_{42}$$

$$\begin{aligned}
 & -K_1(b_4a_{13}a_{22}-b_2a_{13}a_{42}) \\
 & +K_2b_4a_{13}a_{21} \\
 & -K_3\{b_4(a_{12}a_{21}-a_{11}a_{22})+b_2a_{11}a_{42}\}
 \end{aligned} \tag{11.12}$$

11.1 SOLUTION OF QUARTIC

An approximate solution to the quartic

$$\lambda^4 + C_0\lambda^3 + C_1\lambda^2 + C_2\lambda + C_3 = 0 \tag{11.13}$$

can be obtained by the method of reference 13. Using the notation of reference 13, the quartic can be written as the two quadratic factors,

$$(\lambda^2+(\alpha-a)\lambda+\beta-b)(\lambda^2+(\alpha+a)\lambda+\beta+b)=0 \tag{11.14}$$

$$\text{where } \alpha = C_0/2, \quad \beta = (A+\xi)/2,$$

$$a = \xi^{1/2}, \quad b = a(\alpha-B/\xi)/2, \tag{11.15}$$

$$A = C_1 - \alpha^2, \quad B = C_2 - \alpha A$$

and ξ satisfies the cubic equation

$$\xi^3 + (2A-\alpha^2)\xi^2 + (A^2+2B\alpha-4C)\xi - B^2 = 0 \tag{11.16}$$

The approximate solution of this equation is described in reference (13).

By substituting $\xi = x(-B)^{2/3}$ in equation (11.16) it is found that the resulting cubic equation

$$x^3 + (2A - \alpha^2)(-B)^{-2/3}x^2 + (A^2 + 2B\alpha - 4C_3)(-B)^{-4/3}x - 1 = 0 \quad (11.17)$$

has one real root for $0 < x < 1$. Over this interval, the Chebyshev approximation $x^3 \approx 1.5x^2 - 0.5625x + 0.03125$ is substituted, reducing equation (11.17) to the quadratic

$$\begin{aligned} & \{(2A - \alpha^2)(-B)^{-2/3} + 1.5\}x^2 + \{(A^2 + 2B\alpha - 4C_3)(-B)^{-4/3} - 0.5625\}x \\ & - 1 + 0.03125 = 0, \end{aligned} \quad (11.18)$$

which leads to the solution for ξ ,

$$\begin{aligned} \xi = & - \frac{(A^2 + 2B\alpha - 4C_3)(-B)^{-2/3} - 0.5625(-B)^{2/3}}{2(2A - \alpha^2)(-B)^{-2/3} + 3} \\ & \pm \left[\frac{(A^2 + 2B\alpha - 4C_3)(-B)^{-2/3} - 0.5625(-B)^{2/3}}{2(2A - \alpha^2)(-B)^{-2/3} + 3} \right]^2 \\ & + \frac{2(1 - 0.03125)(-B)^{4/3}}{2(2A - \alpha^2)(-B)^{-2/3} + 3} \quad 1/2 \end{aligned} \quad (11.19)$$

This solution can be greatly simplified when the following conditions hold,

$$|(A^2+2B\alpha-4C_3)(-B)^{-4/3}| \gg 0.5626,$$

$$|(2A-\alpha^2)(-B)^{-2/3}| \gg 1.5,$$

$$|4B^2(2A-\alpha^2)/(A^2+2B\alpha-4C_3)^2| \ll 1, \quad (II.20)$$

$$|2B\alpha-4C_3| \ll A^2.$$

and ignoring 0.03125 compared with 1, gives the simple approximation

$$\xi = B^2/A^2 \text{ or } \xi^{1/2} = -B/A. \quad (II.21)$$

In summary, an approximate set of solutions to the quartic equation (II.13) is given by

$$\lambda_{1,2} = -(\alpha-a)/2 \pm [(\alpha-a)^2/4 - (\beta-b)]^{1/2},$$

$$\lambda_{3,4} = -(\alpha+a)/2 \pm [(\alpha+a)^2/4 - (\beta+b)]^{1/2} \quad (II.22)$$

where α , β , a , b , are given by equations (II.15) and the parameter ξ approximated by equation (II.19). An exceptional case⁽¹³⁾ occurs when $B=0$ in equations (II.15), making $\xi=0$ a solution of equation (II.16). In this case the limiting value of b is $0.5(A^2-4C_3)^{1/2}$ unless (A^2-4C_3) is negative in which case the positive root of the quadratic

$$\xi^2 + (2A-\alpha^2)\xi + (A^2-4C_3) = 0 \quad (II.23)$$

is taken as the value of ξ in equations (II.15). A modification to equations (II.22) should be used when β and b are approximately of the same value. In this case, the relationship

$$\beta-b = C_3/(\beta+b) \quad (II.24)$$

obtained by comparing equations (II.13) and (II.14), should be used. Similarly when α and a are approximately of the same value, the

relationship

$$\alpha - a = C_0 - 2\beta/(\alpha + a) \quad (11.25)$$

should be used.

Inserting the values of a_{ij} from Appendix 1 into equations (11.9) to (11.12) with zero feedback gains, it is found that

$$A \approx C_1$$

$$B \approx C_2 - C_1 C_0/2$$

and that all conditions (II.20) are well satisfied. Hence, from equations (II.15) and (II.21)

$$a = \xi^{1/2} = C_0/2 - C_2/C_1,$$

$$\alpha + a = C_0 - C_2/C_1, \quad \alpha - a = C_2/C_1,$$

$$b = (1/2) \{C_1 + (C_0/4)(C_0 - 2C_2/C_1)\},$$

$$\beta = (1/2) \{C_1 + (1/4)(C_0 - 2C_2/C_1)^2\}$$

It is found that $(C_0/2 - C_2/C_1)^2$ and $C_0/2 (C_0/2 - C_2/C_1)$ are negligible compared with C_1 , so that

$$\beta + b = C_1, \text{ and from equation (II.24)}$$

$$\beta - b = C_3/C_1$$

From equations (II.5) to (II.12), the following approximations, in terms of the elements of the plant matrix A, are obtained

$$\alpha + a = -(a_{22} + a_{44} + a_{23}), \quad \alpha - a = a_{23} - a_{11},$$

$$\beta + b = -a_{42}, \quad \beta - b = a_{13}a_{21} - a_{23}a_{11} \quad (11.26)$$

Substituting these results into equation (11.22) shows the short period damping and frequency to be approximated by

$$\sigma_{sp} \approx (1/2)(a_{22} + a_{44} + a_{23}), \quad \omega_{sp}^2 \approx -a_{42} - \sigma_{sp}^2 \quad (11.27)$$

and the long period damping and frequency by

$$\sigma_{lp} \approx (1/2)(a_{11} - a_{23}), \quad \omega_{lp}^2 \approx a_{13}a_{21} - a_{23}a_{11} - \sigma_{lp}^2 \quad (11.28)$$

Using the numerical values of a_{ij} from Appendix I, the initial open loop values of damping, frequency, and period are,

$$\sigma_{sp} = -3.455 \times 10^{-1} \text{ s}^{-1}, \quad \omega_{sp} = 6.036 \text{ s}^{-1}, \quad T_{sp} = 1.041 \text{ s},$$

$$\sigma_{lp} = -1.091 \times 10^{-2} \text{ s}^{-1}, \quad \omega_{lp} = 7.969 \times 10^{-2} \text{ s}^{-1}, \quad T_{lp} = 78.85 \text{ s},$$

and the final values are

$$\sigma_{sp} = -4.015 \times 10^{-1} \text{ s}^{-1}, \quad \omega_{sp} = 6.034 \text{ s}^{-1}, \quad T_{sp} = 1.041 \text{ s},$$

$$\sigma_{lp} = -1.281 \times 10^{-2} \text{ s}^{-1}, \quad \omega_{lp} = 8.634 \times 10^{-2} \text{ s}^{-1}, \quad T_{lp} = 72.78 \text{ s}.$$

The elements a_{ij} can be expressed in terms of the significant aerodynamic coefficients when the gravity components are eliminated through equations (22) and (23). This results in the following approximations

$$\begin{aligned} \sigma_{sp} \approx & -(V_0/2) [(\rho S/2m) \{(\partial C_L/\partial \alpha) + C_D(\alpha_0)\} \\ & + (\rho S b^2/4B) \{(\partial C_m/\partial q + \partial C_m/\partial \alpha)\}] \end{aligned} \quad (11.29)$$

$$\omega_{sp}^2 \approx -(\rho S b/2B) V_0^2 (\partial C_m/\partial \alpha) \quad (11.30)$$

$$\sigma_{lp} \approx -(3/2) V_0 (\rho S/2m) C_D(\alpha_0) \quad (11.31)$$

$$\omega_{1p}^2 \approx \sqrt{2} V_0^2 (\rho S / 2m) C_L(\alpha_0) \quad (11.32)$$

11.2 REDUCED ORDER SYSTEM

The prospect of a reduced order system to represent the long period motion is apparent from consideration of equations (II.14) and (II.26). The first three plant equations of the fourth order system are

$$\dot{x}_1 = a_{11}x_1 + a_{12}x_2 + a_{13}x_3$$

$$\dot{x}_2 = a_{21}x_1 + a_{22}x_2 + a_{23}x_3 + x_4$$

$$\dot{x}_3 = x_4$$

and these can be written as

$$\dot{z}_1 = a_{11}z_1 + a_{13}z_2 + (a_{12} + a_{13})x_2$$

$$\dot{z}_2 = -a_{21}z_1 - a_{23}z_2 - (a_{22} + a_{23})x_2 \quad (11.33)$$

where $z_1 = x_1$

and $z_2 = x_3 - x_2$ (11.34)

Regarding z_1, z_2 as controlled variables and x_2 as the control variable, then the characteristic equation for the open loop part of this system is

$$\lambda^2 + \lambda(a_{23} - a_{11}) + a_{13}a_{21} - a_{23}a_{11} = 0,$$

which from equation (II.26) is equivalent to

$$\lambda^2 + \lambda(\alpha - a) + \beta - b = 0,$$

the long period quadratic component of the complete quartic given by equation (II.14). In terms of the physical variables,

$$z_1 = V_1 \quad \text{the velocity perturbation,}$$

$z_2 = \theta - \alpha_1$, the perturbation in flight path direction, (see figure 4)

and $x_2 = \alpha_1$, the increment in angle of attack.